



UNIVERSITÀ DEGLI STUDI DI MILANO

**SCUOLA DI DOTTORATO
FISICA, ASTROFISICA E FISICA APPLICATA
DIPARTIMENTO DI FISICA**

**CORSO DI DOTTORATO DI RICERCA IN
FISICA, ASTROFISICA E FISICA APPLICATA
CICLO XXVII**

**CHARACTERIZATION OF ATMOSPHERIC AEROSOLS EXPLOITING
SATELLITE MULTISPECTRAL OPTICAL IMAGING. APPLICATIONS TO
RADIATIVE TRANSFER FOR DOWNSTREAM SERVICES IN THE
FIELDS OF RENEWABLE ENERGY AND HEALTHCARE**

Settore Scientifico Disciplinare FIS/07

**Tesi di Dottorato di:
Marco Morelli**

**Supervisore: Dr. Marco Alberto Carlo Potenza
Co-Supervisore: Dr. Emilio Simeone
Coordinatore: Prof. Marco Bersanelli**

A.A. 2014-2015

*A mia moglie, Maria Chiara,
imprescindibile ed amorevole sostegno a tutta la mia vita*

*Ai miei genitori, Renzo e Margherita,
per il loro enorme aiuto in tutto da sempre*

*Alla mia "famiglia abruzzese", Nino, Patrizia, Emanuela, Nicola e Cecilia,
per la loro attenzione per me, i consigli ed il tifo dall'Abruzzo*

*A Emilio e a tutti gli amici e colleghi della Flyby,
senza cui questo Dottorato semplicemente non sarebbe stato possibile*

ACKNOWLEDGEMENTS

My PhD work (and the realization of this Thesis itself) has been performed in collaboration with Flyby S.r.l., a small Italian company devoted to applied research and innovative technology development in remote sensing.

So first of all I would like to express my gratitude to Flyby, that fully funded and supported my PhD scholarship and my attendance to conferences, courses and meetings at national and international level.

Then I would like to thank my Supervisors, Dr. Marco Alberto Carlo Potenza of the University of Milano and Dr. Emilio Simeone, CEO of Flyby. I greatly appreciated the expertise, passion, humanity and patience of Dr. Potenza, who fully understood the best way to conduct my “untypical” PhD in collaboration with an external company, constantly supporting me in my work and helping me in many circumstances. I’m very grateful also to Dr. Simeone, who firstly proposed me this PhD possibility and supported me from professional, scientific and human point of views, greatly contributing to my personal education and growth.

I would like to thank also Prof. Danilo Giuliotti of the University of Pisa, Referee of this Thesis, for the very interesting collaboration that we are developing (also aside this Thesis) and for his great passion, support and confidence in me.

For what concern PhD activities, I’m thankful also to Prof. Marco Bersanelli, Coordinator of the PhD school, and to Andrea Zanzani, Secretary of the PhD School, for their support. I would like to thank also Dr. Roberta Vecchi and Dr. Gianluigi Valli of the University of Milano for their collaboration and for the scientific advices on atmospheric physics.

I’m grateful also to all my colleagues at Flyby, that contributed a lot to my education and to the PhD research activities. Unfortunately I cannot cite them all, but I would like to mention some of them who particularly contributed to this Thesis: Dr. Andrea Masini, co-author in almost all my publications and great support for my scientific activities; Eng. Ciro Lanzetta, who supported me in the development of applications in the solar energy sector; Eng. Antonio Piazzi and Eng. Enrico Gabriele, for the technical realization of the solar measurement station at Flyby; Dr. Fabrizio Ruffini, who contributed to the validation of the satellite-based application dedicated to solar energy plant monitoring.

Furthermore, I would like to thank all the colleagues involved in the research projects in which I participated. In particular I would like to mention Prof. Lucien Wald of ARMINES-ParisTech, coordinator of the FP7-ENDORSE project, for all his important advices and for his great confidence in me (as demonstrated by nominating me leader of one of the most important Work Packages of ENDORSE at my first year of PhD and in spite of my initial worry).

Finally I would like to acknowledge Dr. Henri Diémoz of the Environmental Protection Agency of the Italian region of Valle d’Aosta (ARPA – Valle d’Aosta) who greatly contributes to the realization and validation of the satellite-based UV dosimeter. And I would like to thank also Dr. Joe Michalsky, coordinator of the BSRN international project, for my involvement in the BSRN expert group on spectral measurements.

CONTENTS

1	INTRODUCTION	1
2	RADIATIVE TRANSFER IN THE ATMOSPHERE	3
2.1	Earth atmosphere.....	3
2.1.1	Gases.....	4
2.1.2	Aerosols	8
2.1.3	Clouds	13
2.2	Solar radiation.....	15
2.2.1	Common definitions	16
2.2.2	Approximations.....	18
2.2.3	Components of the solar irradiance	18
2.2.4	Solar shortwave radiation.....	20
2.2.5	Solar UV radiation.....	21
2.3	Radiative transfer.....	23
2.4	Satellite multispectral optical imagery	25
2.5	Solar radiation measurements at ground	28
3	AEROSOL IMPACT ON RADIATIVE TRANSFER	32
3.1	Satellite near real-time monitoring of cloudiness.....	32
3.2	Aerosols impact on cloudless-sky solar radiation	35
3.2.1	Observations.....	39
3.2.2	Simulations	47
3.2.3	Innovative concepts for the near real-time assessment of aerosols impact	55
4	APPLICATIONS	56
4.1	Solar energy: near real-time monitoring of solar plants	56
4.1.1	Concept.....	56
4.1.2	Results.....	57
4.2	Healthcare: satellite-based UV dosimetry	59
4.2.1	Concept.....	59
4.2.2	Results.....	60

5	REPORT OF THE ACTIVITIES IN RESEARCH PROJECTS	63
5.1.1	FP7 “MACC” project.....	63
5.1.2	FP7 “ENDORSE” project	64
5.1.3	ASI “SATENERG” project	64
6	CONCLUSIONS	66
6.1	Achieved results	66
6.2	Future developments	67
7	REFERENCES	68
8	APPENDICES	72
8.1	Appendix A: Publications	72
8.1.1	List of publications	72
8.1.2	Published peer-reviewed papers	74
8.2	Appendix B: Presentations at conferences	95
8.2.1	International	95
8.2.2	National	102
8.3	Appendix C: Presentations at project meetings	105
8.3.1	International	105
8.3.2	National	109
8.4	Appendix D: Awards	111
8.4.1	EMS Young Scientist Travel Awards (YSTAs) – Fee Waiver	111
8.5	Appendix E: other relevant activities performed during the PhD	112
8.5.1	Attended courses.....	112
8.5.2	BSRN “Spectral measurements” expert group	112
8.5.3	Teaching activities.....	113
8.5.4	Reviewer activities	113
8.5.5	Thesis supervision	114
8.6	Appendix F: Project deliverables	115
8.6.1	Non-public	115
8.6.2	Public	123

LIST OF TABLES

Table 1: Altitude ranges of different atmospheric layers. Taken from (Seinfeld and Pandis 1998).	3
Table 2: Normal composition of clean atmospheric air. Taken from (NOAA 1976).....	6

LIST OF FIGURES

Figure 1: Scheme of the different atmosphere layers. Courtesy of NASA.....	4
Figure 2: Scheme of the scattering and absorption processes in the atmosphere. Courtesy of Flyby..	6
Figure 3: Vertical distribution of the ozone density in the atmosphere at mid-latitudes. Taken from (Manins 2001).....	7
Figure 4: Total precipitable water retrieved during May 2009 by the Atmospheric Infrared Sounder (AIRS) on the Aqua satellite. Courtesy of NASA.....	8
Figure 5: Aerial photo of aerosols over Los Angeles (USA). Courtesy of the Department of Physics of University of Oxford.....	9
Figure 6: Scanning electron photographs of dried sea-salt aerosol particles collected at Mace Head in Ireland. The width of the picture is 2.7 μm . Taken from (Chamaillard, et al. 2003).....	10
Figure 7: Scanning electron photographs of dust aerosol particles. Taken from (Klashnikova and Sokolik 2004).....	11
Figure 8: A street sample of aerosols submitted for examination as the result of a nuisance complaint. The magnification is equal to 40. The white snowballs are spheres of sodium carbonate from a nearby paper plant. In addition, the sample contains dried leaves, glass, glass fibers, paper fibers, cement dust, hematite, limestone, olivine, coal dust, soot, and burned wood. There is a great deal of quartz, covered wholly or partially by asphalt. Taken from (McCrone 1967).....	12
Figure 9: Effects of volcanic aerosols on the climate. Courtesy of United States Geological Survey. .	13
Figure 10: Radiation arriving on the ground under cloudy skies. Taken from (Iqbal 1983).....	14
Figure 11: Comparison of the observed solar spectral irradiance at TOA and the spectral irradiance emitted by a black body with temperature of 5777 K. Derived from (Iqbal 1983).....	15
Figure 12: Scheme for the radiance definition. Courtesy of Flyby.	16
Figure 13: Scheme for the irradiance definition. Courtesy of Flyby.	17
Figure 14: Different components of the solar irradiance incident on a plane. Courtesy of Flyby.....	18
Figure 15: Scheme of a plane normal to sun rays (surface B) and of an horizontal plane (surface A). Courtesy of Flyby.	19
Figure 16: Spectrum of the solar shortwave radiation at ground level, reported also with the spectrum at TOA level and the sun's blackbody spectrum. Courtesy of the American Society for Testing and Materials (ASTM).....	20
Figure 17: Scheme of the propagation of solar ultraviolet radiation into the atmosphere. Courtesy of the National Institute for Environmental Studies of Japan.....	21
Figure 18: Erythral Action Spectrum (weight function) for converting UV spectral irradiance into the UV-Index. Taken from (McKinlay and Diffey 1987).....	22
Figure 19: Distribution of direct (beam), diffuse and absorbed solar radiation. Taken from (Iqbal 1983).....	23

Figure 20: Geometry of a monochromatic beam of radiation passing through a thin layer of atmosphere. Courtesy of the Department of Geology of the University of California at Santa Barbara (USA)..... 24

Figure 21: Atmospheric scattering processes occurring at different radiation wavelengths for different molecules radii. Courtesy of the Department of Geology of the University of California at Santa Barbara (USA)..... 24

Figure 22: Characteristics of then SEVIRI mutispectral channels. Taken from(EUMETSAT 2005)....25

Figure 23: SEVIRI solar channels spectral response, together with typical atmospheric transmittance spectra. Taken from www.eumetsat.org. 26

Figure 24: SEVIRI thermal channels spectral response, together with typical atmospheric transmittance spectra. Taken from www.eumetsat.org. 26

Figure 25: Spatial coverage of the SEVIRI sensor on the MSG satellite. Courtesy of Flyby. 27

Figure 26: An example of the full-disk image observed by the SEVIRI sensor on the MSG satellite in the 0.8 μm visible channel on September 2nd 2014 at 12.00 UTC. Source data are provided by EUMETSAT. 27

Figure 27: The solar measurements site at Flyby (Livorno, Italy), represented by a red square on the image. The geographical coordinates are 43.506°N, 10.322°E . Image has been retrieved from Google Earth service (<http://earth.google.it>)..... 28

Figure 28: Scheme of the solar measurement station at Flyby (Livorno, Italy)..... 28

Figure 29: Photo during the installation of the solar measurement station at Flyby (Livorno, Italy). The Author is setting the position of one of the UV sensors. 29

Figure 30: Photo of the complete solar measurement station at Flyby (Livorno, Italy)..... 29

Figure 31: Technical characteristics of the UV sensor provided by Davis Instruments. Taken from (Davis Instruments 2006)..... 30

Figure 32: Cosine and spectral responses of the UV sensor provided by Davis Instruments. Taken from (Davis Instruments 2006). 31

Figure 33: Photo of the Davis Instruments UV Sensor model 7841. Taken from www.davisnet.com. 31

Figure 34: Scheme of a EO satellite acquisition geometry. Courtesy of Flyby. 33

Figure 35: Aerosols and clouds interactions with incident solar radiation. Courtesy of the Lawrence Livermore National Laboratory (USA) 35

Figure 36: Line of sight from Livorno to the island of Capraia. Image taken from the Google Earth service..... 36

Figure 37: Photo of the solar radiation measurements station and the horizon seen from the roof of Flyby (Livorno, Italy) on September 2nd 2014..... 37

Figure 38: Photo of the horizon seen from the roof of Flyby (Livorno, Italy) on September 2nd 2014. The Capraia island can be detected on the horizon..... 37

Figure 39: Photo of the solar radiation measurements station and the horizon seen from the roof of Flyby (Livorno, Italy) on September 6th 2014..... 38

Figure 40: Photo of the horizon seen from the roof of Flyby (Livorno, Italy) on September 6th 2014. The Capraia island cannot be detected on the horizon. 38

Figure 41: Comparison of the AC power produced by the photovoltaic plant at Flyby (Livorno, Italy) on September 2nd and on September 6th 2014. Data have been sampled every 15 minutes from 4.00 UTC to 19.00 UTC. Source data are provided by Flyby..... 40

Figure 42: Comparison of the UV index on the horizontal plane measured at Flyby (Livorno, Italy) on September 2nd and on September 6th 2014. Data have been sampled every 1 minute from 4.00 UTC to 19.00 UTC. Source data are provided by Flyby..... 41

Figure 43: Full-disk image observed by the SEVIRI sensor on the MSG satellite in the 1.6 μm infrared channel on September 2nd 2014 at 12.00 UTC. Source data are provided by EUMETSAT..... 42

Figure 44: Full-disk image observed by the SEVIRI sensor on the MSG satellite in the 3.9 μm infrared channel on September 2nd 2014 at 12.00 UTC. Source data are provided by EUMETSAT..... 43

Figure 45: Full-disk image observed by the SEVIRI sensor on the MSG satellite in the 1.6 μm infrared channel on September 6th 2014 at 12.00 UTC. Source data are provided by EUMETSAT..... 43

Figure 46: Full-disk image observed by the SEVIRI sensor on the MSG satellite in the 3.9 μm infrared channel on September 6th 2014 at 12.00 UTC. Source data are provided by EUMETSAT..... 44

Figure 47: Comparison of the spectral radiance observed by the SEVIRI sensor on the MSG satellite in the 1.6 μm infrared channel for the Flyby site (Livorno, Italy) on September 2nd and on September 6th 2014. Data have been sampled every 15 minutes from 4.00 UTC to 19.00 UTC. Source data are provided by EUMETSAT..... 45

Figure 48: Comparison of the spectral radiance observed by the SEVIRI sensor on the MSG satellite in the 3.9 μm infrared channel for the Flyby site (Livorno, Italy) on September 2nd and on September 6th 2014. Data have been sampled every 15 minutes from 4.00 UTC to 19.00 UTC. Source data are provided by EUMETSAT..... 46

Figure 49: Comparison of the simulated spectral solar (shortwave) irradiance at Flyby (Livorno, Italy) on September 2nd and on September 6th 2014. Data have been obtained exploiting the libRadtran RTM..... 49

Figure 50: Simulated spectral solar (shortwave) irradiance at Flyby (Livorno, Italy) on September 2nd for different values of aerosols visibility. Data have been obtained exploiting the libRadtran RTM..... 50

Figure 51: Simulated solar shortwave irradiance at Flyby (Livorno, Italy) on September 2nd (0 UTC - 24 UTC) for different values of aerosols visibility. Data have been obtained exploiting the libRadtran RTM..... 51

Figure 52: Simulated UV index at Flyby (Livorno, Italy) on September 2nd (5 UTC - 17.30 UTC) for different values of aerosols visibility. Data have been obtained exploiting the libRadtran RTM. 51

Figure 53: Simulation of the radiance observed by the SEVIRI sensor on the MSG satellite in the 1.6 μm channel for the Flyby site (Livorno, Italy) on September 2nd 2014 (0 UTC - 24 UTC). Data have been obtained exploiting the libRadtran RTM. 53

Figure 54: Simulation of the radiance observed by the SEVIRI sensor on the MSG satellite in the 3.9 μm channel for the Flyby site (Livorno, Italy) on September 2nd 2014 (0 UTC - 24 UTC). Data have been obtained exploiting the libRadtran RTM. 54

Figure 55: Scheme of a possible innovative method for the satellite-based near real-time monitoring of solar radiation at ground that takes into account also aerosols impact in cloudless-sky conditions. 55

Figure 56: Scheme of our modelling technique for the satellite-based near real-time monitoring of solar energy photovoltaic plants.57

Figure 57: Equivalent circuit of a PV cell exploited in the opto-electronic model. Taken from (De Soto, Klein and Beckman 2006).57

Figure 58: Scatter plot comparing the hourly AC power produced by three different PV plants as calculated by the satellite-based method and as obtained from in-situ measured data. Source data are referred to a 4.86 kWp plant in Veneto (North Italy), a 3.89 kWp plant in Lazio (Centre Italy) and a 20.0 kWp plant in Sicily (South Italy). The considered periods are November 2013, January 2014, March 2014, May 2014, July 2014 and September 2014, for a total of 5383 time instants that range from 05:00 UTC to 20:00 UTC. Taken from (Morelli, Masini and Ruffini, et al. 2015 - in press).58

Figure 59: Comparison between the behaviour of the satellite-based hourly AC power and the in-situ measured one. Data are referred to a single month (September 2014) for the PV plant in Veneto. Taken from (Morelli, Masini and Ruffini, et al. 2015 - in press).58

Figure 60: An example of the behaviour of the NMAE resulting from the comparison between satellite-based and in-situ measured hourly AC power. Data are referred to a single month (September 2014) for the PV plant in Veneto. Taken from (Morelli, Masini and Ruffini, et al. 2015 - in press).59

Figure 61: Photo of the UVS-AE-T radiometer exploited for the validation of the satellite-based UV dosimeter. Courtesy of Kipp&Zonen.60

Figure 62: Comparison between the UV dose derived from the satellite-based dosimeter and the UV data provided by the in-situ measurements performed by ARPA Valle d'Aosta in stable weather conditions. Data are referred to the period June-July 2014. Taken from (Morelli, Masini and Diémoz, et al. 2014).61

Figure 63: Maximum relative difference between satellite-based and in-situ measured UV dose data with respect to SZA in stable weather conditions. Data are referred to the Saint Christophe (Aosta, Italy) station in the period June-July 2014. Taken from (Morelli, Masini and Diémoz, et al. 2014).61

Figure 64: Comparison between the UV dose derived from the satellite-based dosimeter and the UV data provided by the in-situ measurements performed by ARPA Valle d'Aosta in unstable weather conditions. Data are referred to the period June-July 2014. Taken from (Morelli, Masini and Diémoz, et al. 2014).62

Figure 65: Maximum relative difference between satellite-based and in-situ measured UV dose data with respect to SZA in unstable weather conditions. Data are referred to the Saint Christophe (Aosta, Italy) station in the period June-July 2014. Taken from (Morelli, Masini and Diémoz, et al. 2014).62

Figure 66: Copy of the Diploma released to the Author for the participation to the ESA EO Summer School in August 2014 at Frascati (Rome, Italy).112

LIST OF ABBREVIATIONS AND ACRONYMS

AERONET	AERosol RObotic NETwork
ASI	Italian Space Agency
BHI	Beam Horizontal Irradiance
BNI	Beam Normal Irradiance
BSRN	Baseline Surface Radiation Network
BTI	Beam Tilted Irradiance
CIE	International Commission on Illumination
DHI	Diffuse Horizontal Irradiance
DNI	Diffuse Normal Irradiance
DTI	Diffuse Tilted Irradiance
EC	European Commission
EO	Earth Observation
ENDORSE	ENergy DOWnstReam SErvices
ESA	European Space Agency
EU	European Union
EUMETSAT	European Organisation for the Exploitation of Meteorological Satellites
FP	Framework Programme
GHI	Global Horizontal Irradiance
GNI	Global Norma Irradiance
GTI	Global Tilted Irradiance
IARC	International Agency for Research on Cancer
IR	InfraRed
MACC	Monitoring Atmospheric Composition and Climate
MED	Minimum Erythemat Dose
MSG	Meteosat Second Generation
NASA	National Aeronautics and Space Administration
RNI	ground Reflected Normal Irradiance
RTE	Radiative Transfer Equation
RTI	ground Reflected Tilted Irradiance
RTM	Radiative Transfer Model

SEVIRI	Spinning Enhanced Visible and Infrared Imager
TOA	Top Of Atmosphere
UV	UltraViolet
UVI	UltraViolet Index
WMO	World Meteorological Organization

1 INTRODUCTION

In this Thesis we present some of the most important results obtained in the PhD concerning with multispectral satellite remote sensing and radiative transfer modelling.

The effects of atmospheric aerosols on the solar radiative transfer have been investigated by exploiting both satellite optical imagery and ground-based solar radiation measurements. In particular almost clear-sky weather conditions have been taken into account in order to focus aerosols impact on radiative transfer avoiding the effects related to clouds.

We observed the solar radiation measured at ground (i.e. the solar radiation transmitted through the atmosphere) and the backscattered radiation observed by a geostationary Earth Observation (EO) satellite in different spectral bands. The contemporaneous observation of solar radiation “below” and “above” aerosols layer in cloudless-sky conditions can be extremely important for aerosols impact assessment and for the development of an innovative method for satellite-based solar radiation monitoring taking also into account a near real-time aerosols impact detection.

Besides also the effects of clouds on solar radiation have been modelled, allowing several applications in the fields of renewable energies and healthcare.

In particular some methodologies for the near real-time monitoring of the performances of solar energy plants (Photovoltaic or PV, Concentrating Solar Power or CSP, Concentrated Photovoltaic or CPV) have been developed also in the frame of different research project (FP7-MACC, FP7-ENDORSE, ASI-SATENERG). These methodologies are based on the satellite monitoring of the solar radiation incident at ground level and on a analytic modelling of the solar energy plant, allowing a near-real time comparison between the actual AC power produced by the plant and the satellite-based expected one.

In the healthcare sector instead, an application dedicated to the satellite-based monitoring of UV effects on human skin has been developed. This application starts from the near-real time assessment of UV erythemal dose and makes a comparison whit user’s Minimum Erythemal Dose (MED) in order to provide a “safe sun exposure time” for avoiding sunburns or other skin diseases (such as melanoma).

The Thesis has been structured as follows. In Chapter 2 we introduce the theoretical fundamentals by describing Earth atmosphere (Section 2.1), solar radiation (Section 2.2) and radiative transfer (i.e. the interaction of solar radiation with the atmosphere). Then the Chapter is concluded with a general description of the satellite optical imagery exploited in this Thesis (Section 2.4).

Chapter 3 is dedicated instead to the scientific results obtained on satellite-based monitoring of solar radiation. The effects of clouds are taken into account in Section 3.1, while the results on aerosols impact in cloudless conditions are presented in the Section 3.2. At the end of the Chapter (Section 3.2.3) we present some innovative concepts on satellite-based aerosols impact monitoring derived from the results obtained in Section 3.2.

The main applications developed starting from our scientific results (presented in Chapter 3) are described in Chapter 4 and the related results obtained are reported.

In Chapter 5 we briefly report the main activities performed during the PhD in the frame of national and international research project.

Finally we summarize the main achieved results and the further research activities currently envisaged in Chapter 6 (Conclusions).

2 RADIATIVE TRANSFER IN THE ATMOSPHERE

In this Chapter the theoretical background for the study of the radiative transfer of solar radiation into the atmosphere is described, starting from a general description of the Earth atmosphere (Section 2.1) and then describing the main characteristics of the solar radiation (Section 2.2) and its transmission through the atmosphere (Section 2.3). Finally the focus is put on the backscattered radiation observed by a Earth Observation (EO) satellite in different spectral bands (Section 2.4).

2.1 Earth atmosphere

Solar radiation is attenuated, before reaching the ground, by the Earth's atmosphere, i.e. the layer of gases and particles that surrounds the Earth. The atmosphere is modelled into a number of concentric spheres: troposphere, stratosphere, mesosphere, thermosphere and exosphere (going upward).

Atmospheric layer	Altitude range
Exosphere	600 – 10000 km
Thermosphere	85 – 600 km
Mesosphere	50 – 85 km
Stratosphere	16 - 50 km
Troposphere	0 – 16 km

Table 1: Altitude ranges of different atmospheric layers. Taken from (Seinfeld and Pandis 1998).

Density and pressure decrease continuously, while temperature has important variations in each of these layers (see Figure 1).

The atmosphere consists mainly of molecular nitrogen and molecular oxygen: in cloud-free conditions air contains about 78% nitrogen, 21% oxygen, 1% argon and 0.33% carbon dioxide by volume (Iqbal 1983).

In addition the Earth's atmosphere contains water vapour and also particulate matter such as dust, soot, water drops, ice crystals, which are highly variable in time and space. These particles suspended into the atmosphere are called atmospheric aerosols.

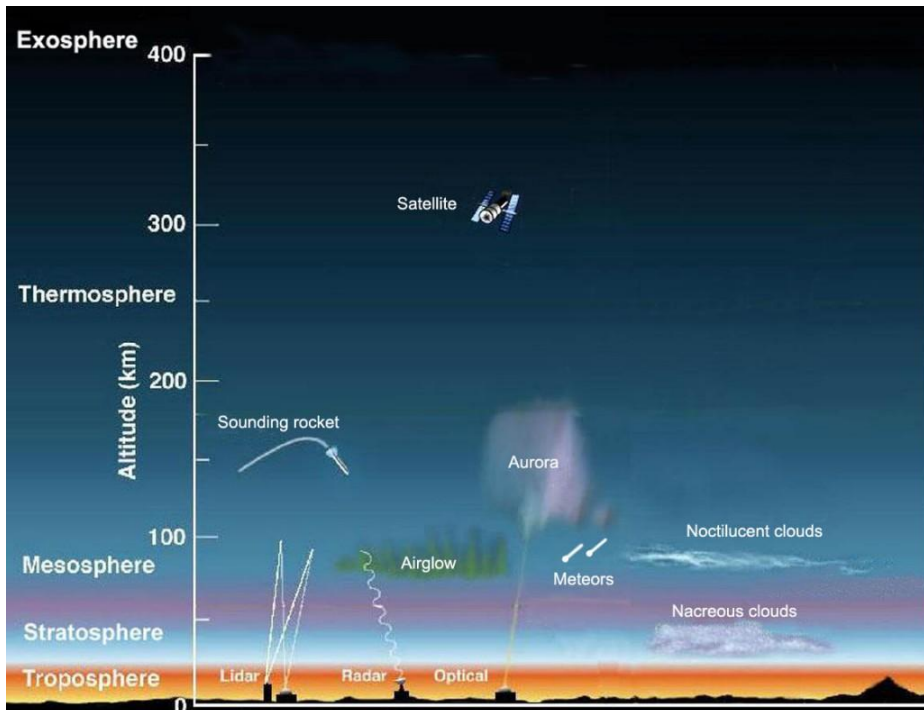


Figure 1: Scheme of the different atmosphere layers. Courtesy of NASA.

The transmittance of the atmosphere to solar radiation is usually determined by dividing the total atmosphere into three main groups: gaseous molecules, clouds and aerosols.

2.1.1 Gases

A clear-sky clean atmosphere (i.e. without clouds and aerosols) has a composition of gases that with geographical location, elevation and season. The concentration of some atmospheric gases such as carbon dioxide (CO_2), ozone (O_3), carbon monoxide (CO) and methane (CH_4) can be

highly variable. These gases are not homogeneously distributed, in space or in time, throughout the atmosphere.

A typical composition of the clean atmosphere has been realized in 1976 and it's called "U.S. Standard Atmosphere" (see Table 2).

Constituent gas	Content (% by volume)
Nitrogen (N ₂)	78.084
Oxygen (O ₂)	20.948
Argon (Ar)	0.934
Carbon dioxide (CO ₂)	0.333
Neon (Ne)	18.18 · 10 ⁻⁴
Helium (He)	5.24 · 10 ⁻⁴
Krypton (Kr)	1.14 · 10 ⁻⁴
Xenon (Xe)	0.089 · 10 ⁻⁴
Hydrogen (H)	0.5 · 10 ⁻⁴
Methane (CH ₄)	1.5 · 10 ⁻⁴
Nitrous oxide (N ₂ O)	0.27 · 10 ⁻⁴
Ozone (O ₃)	0 ÷ 12 · 10 ⁻⁴
Sulphur dioxide (SO ₂)	0.001 · 10 ⁻⁴
Nitrogen dioxide (NO ₂)	0.001 · 10 ⁻⁴
Ammonia (NH ₄)	0.004 · 10 ⁻⁴
Carbon monoxide (CO)	0.19 · 10 ⁻⁴
Water vapour (H ₂ O)	0 ÷ 004 · 10 ⁻⁴
Nitric oxide (NO)	0.0005 · 10 ⁻⁴
Hydrogen sulphide (H ₂ S)	0.00005 · 10 ⁻⁴

Nitric acid vapour	traces
--------------------	--------

Table 2: Normal composition of clean atmospheric air. Taken from (NOAA 1976).

Variations of the gaseous composition are a function of the industrial and agricultural activity of the place, its surroundings and the general dynamic nature of the atmosphere.

For example, solar ultraviolet radiation dissociates molecular oxygen (O_2) from about 90 km in altitude above. So as altitude increases, concentration of O_2 decreases and concentration of atomic oxygen (O) increases. Instead molecular nitrogen (N_2) is much more difficult to dissociate, so concentration of atomic nitrogen (N) remains very small also at high altitudes.

At very high altitudes (above 500 km) helium becomes one of the principal constituents and at about 2000 km the principal constituents becomes ionized helium, ionized hydrogen and electrons.

All molecules of air deplete solar energy by extinction, that is caused both by scattering and by absorption processes. Scattering happens at all wavelengths and is therefore called a continuum process. The absorption by air molecules of solar radiation takes place instead at selective wavelengths only (discrete process).

The most important gaseous absorbers in clean atmosphere are ozone, carbon dioxide, oxygen, oxides of nitrogen, nitrogen and hydrocarbons combinations.

For what concern the radiative transfer of ultraviolet (UV) solar radiation, the most important absorber is ozone. In the upper atmosphere, ozone is created mainly by ultraviolet solar radiation itself. Indeed the formation of ozone in the stratosphere results from the photolysis of molecular oxygen by solar UV radiation followed by the recombination of the oxygen atoms by O_2 (Zerefos and Bais 1996).

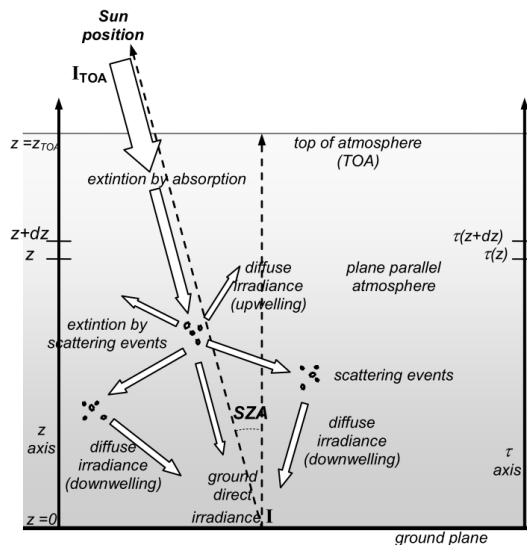


Figure 2: Scheme of the scattering and absorption processes in the atmosphere. Courtesy of Flyby.

On the ground instead ozone is formed through the decomposition of nitrogen oxide that enters the atmosphere from factory smoke and forest fires, for example.

Usually the mean density of ozone in a vertical column of air (called total columnar ozone density), that is dominated by the stratospheric ozone density, is measured in Dobson Units (DU). One DU refers to a layer of gas that would be 10 μm thick under standard temperature and pressure (i.e. 0°C temperature and 1 atm of pressure) and it's equivalent to $2.69 \cdot 10^{20}$ molecules/ m^2 (McNaught and Wilkinson 1997). A typical value of ozone density is 300 DU at European latitudes.

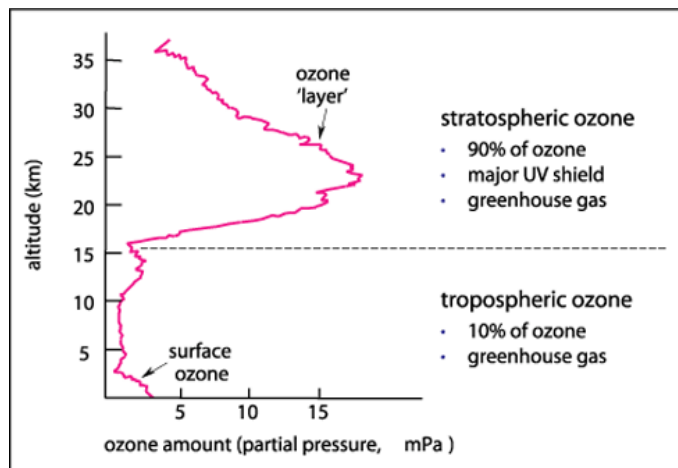


Figure 3: Vertical distribution of the ozone density in the atmosphere at mid-latitudes. Taken from (Manins 2001).

The amount of ozone increases with latitude and at high latitudes there are distinct seasonal variations: in each hemisphere it is maximum in the spring and minimum in the fall. Also the vertical distribution of ozone varies with latitude and seasons, but it is mainly concentrated between 10 km and 35 km of altitude (Figure 3).

Another important absorber of solar radiation in clean atmosphere is the water vapour. Water can exist in the atmosphere in three states: gas, liquid and ice. Water in gaseous state is called water vapour. The amount of water vapour present in the atmosphere can be usually defined in two ways: mixing ratio M_r and precipitable water w' (Iqbal 1983). The mixing ratio is the ratio of the mass of water vapour present to the mass of dry air present in a unit volume (unitless), while precipitable water is the total amount (depth) of water vapour in the zenith direction between the surface and the top of atmosphere (measured in meters unit).

AIRS TOTAL PRECIPITABLE WATER VAPOR (mm), May 2009

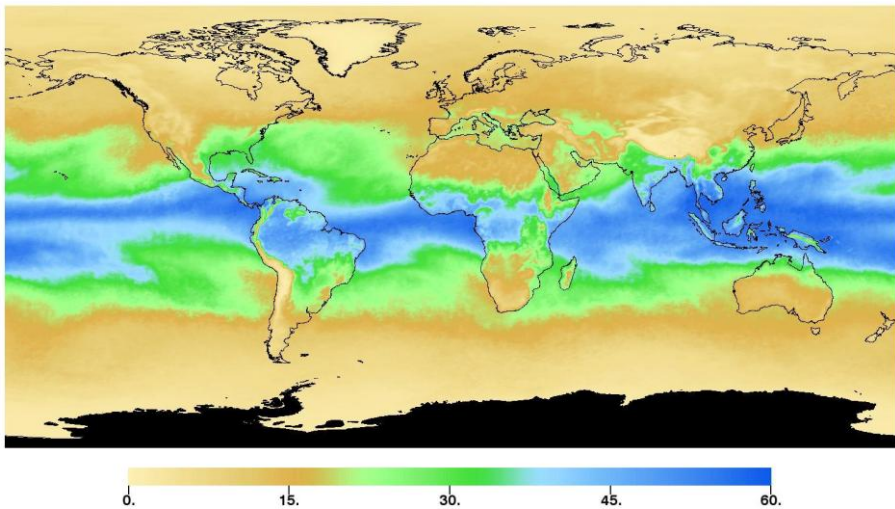


Figure 4: Total precipitable water retrieved during May 2009 by the Atmospheric Infrared Sounder (AIRS) on the Aqua satellite. Courtesy of NASA.

About one-half the precipitable water is concentrated in the first 2 km above sea level and above 12 km in altitude precipitable water is practically nonexistent. The amount of precipitable water varies with seasons. An extremely dry atmosphere may contain as little as 1 mm of precipitable water while a humid atmosphere may contain more than 40 mm (Figure 4).

2.1.2 Aerosols

An aerosol is a small solid or liquid particle that remains suspended in the air and follows the motion of the air within certain broad limits. Rain, snow and hail are not aerosol particles, while coagulated water vapour molecules that follow the motion of the air are considered aerosols.

In contrast to molecules of the permanent atmospheric gases (Section 2.1.1), suspended particles within the atmosphere display considerable diversity in volume, size, distribution, form and material composition.

The optical properties of atmospheric aerosols are determined by chemical composition, concentration, shape and internal liquid or solid structure. All these characteristics vary in space and time. At any time new particles can enter or leave the atmospheric volume under study. Depending on the aerosol type, we can identify among the particles different minerals, sulphates, nitrates, biological particles such as bacteria or pollen, organic particles, soot, sea salt, etc...



Figure 5: Aerial photo of aerosols over Los Angeles (USA). Courtesy of the Department of Physics of University of Oxford.

Aerosol particles are very tiny objects with sizes typically around 100 nm, therefore usually they are not visible to the naked eye. Nevertheless, aerosols considerably reduce visibility, influence climate, and can cause health problems in humans (Kokhanovsky 2008).

There are three main sources of particulate matter in the atmosphere:

- particles can enter the atmosphere from the surface (e.g. dust and sea salt);
- particles can be generated in atmosphere by gas-to-particle conversions;
- particles can enter the atmosphere from space (cosmic aerosols).

Surface-derived aerosols constitute the main mass of suspended particulate matter (with about 50% contribution on a global scale). Particles born in the atmosphere dominate the aerosol number concentration. Cosmic aerosols have little influence on the lower atmosphere while their contribution on atmospheric air properties is important in the higher atmospheric layers.

Water and ice aerosols form clouds: they will be treated in Section 2.1.3 .

The concentration of aerosols increased considerably due to industrial activities and transportation. In particular the contribution of the anthropogenic aerosols to the total aerosol mass is significant. This has several effects, such as health problems in highly populated areas and climate change. Globally the increment of aerosols leads to a global cooling in contrast to the global warming caused by the greenhouse effect.

Atmospheric aerosols are usually classified in terms of their origin and chemical composition (Jaenicke 1988):

- Sea-salt aerosols
- Aerosol formed in atmosphere from a gaseous phase
- Dust aerosols
- Biological aerosols

- Smoke from forest fires
- Volcanic aerosols
- Anthropogenic aerosols

Sea-salt aerosols originates from the oceanic surface due to wave breaking phenomena. The largest droplets fall close to their area of origin. Only the smallest aerosol particles with sizes from approximately 0.1 to 1 μm are of primary importance to the large scale atmospheric properties.

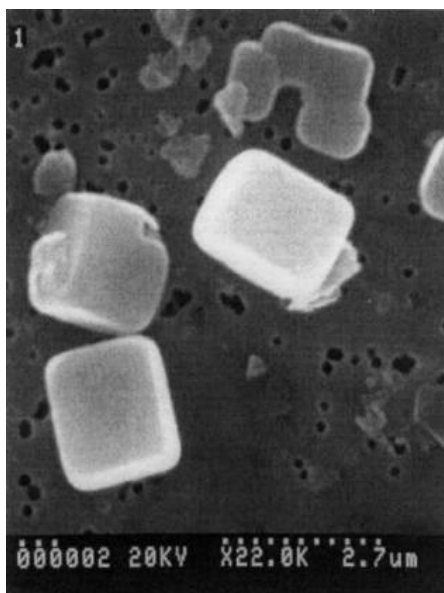


Figure 6: Scanning electron photographs of dried sea-salt aerosol particles collected at Mace Head in Ireland. The width of the picture is 2.7 μm . Taken from (Chamaillard, et al. 2003)

The shape of sea-salt aerosol particles depend on the humidity. Cubic particles are found at low humidity, due to the cubic structure of sodium chloride (NaCl) that mainly constitutes these particles. Given that NaCl easily dissolves in water, cubic forms transform into spherical shapes in high-humidity conditions. The typical numerical concentration of sea-salt aerosols is 250 cm^{-3} (Clarke, et al. 2003).

Dust aerosols originates from the land surface and are composed by solid particles. Most of them are not soluble in water (e.g. silicon), so changes in particle shapes are rare events as compared to sea-salt aerosols. However the mineral core can be covered by a water or ice shell in high-humidity conditions and this can modify the optical properties of these particles.

The numerical concentration of dust aerosols varies considerably depending in the aerosol mode. There are three main modes of aggregation for this type of aerosol (Hess, Koepke and Schult 1998) with three different concentrations: 269.5, 30.5 and 0.142 cm^{-3} .

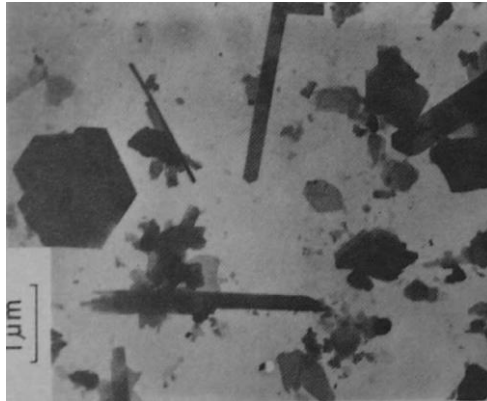


Figure 7: Scanning electron photographs of dust aerosol particles. Taken from (Klashnikova and Sokolik 2004).

The atmospheric borne aerosols, called secondary aerosols, originate in the atmosphere due to gas-to-particle conversion. This aerosol is composed of mostly sulphates and nitrates. Also various organic substances can make a large contribution in the total aerosol mass (Seinfeld and Pandis 1998). The generated particles are mostly of spherical shapes with a numerical concentration usually in the range $3000 \div 7000 \text{ cm}^{-3}$. This type of aerosol is found at all locations, so it plays an important role in the global aerosol budget.

Biological aerosols (bioaerosols) are characterized by the extreme particle size range and enormous heterogeneity. Biological material is present into the atmosphere in the form of pollens, fungal spores, bacteria, viruses, insects, fragments of plants and animals, etc..

The concentration of bioaerosols depends on season, location, height. This type of aerosols can occupy up to 30% of the total atmospheric volume at a given location (particularly in remote continental areas) and its concentration is at least three times smaller in remote marine environments. Nevertheless, biological aerosols produced inland can travel very long distances due to their low density.

The origins of smoke aerosols are fires of forest, grass or other types of fires. In spite of their relative small number (with respect to other types of aerosols), smoke aerosols have important local effects (such as human, animal and plant disease, reduction of visibility) and effects on global climate change due to generally larger values of light absorption by smoke aerosols (e.g. black carbon) as compared to other aerosol species. Smoke aerosols may lead to a number of spectacular optical atmospheric effects such as the blue Moon and Sun (van de Hulst 1957).

Combustion processes produce tremendous numbers of small particles with radii below $0.1 \mu\text{m}$. They also produce particles in the so-called accumulation mode ($0.1 - 1 \mu\text{m}$) and relatively giant particles with radii greater than $1 \mu\text{m}$. This means that particles of smoke can easily penetrate the respiratory system of humans leading to various health problems.

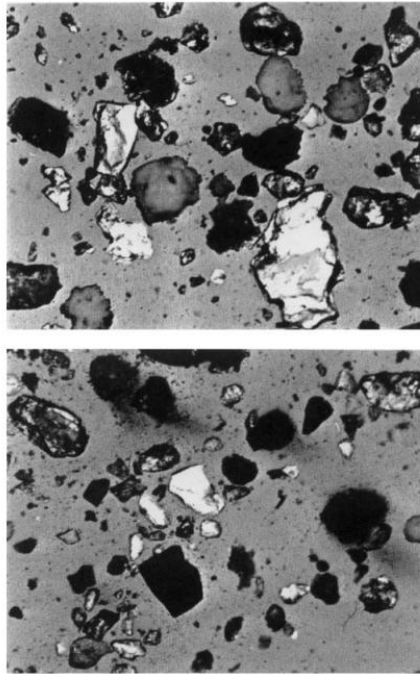


Figure 8: A street sample of aerosols submitted for examination as the result of a nuisance complaint. The magnification is equal to 40. The white snowballs are spheres of sodium carbonate from a nearby paper plant. In addition, the sample contains dried leaves, glass, glass fibers, paper fibers, cement dust, hematite, limestone, olivine, coal dust, soot, and burned wood. There is a great deal of quartz, covered wholly or partially by asphalt. Taken from (McCrone 1967).

Volcanic aerosols originate due to emissions of primary particles and gases (e.g. gaseous sulphur) by volcanic activity. Most of them are water-insoluble mineral particles, silicates and metallic oxides such as SiO_2 which remain mostly in the atmosphere.

Volcanic sources can be important for the sulphate aerosols burden changes in the upper troposphere, where might act as condensation nuclei for ice particles and thus represent a potential for a large indirect radiative forcing. Sulphate aerosols leads generally to a cooling of a climate system.

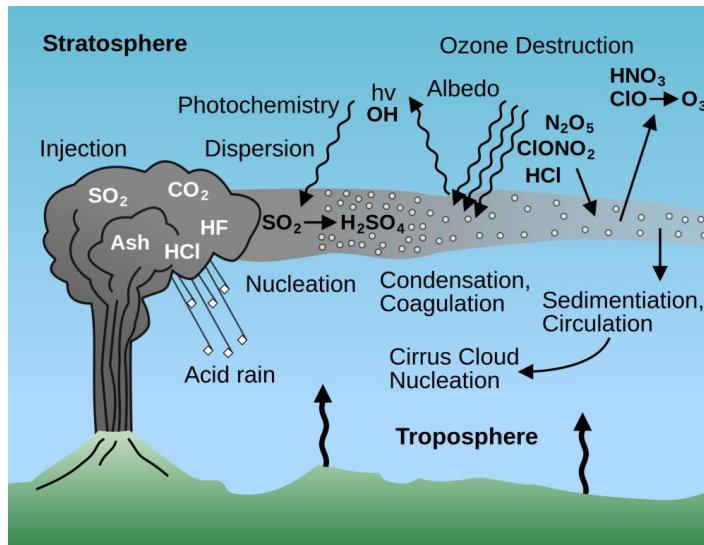


Figure 9: Effects of volcanic aerosols on the climate. Courtesy of United States Geological Survey.

Anthropogenic aerosols consist of both primary particles (e.g. diesel exhaust and dust) and secondary particles formed from gaseous anthropogenic emissions. They contribute about 10% of the total aerosol loading. The influence of this small but growing contribution on the climate system is not exactly known and should be assessed in future research.

Although the increased gaseous concentrations lead to larger atmospheric absorption and, therefore, to the warming of the atmospheric system, aerosol could increase or decrease the level of light reflection by the Earth-atmosphere system depending on the ground albedo (Meehl and Tebaldi 2004).

2.1.3 Clouds

Clouds are one of the most significant elements of the atmospheric system, playing several key roles (Seinfeld and Pandis 1998):

- clouds are a major factor in the Earth's radiation budget, reflecting sunlight back to space or blanketing the lower atmosphere and trapping infrared radiation emitted by the Earth's surface;
- clouds deliver water from the atmosphere to the Earth's surface as rain or snow and are thus a key step in the hydrologic cycle;
- clouds scavenge gaseous and particulate materials and return them to the surface;
- clouds provide a medium for aqueous-phase chemical reactions and production of secondary species;

- clouds significantly affect vertical transport in the atmosphere. Updrafts and downdrafts associated with clouds determine in a major way the vertical redistribution of trace species in the atmosphere.

The solar beam radiation (coming directly from the solar disk) is attenuated by the presence of clouds in its path as well as by the various elements of the cloudless atmosphere presented above. The depletion of the direct beam by the clouds depends on the type of clouds, their thickness and the number of layers (Iqbal 1983).

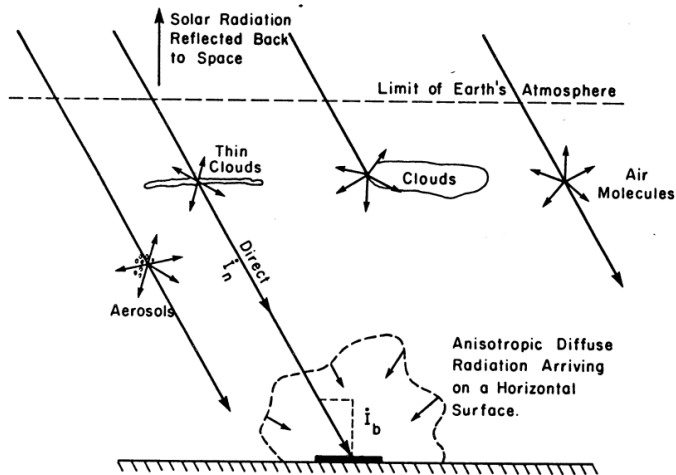


Figure 10: Radiation arriving on the ground under cloudy skies. Taken from (Iqbal 1983).

The diffuse component of the solar radiation has contributions from the interaction of solar radiation with both air molecules and aerosols, but also the interaction of beam solar radiation with the clouds (and cloud layers if the clouds are in layers) contributes to the diffuse solar radiation at incident at ground level. Further a portion of the beam and the diffuse solar radiation reaching the ground after the first pass through the atmosphere is reflected back to the sky, contributing to the multiply reflected irradiance that can increase further the diffuse irradiance at ground (see Figure 10).

Theoretical determination of direct, diffuse and directional intensity of diffuse irradiance is quite difficult, requiring data on the type and optical properties of clouds, clouds amount, thickness, position, number or layers, etc.. A common approach is to estimate the diffuse solar radiation from the solar global radiation and the global radiation in cloudless sky conditions (modelled).

2.2 Solar radiation

The radiant energy of the Sun is practically the only source of energy that influences atmospheric motions on the Earth and our climate.

The temperature of the Sun varies from one part to another. Radiation arriving outside the Earth's atmosphere is a complicated function of the convection and re-radiation processes in the outer layers of the Sun and other factors. Sun effective temperature is calculated by taking into account the solar radiation arriving at the Top of Atmosphere (TOA), its spectral distribution and the Stefan-Boltzmann equation in the following way (Iqbal 1983):

$$T = [(I_{sc} r_{se}^2) / (\sigma R_s^2)]^{1/4}$$

where

- I_{sc} is the solar constant, i.e. the rate of total solar energy at all wavelengths incident on a unit area exposed normally to sun rays at one astronomical unit, equal to 1367 W/m^2 ;
- r_{se} is the mean Sun-Earth distance, equal to $149\,597\,890 \text{ km}$;
- R_s is the mean radius of the solar disk, equal to $695\,980 \text{ km}$;
- σ is the Stefan-Boltzmann constant.

This relation yield an effective temperature of 5777 K , so we can approximate the solar radiation incident on the TOA as the radiation emitted by a black body with temperature 5777 K (Figure 11).

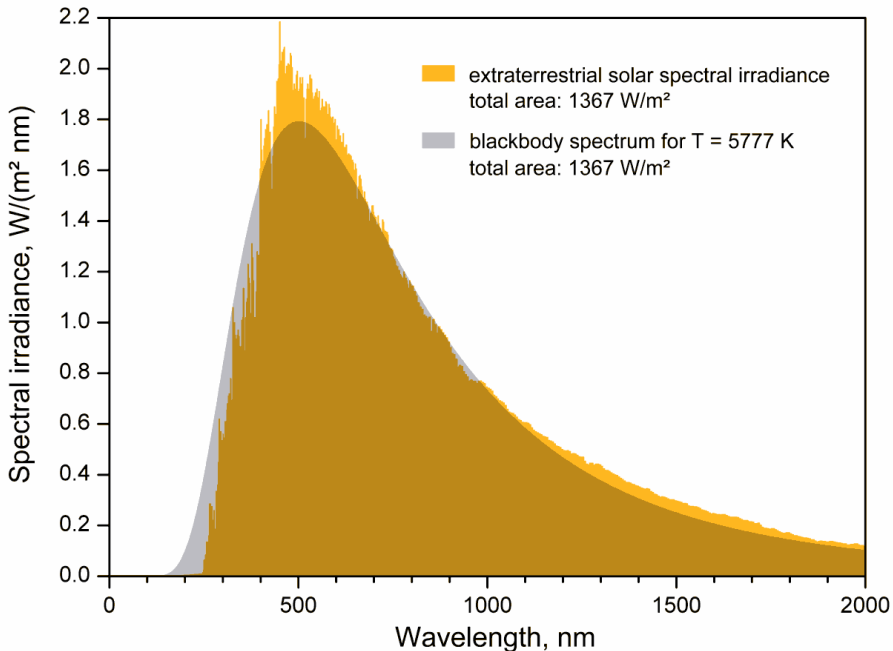


Figure 11: Comparison of the observed solar spectral irradiance at TOA and the spectral irradiance emitted by a black body with temperature of 5777 K . Derived from (Iqbal 1983).

The solar radiation at TOA is the basis of the radiative transfer modelling of solar radiation in the atmosphere.

2.2.1 Common definitions

In studying the propagation of light in the atmospheric medium, the variable of interest is the radiance (intensity, surface brightness). The radiance L_λ crossing a surface dA (see Figure 12) is defined as the mean power crossing the unit of surface normal to the direction defined by \hat{s} , for unit of wavelength λ , for unit of solid angle Ω around \hat{s} :

$$L_\lambda = \frac{dP}{d\lambda d\Omega dA \hat{n} \cdot \hat{s}}$$

Thus radiance units are $W m^{-2} sr^{-1} \mu m^{-1}$.

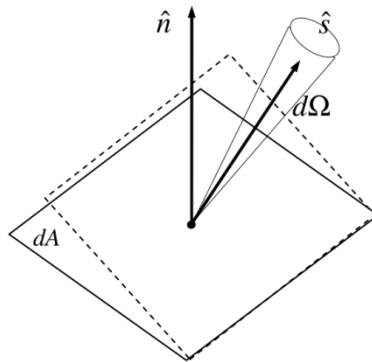


Figure 12: Scheme for the radiance definition. Courtesy of Flyby.

The irradiance (or flux) E_λ is defined by fixing a plane (i.e. the ground) and integrating in the semi-solid angle the radiance L_λ (see Figure 13):

$$E_\lambda = \int_{2\pi} \cos\theta L_\lambda d\Omega$$

Depending on the semi solid angle chosen for the integration, the considered irradiance is named downwelling (light incident on the upper surface from the overlying strata) or upwelling (i.e. ground or cloud reflected toward the sky).

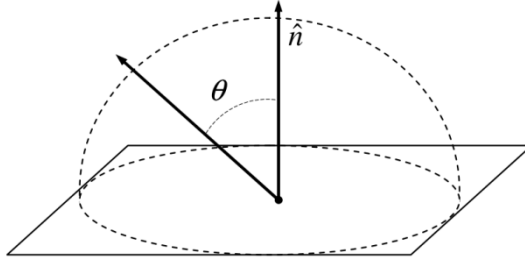


Figure 13: Scheme for the irradiance definition. Courtesy of Flyby.

In the latter case, considering the ground as a Lambertian diffuser (i.e. reflected radiance is distributed isotropically: $L_\lambda = L_{0\lambda}$), the irradiance takes the form of:

$$E_\lambda = \int_0^{\frac{\pi}{2}} \int_0^{2\pi} \cos\theta L_{0\lambda} \sin\theta d\theta d\varphi = \pi L_{0\lambda}$$

In case of a mono-directional radiance (represented by a Dirac Delta distribution):

$$L_\lambda = \delta(\Omega - \Omega_0) L_{0\lambda}$$

(i.e. extra atmospheric radiance from the Sun impinging at the top of the last atmospheric layer) the corresponding irradiance is:

$$E_\lambda = \int_{2\pi} \cos\theta \delta(\Omega - \Omega_0) L_{0\lambda} d\Omega = L_{0\lambda} \cos\theta_0$$

where θ_0 is the angle of incidence of the radiation on the plane.

Fixing a wavelength range $[\lambda_0, \lambda_1]$, we can define the spectrally integrated radiance for a fixed position in the space as:

$$L = \int_{\lambda_0}^{\lambda_1} L_\lambda d\lambda$$

and the spectrally integrated irradiance as:

$$E = \int_{\lambda_0}^{\lambda_1} E_\lambda d\lambda$$

2.2.2 Approximations

The source of radiance in Earth atmosphere in the wavelength of interest of this Thesis (UV, visible and near infrared) is the Sun. Thus, in the following equations the contribution due to thermal emission of ground and atmosphere itself is neglected.

The system is considered to be in steady state, that is the propagation of light in the medium is considered instantaneous, and the polarization of the photons is not considered, so we are dealing with radiation averaged over all polarizations, ignoring the dependence of the scattering on the polarization.

Following the literature (Kylling and Mayer 2005), in this work the Top Of Atmosphere (TOA) has been fixed at 120 km, a value that allows the atmosphere to be considered transparent in the wavelength of UV, visible and near infrared.

2.2.3 Components of the solar irradiance

The solar irradiance incident on a plane could be divided in different components (see Figure 14):

- the component arriving directly from the sun that hasn't been affected by scattering processes in the atmosphere, that is called beam (or direct) component;
- the component deriving from scattering processes of the solar radiation in the atmosphere, called diffuse component;
- the component due to the reflection from the surrounding ground, that is called reflected component.

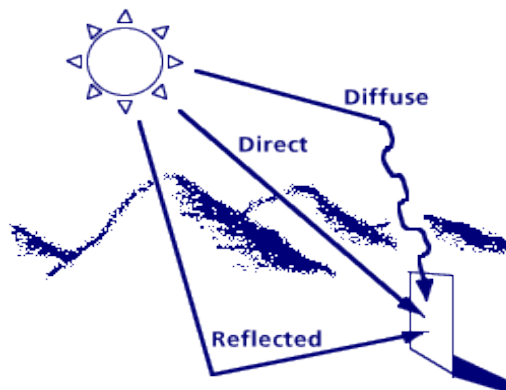


Figure 14: Different components of the solar irradiance incident on a plane. Courtesy of Flyby.

Given that the solar irradiance actually measured is the one incident orthogonally (i.e. the plan orthogonal component) with respect to the plane of measurement, the type of solar irradiance considered changes depending on the plane considered for its measurement (see Figure 15) :

- if the plane is horizontal with respect to the ground, the irradiance is called horizontal;
- if the plane is oriented normally with respect to incident solar rays (following sun's apparent motion), the irradiance is called normal ;
- if the plane is fixed in a tilted position (i.e. not horizontal), the irradiance is called tilted.

In this work we mainly consider two spectral ranges:

- ultraviolet spectral range (UV): 100 nm – 400 nm ;
- shortwave spectral range: 280 nm – 2500 nm ;

and the following solar radiation components:

- Global Horizontal Irradiance (GHI), i.e. the solar irradiance measured on a plane horizontal with respect to the ground ;
- Global Tilted Irradiance (GTI), i.e. the solar irradiance incident on a fixed tilted plane (e.g. a solar photovoltaic cell) ;
- Global Normal Irradiance (GNI), i.e. the solar irradiance incident on a plane normal to the sun rays (that is usually the plane where the skin absorbs the maximum dose of UV radiation) .

Every "global" quantity is sum of the related beam, diffuse and reflected components of the solar radiation, that is:

- $GHI = BHI + DHI$ (there is no ground reflected component incident on a horizontal plane) ;
- $GTI = BTI + DTI + RTI$;
- $GNI = BNI + DNI + RNI$.

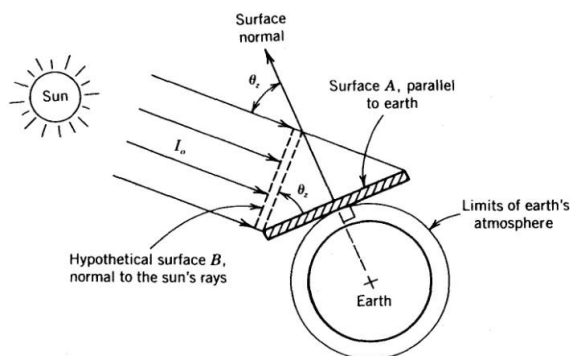


Figure 15: Scheme of a plane normal to sun rays (surface B) and of an horizontal plane (surface A). Courtesy of Flyby.

2.2.4 Solar shortwave radiation

The spectral range of the solar radiation incident on Earth's atmosphere is commonly called "shortwave", in contrast to the "longwave" radiation emitted by Earth and the atmosphere that has spectral range from 4 μm to 25 μm (thermal infrared).

Shortwave radiation ranges from 100 nm (ultraviolet) to 3000 nm (infrared). The solar shortwave radiation it's detectable only during daylight and its maximum occurs at 480 nm (visible). The typical spectrum of the solar shortwave radiation at TOA and at surface is shown in Figure 16.

In this work we will consider solar shortwave radiation only (both from ground and from EO satellite point of views), that is composed by (IARC 1992):

- UV radiation (100 nm – 400 nm);
- visible radiation (400 nm – 780 nm);
- shortwave infrared radiation (780 nm – 3000 nm, i.e. IRA and IRB).

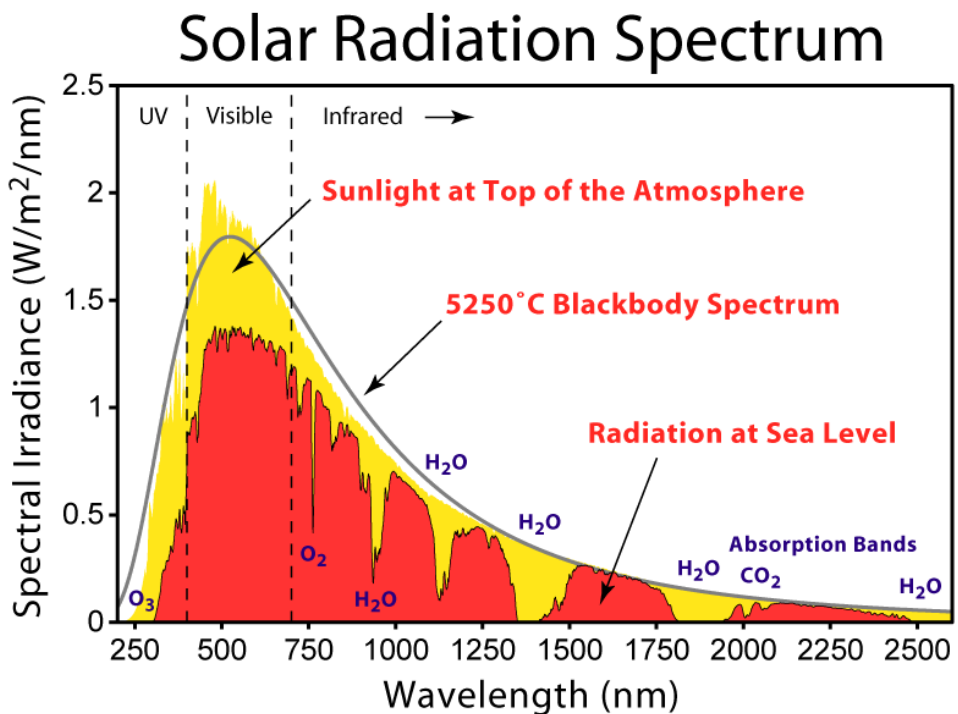


Figure 16: Spectrum of the solar shortwave radiation at ground level, reported also with the spectrum at TOA level and the sun's blackbody spectrum. Courtesy of the American Society for Testing and Materials (ASTM).

2.2.5 Solar UV radiation

The ultraviolet (UV) wavelength range considered in this work is divided in UV-A (between 315 nm and 400 nm) and the UV-B (between 280 nm and 315 nm). The other part of UV radiation coming from the sun, i.e the UV-C (between 100 nm and 280 nm), is completely blocked by the atmosphere and typically doesn't arrive at ground level.

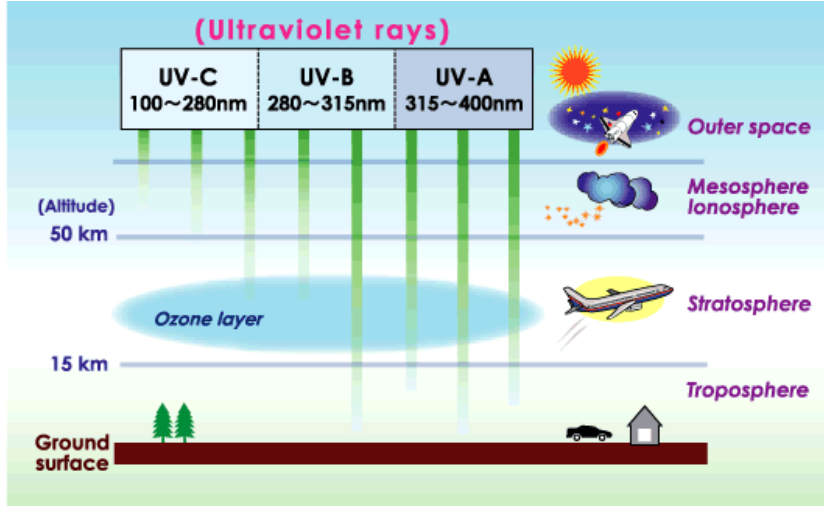


Figure 17: Scheme of the propagation of solar ultraviolet radiation into the atmosphere. Courtesy of the National Institute for Environmental Studies of Japan.

To estimate the danger for the human skin for the UV radiation, the UV-Index (UVI) estimative index will be used.

The UVI is defined as the integral on the wavelength of the UV spectral irradiance weighted with the Erythemal (skin burn) Action Spectrum (EAS) $f_{ery}(\lambda)$ as defined in (McKinlay and Diffey 1987). The EAS is a function that estimates the seriousness of UV exposure with respect to the wavelength and applying a scaling factor of $25mW$:

$$UVI = \frac{1}{25mW} \int_{\lambda=280}^{\lambda=400} E_{\lambda} \cdot f_{ery}(\lambda) d\lambda$$

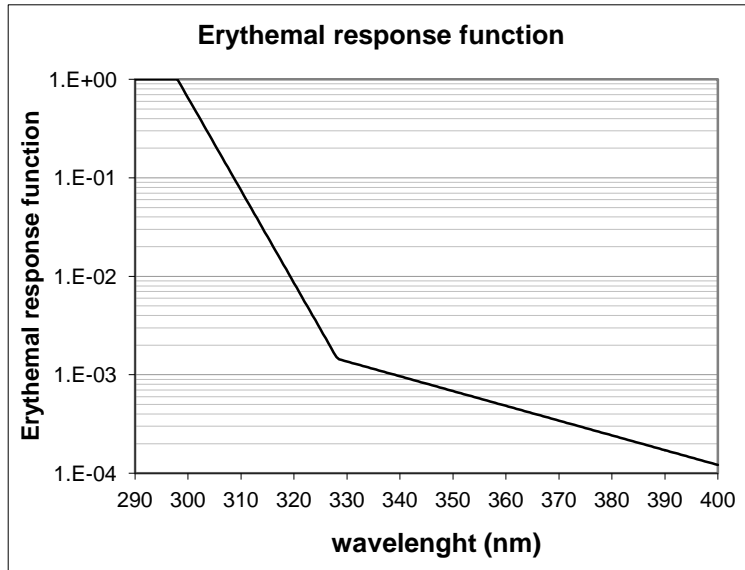


Figure 18: Erythema Action Spectrum (weight function) for converting UV spectral irradiance into the UV-Index. Taken from (McKinlay and Diffey 1987).

2.3 Radiative transfer

When solar radiation enters the Earth's atmosphere, a part of the incident energy is removed by scattering and a part by absorption. Both these processes are part of the so-called extinction of solar radiation and considerably modify the spectral energy passing through the atmosphere (Iqbal 1983).

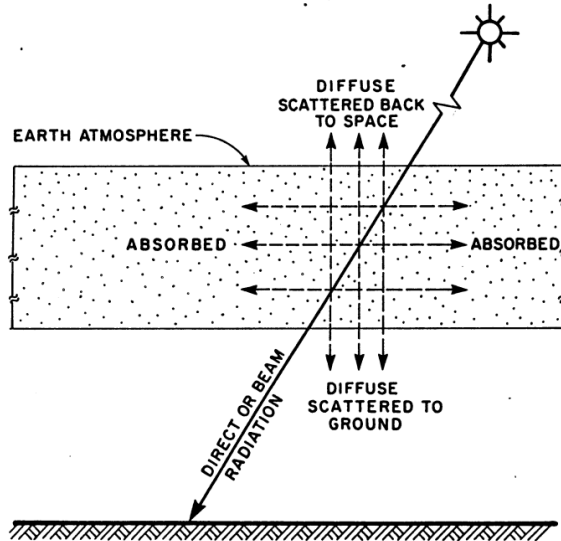


Figure 19: Distribution of direct (beam), diffuse and absorbed solar radiation. Taken from (Iqbal 1983).

Considering a beam of parallel monochromatic radiation I_λ (with wavelength λ) entering a homogenous medium, the flux emerging from the medium is reduced by a certain quantity dI_λ after traversing a distance dz . The resulting flux is then $(I_\lambda - dI_\lambda)$, as shown in Figure 20. The amount attenuated in passing through the medium can be evaluated by the so-called Lambert-Beer's law. According to this law, the attenuation of light through a medium is proportional to the distance transverse in the medium and to the local flux of radiation as follows:

$$I_\lambda - dI_\lambda = I_\lambda e^{(-k_\lambda dz)}$$

where k_λ is the monochromatic extinction or attenuation coefficient and dz is the optical path length.

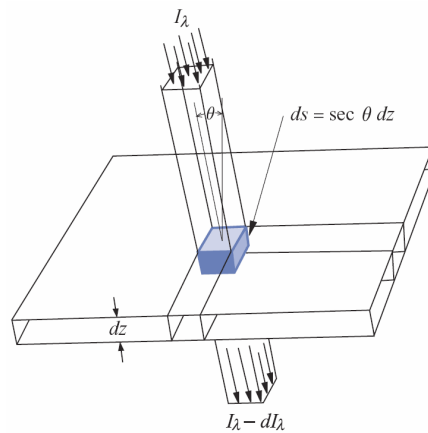


Figure 20: Geometry of a monochromatic beam of radiation passing through a thin layer of atmosphere. Courtesy of the Department of Geology of the University of California at Santa Barbara (USA).

This is the starting point for the study of the radiative transfer in the atmosphere, that is a complex problem affected by a lot of different scattering and absorption processes highly variable in space and time. As an example, scattering of solar radiation by atmospheric particles occurs in different ways depending on the dimension of the particle and the wavelength, as shown in Figure 21.

Radiative transfer could be modelled by complex models called Radiative Transfer Models (RTM) that takes into account typical compositions of the atmosphere. Atmosphere is divided a lot of layers and the RTM models the incoming and the outgoing radiation for each layer from TOA to surface.

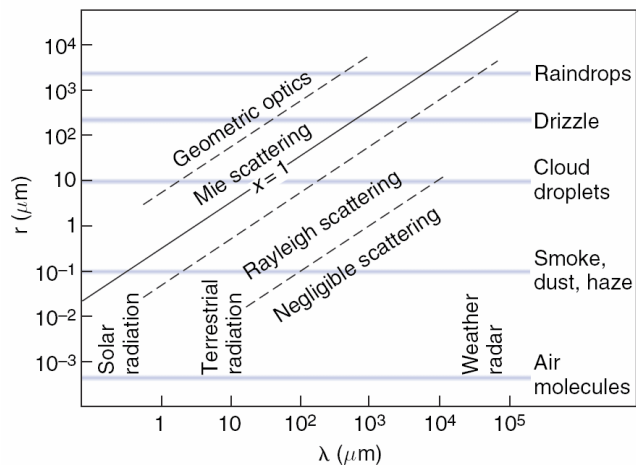


Figure 21: Atmospheric scattering processes occurring at different radiation wavelengths for different molecules radii. Courtesy of the Department of Geology of the University of California at Santa Barbara (USA).

2.4 Satellite multispectral optical imagery

In this Thesis we consider the multispectral optical images provided by an optical sensor on the Meteosat Second Generation (MSG) Earth Observation (EO) geostationary satellite.

Meteosat Second Generation (MSG) is a meteorological satellite with a radiometer, the Spinning Enhanced Visible and InfraRed Imager (SEVIRI), that delivers daylight radiance images plus thermal information with a spatial resolution at sub-satellite point (located at 0° in latitude and 0° in longitude, above the gulf of Guinea) of 3 km.

Channel ID	Absorption Band Channel Type	Nominal Centre Wavelength (µm)	Spectral Bandwidth (µm)	Spectral Bandwidth As % of energy actually detected within spectral band
HRV	Visible High Resolution	Nominally 0.75	0.6 to 0.9	Precise spectral characteristics not critical
VIS 0.6	VNIR Core Imager	0.635	0.56 to 0.71	98.0 %
VIS 0.8	VNIR Core Imager	0.81	0.74 to 0.88	99.0 %
IR 1.6	VNIR Core Imager	1.64	1.50 to 1.78	99.0 %
IR 3.9	IR / Window Core Imager	3.92	3.48 to 4.36	98.6 % ⁽¹⁾
IR 6.2	Water Vapour Core Imager	6.25	5.35 to 7.15	99.0 %
IR 7.3	Water Vapour Pseudo-Sounding	7.35	6.85 to 7.85	98.0 %
IR 8.7	IR / Window Core Imager	8.70	8.30 to 9.10	98.0 %
IR 9.7	IR / Ozone Pseudo-Sounding	9.66	9.38 to 9.94	99.0 %
IR 10.8	IR / Window Core Imager	10.80	9.80 to 11.80	98.0 %
IR 12.0	IR / Window Core Imager	12.00	11.00 to 13.00	98.0 %
IR 13.4	IR / Carbon Dioxide Pseudo-Sounding	13.40	12.40 to 14.40	96.0 %

Figure 22: Characteristics of then SEVIRI multispectral channels. Taken from(EUMETSAT 2005).

A description of SEVIRI bands is reported in Figure 22, Figure 23 and Figure 24, showing also a diagram of the atmospheric transmittance (due to molecular scattering, aerosol scattering and total contribution of absorption plus scattering).

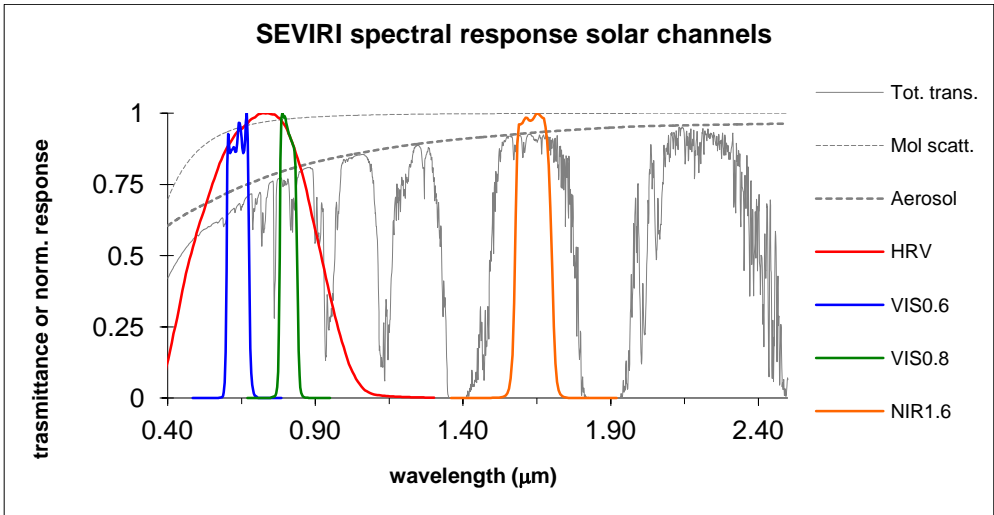


Figure 23: SEVIRI solar channels spectral response, together with typical atmospheric transmittance spectra. Taken from www.eumetsat.org.

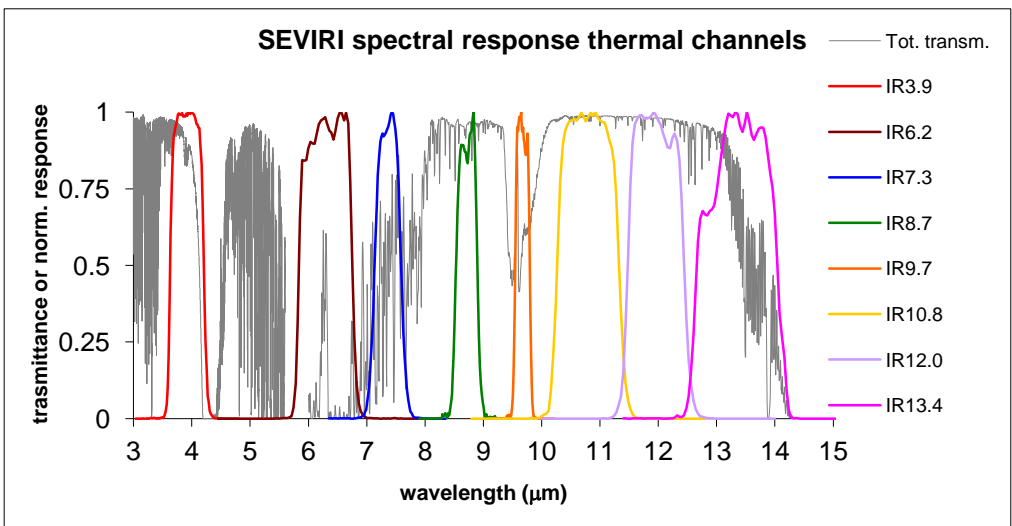


Figure 24: SEVIRI thermal channels spectral response, together with typical atmospheric transmittance spectra. Taken from www.eumetsat.org.

The spatial coverage of the provided images is comprised from -66° to 66° both in latitude and longitude (Figure 25), while the temporal resolution 15 minutes.

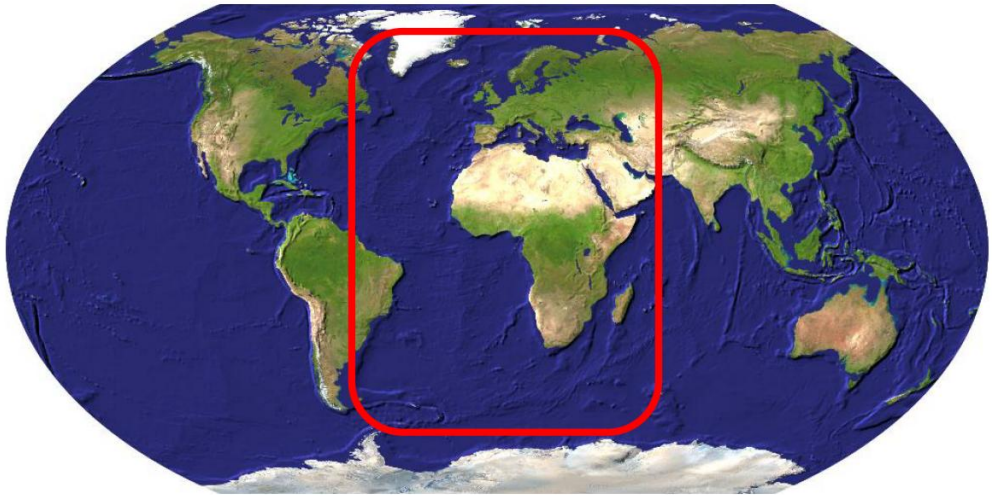


Figure 25: Spatial coverage of the SEVIRI sensor on the MSG satellite. Courtesy of Flyby.

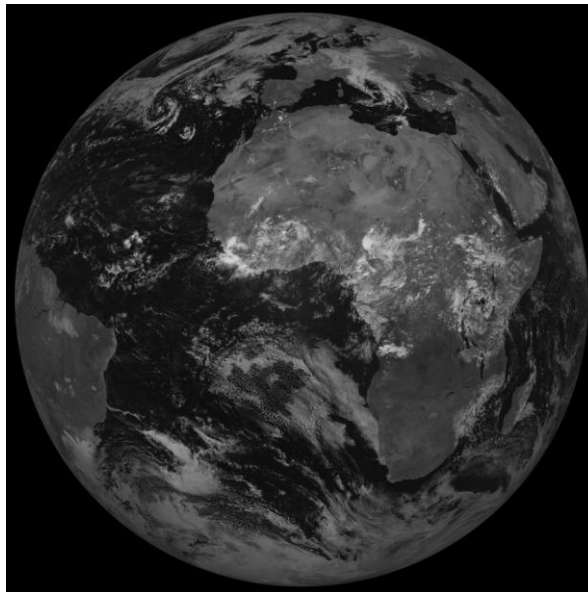


Figure 26: An example of the full-disk image observed by the SEVIRI sensor on the MSG satellite in the $0.8 \mu\text{m}$ visible channel on September 2nd 2014 at 12.00 UTC. Source data are provided by EUMETSAT.

2.5 Solar radiation measurements at ground

We designed and installed, with the financial support of Flyby S.r.l., a solar radiation measurement station on Flyby's roof at Livorno (Italy). The installation site is in plain, near to the sea (about 200 meters from the coast) and with no relevant obstacles in the surroundings (such as mountains or high buildings).

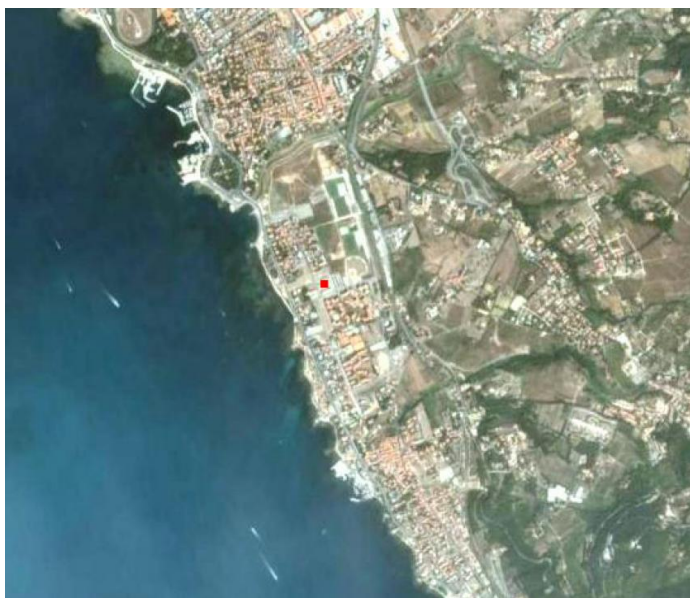


Figure 27: The solar measurements site at Flyby (Livorno, Italy), represented by a red square on the image. The geographical coordinates are 43.506°N, 10.322°E . Image has been retrieved from Google Earth service (<http://earth.google.it>).

The scheme of the measurement station is shown in Figure 28, while in Figure 29 we reported a photo of the installation phase and in Figure 30 a photo of the complete solar measurement station is shown.

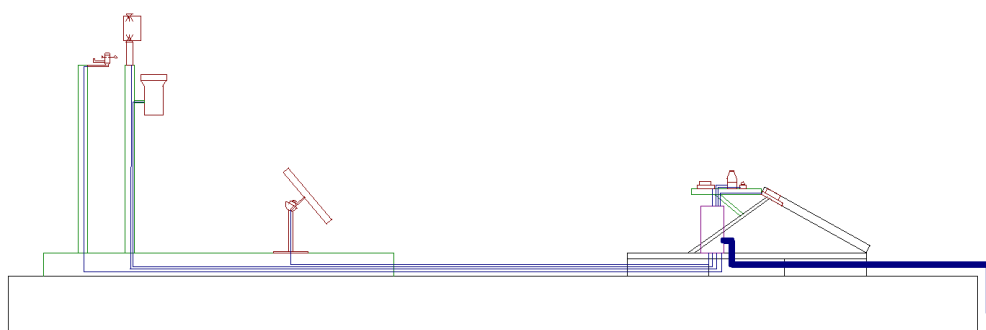


Figure 28: Scheme of the solar measurement station at Flyby (Livorno, Italy).



Figure 29: Photo during the installation of the solar measurement station at Flyby (Livorno, Italy). The Author is setting the position of one of the UV sensors.



Figure 30: Photo of the complete solar measurement station at Flyby (Livorno, Italy).

The following instruments have been installed:

- three UV sensors provided by Davis Instruments, that constantly measure the UV index with 1 minute intervals (installed at different tilt angles);

- one first class pyranometer and one second class pyranometer provided by Delta Ohm, that constantly measure the solar shortwave irradiance with 1 minute intervals (both installed in horizontal position)
- one ultrasonic anemometer provided by Delta Ohm (for temperature, pressure and wind measurements).

In addition to this instrumentation, there is also a small photovoltaic plant (3 PV cells with a total nominal power production of 0.5 kW) on the same roof that is constantly monitored by Flyby S.r.l. : the AC power produced is measured every 15 minutes.

For the scope of this Thesis we take into account only the measurements provided by one of the UV sensors (the one installed in horizontal position) and the AC power produced by the PV plant. Some technical details about the UV sensor used have been reported in Figure 31 and Figure 32 (as provided by sensor manufacturer).

General

Operating Temperature	-40° to +150° F (-40° to +65° C)
Storage Temperature	-50° to +158°F (-45° to +70°C)
Transducer	Semiconductor photodiode
Spectral Response	280 to 360 nm (Erythema Action Spectrum)
Cosine Response	±4% of reading (0° to 65° incident angle); ±9% of reading (65° to 85° incident angle)
Supplied Cable Length	2' (0.6 m)
Cable Type	4-conductor, 26 AWG
Connector	Modular RJ-11
I/O Specs	
Green wire	Output (0 to 2.5VDC); 150 mV per UV Index, 364 mV per MED/hour
Black & Red wires	Ground
Yellow wire	+3V ±10%, 2.4 mA
Housing Material	UV-resistant ABS plastic
Dimensions (length x width x height)	2" x 2.75" x 2.25" (51 mm x 70 mm x 57 mm)
Weight	0.5 lbs. (226 g)

Sensor Output

Ultra Violet (UV) Radiation Dose	
Resolution and Units	0.1 MEDs to 19.9 MEDs; 1 MED above 19.9 MEDS
Range	0 to 199 MEDs
Accuracy	±5% of daily total
Drift	up to ±2% per year
Update Interval	50 seconds to 1 minute (5 minutes when dark)
Ultra Violet (UV) Radiation Index	
Resolution and Units	0.1 Index
Range	0 to 16 Index
Accuracy	±5% of full scale (Reference: Yankee UVB-1 at UV Index of 10 [extremely high]) plus 0.5 UV Index per 100' (30 m) of additional cable
Cosine Response	±4% (0° to 65° incident angle); 9% (65° to 85° incident angle)

Figure 31: Technical characteristics of the UV sensor provided by Davis Instruments. Taken from (Davis Instruments 2006).

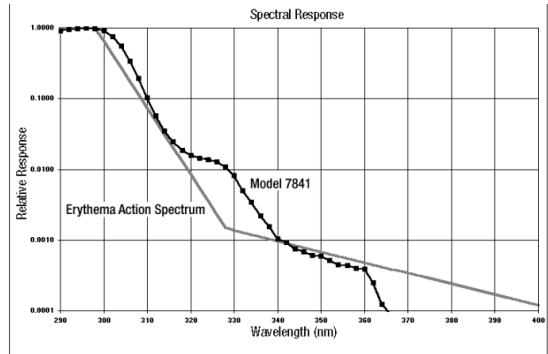
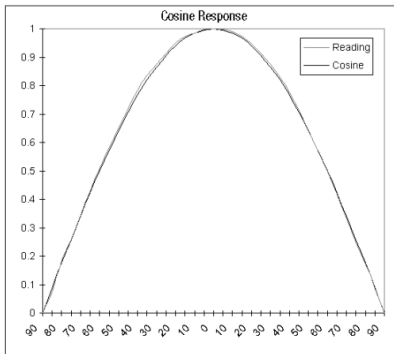


Figure 32: Cosine and spectral responses of the UV sensor provided by Davis Instruments. Taken from (Davis Instruments 2006).



Figure 33: Photo of the Davis Instruments UV Sensor model 7841. Taken from www.davisnet.com.

The other measurements will be useful for future research activities and for the further development of the methodologies presented in this Thesis.

3 AEROSOL IMPACT ON RADIATIVE TRANSFER

In this Chapter the main scientific results obtained on aerosols impact detection are presented. In particular in Section 3.1 we describe the methodology used to identify clouds (and model their impact on radiative transfer) starting from satellite visible imagery. Then in Section 3.2 we take into account cloudless (or clear-sky) weather conditions (identified also exploiting the methodology presented in Section 3.1), analyzing:

- the simulations of cloudless solar radiation at ground level and at satellite sensor in different spectral bands (exploiting a RTM);
- the solar irradiance actually observed both at ground and by the SEVIRI sensor on MSG satellite for the same site and date.

From the comparison of these simulated and observed quantities we derived some innovative concepts for the satellite-based near real-time assessment of aerosols impact on solar radiation (Section 3.2.3) that could increase the accuracy of related applications (such as in the solar energy and in the healthcare fields, as explained in Chapter 4).

3.1 Satellite near real-time monitoring of cloudiness

Satellite visible imagery can be exploited to detect clouds, that are very responsive in the visible part of the spectrum (i.e. cloud have a high reflectance of incident visible radiation). This idea is the basis of a method for satellite-based assessment of clouds impact on solar radiation at ground described in (Cano, et al. 1986) . We started from this method, called “Heliosat”, for the development of a satellite-based monitoring of solar radiation at ground and its related applications (described in Chapter 4).

In addition to this, the Heliosat method can be exploited to identify in near real-time cloudless-sky conditions, allowing a further analysis of aerosols impact in this conditions (Section 3.2).

Basically Heliosat method can be used to determine in near real-time an index related to the amount of cloudiness (called “cloud index”). This index can be further exploited to determine the solar radiation incident at ground by taking into account modelled values of cloudless solar radiation (the so-called “clear-sky model”).

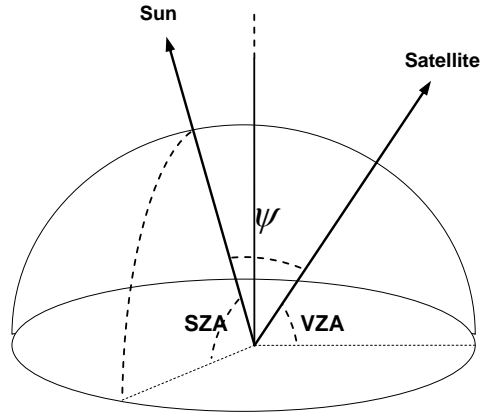


Figure 34: Scheme of a EO satellite acquisition geometry. Courtesy of Flyby.

For each single pixel of the satellite image the radiance contribution can be calculated for the MSG visible band:

$$r_{atm} = I_o \frac{3(1 + \cos^2(\psi))}{16\pi} \frac{\cos(SZA)}{\cos(\nu) + \cos(SZA)} \left(1 - \exp \left[-\tau \left(\frac{1}{\cos(SZA)} + \frac{1}{\cos(\nu)} \right) \right] \right)$$

with:

ν : observer - satellite angle with the normal direction to the ground;

ψ : Sun-satellite relative angle;

I_o is the solar constant (1367 W m^{-2});

τ is the equivalent optical depth in the MSG visible band.

The apparent albedo ρ is thus calculated by (Dagestad and Olseth 2005):

$$\rho = \frac{\pi R}{I_{HRV} \cos(SZA)} - \frac{\pi r_{atm}}{I_0 \cos(SZA)},$$

being:

R the calibrated at sensor radiance in the visible band;

I_{HRV} : the TOA irradiance in the visible band.

If we consider a cloudless atmosphere, the apparent albedo ρ is equal to the ground albedo ρ_g , (clear sky albedo).

Then ρ_g can be written as:

$$\rho_g(\psi) = \rho_{g_0} \rho_{shape}(\psi)$$

being ρ_{g_0} the reflectance for $\psi = 0$ and ρ_{shape} a shape function for taking into account any non-Lambertian behaviour of the ground surface reflection, shading due to the ground structure and contributions of multiple scattering events and molecular and aerosol absorption.

ρ_{shape} is empirically modelled as (Dagestad and Olseth 2005):

$$\rho_{shape}(\psi) = 1 - 0.59\psi + 0.11\psi^2 + 0.05\psi^3$$

From the ground albedo for a clear sky situation, a cloud index n is then calculated for each pixel of the image as (Rigollier, Bauer and Wald 2000):

$$n = \frac{\rho - \rho_g}{\rho_c - \rho_g}$$

with:

ρ_g : albedo calculated for cloud free case;

ρ_c : albedo in the total cloud cover case (value of 0.81 is chosen).

3.2 Aerosols impact on cloudless-sky solar radiation

In cloudless weather conditions, solar radiation is attenuated by the other constituents of the atmosphere. In particular one of the most variable (but relevant) contribution to this attenuation is due to aerosols extinction of solar radiation.

As schematically shown in Figure 35, aerosols play a role similar to clouds in cloudless-sky conditions. In spite of their low reflectance of visible light with respect to clouds (indeed they are relatively less visible to human eye), their impact on the radiative transfer of solar shortwave radiation is relevant and can be observed both at ground (impact on the solar shortwave radiation incident at ground) and by a satellite optical sensor (solar backscattered radiation at satellite level).

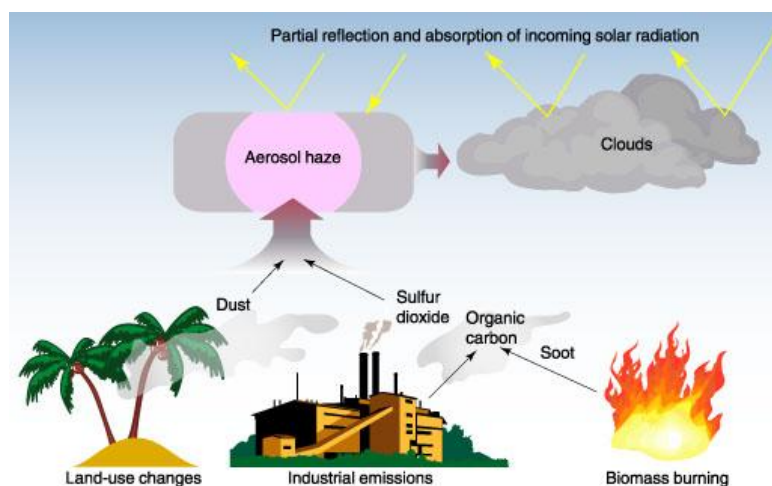


Figure 35: Aerosols and clouds interactions with incident solar radiation. Courtesy of the Lawrence Livermore National Laboratory (USA).

Starting from the results of (Oumbe, et al. 2014) on the decoupling of the effects of clear atmosphere and clouds on shortwave solar irradiance, we supposed that a similar approach could be adopted in cloudless-sky conditions taking the aerosol layer as a “clouds-like” layer affecting the solar radiative transfer.

In particular we tried to exploit solar radiation measurement at ground, backscattered radiation measurements at satellite level and the RTM simulation of both in order to find a possible correlation between aerosols impact on solar radiation at ground and satellite observations.

We selected two days (close in time) at the beginning of September 2014 for the weather observed in Livorno (Italy):

- September 2nd 2014, a cloudless-sky day with very low aerosols presence due to a heavy rain during the preceding night ;
- September 6th 2014, a cloudless-sky day with high aerosols presence due to a total absence of rain and low windiness from September 2nd .

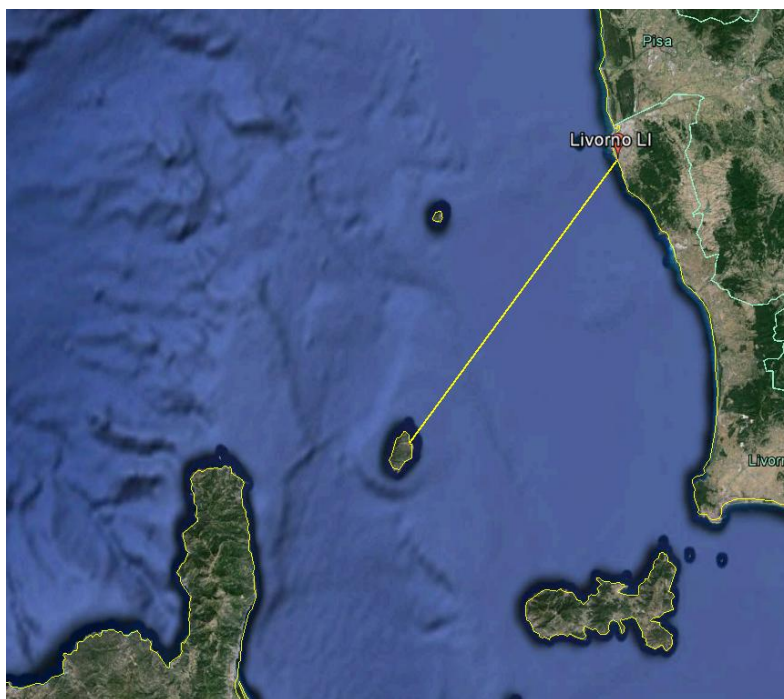


Figure 36: Line of sight from Livorno to the island of Capraia. Image taken from the Google Earth service.

In this case the high difference in aerosols presence between the two days could be also detected directly observing the horizon by naked eye. Indeed we observed an evident difference from the roof of Flyby (solar radiation measurements site): in the first day (September 2nd) the island of Capraia (about 65 km from Livorno in line of sight, see Figure 36) was clearly detectable on the horizon (see Figure 37 and Figure 38), while in the second day (September 6th) it was not (see Figure 39 and Figure 40).



Figure 37: Photo of the solar radiation measurements station and the horizon seen from the roof of Flyby (Livorno, Italy) on September 2nd 2014.



Figure 38: Photo of the horizon seen from the roof of Flyby (Livorno, Italy) on September 2nd 2014. The Capraia island can be detected on the horizon.



Figure 39: Photo of the solar radiation measurements station and the horizon seen from the roof of Flyby (Livorno, Italy) on September 6th 2014.



Figure 40: Photo of the horizon seen from the roof of Flyby (Livorno, Italy) on September 6th 2014. The Capraia island cannot be detected on the horizon.

So we decided to compare observed (Section 3.2.1) and simulated (Section 3.2.2) quantities for these two days in order to possibly find evidences of the different aerosols presence in the atmosphere.

3.2.1 Observations

3.2.1.1 At surface

We analyzed the following quantities at surface (measured with the solar measurements station described in Section 2.5) in order to emphasize aerosols impact for the applications in solar energy and healthcare sectors (Chapter 4):

- AC power produced by the photovoltaic plant (nominal power production of 0.5 kW);
- UV index on the horizontal plane, measured by the UV sensor provided by Davis Instruments.

For both these types of measurement we observed aerosols impact: indeed both UV index and AC power are lower on September 6th due to higher aerosols presence in the atmosphere (as shown in Section 3.2.1.1).

The comparison of the AC power produced by the PV plant on September 2nd and September 6th (sampled every 15 minutes) is reported in Figure 41. The mean relative difference (considering only non-zero values) is 10.24 % (corresponding to a mean difference of 16.51 W), while the relative difference at noon is 6.06 % (corresponding to 20 W).

Instead the comparison of the horizontal UV index measured on September 2nd and September 6th (sampled every 1 minute) is reported in Figure 42. In this case the mean relative difference (considering only non-zero values) is 11.28 % (corresponding to a mean difference of 0.32 UV index), while the relative difference at noon is 8.20 % (corresponding to 0.5 UV index).

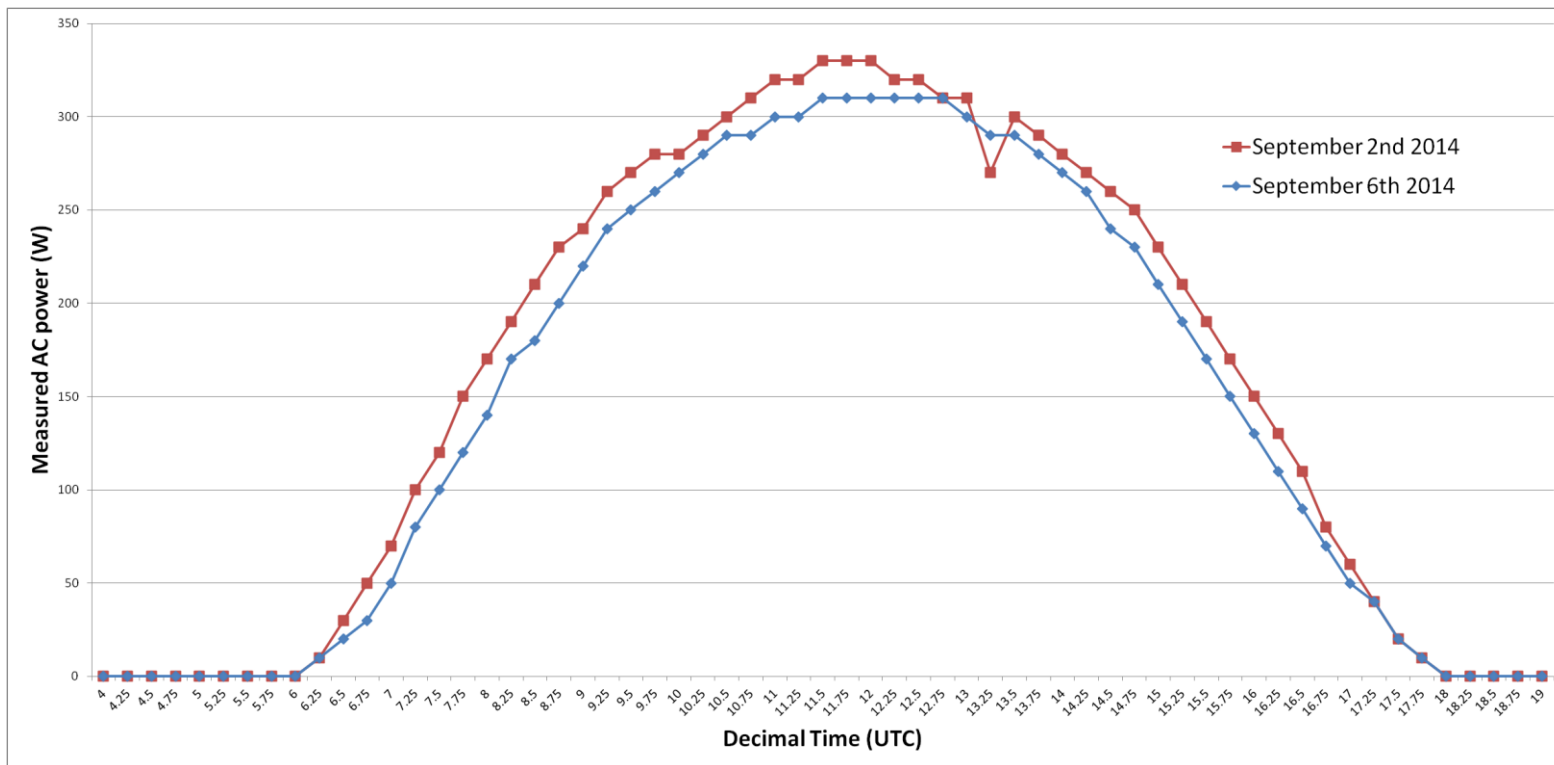


Figure 41: Comparison of the AC power produced by the photovoltaic plant at Flyby (Livorno, Italy) on September 2nd and on September 6th 2014. Data have been sampled every 15 minutes from 4.00 UTC to 19.00 UTC. Source data are provided by Flyby.

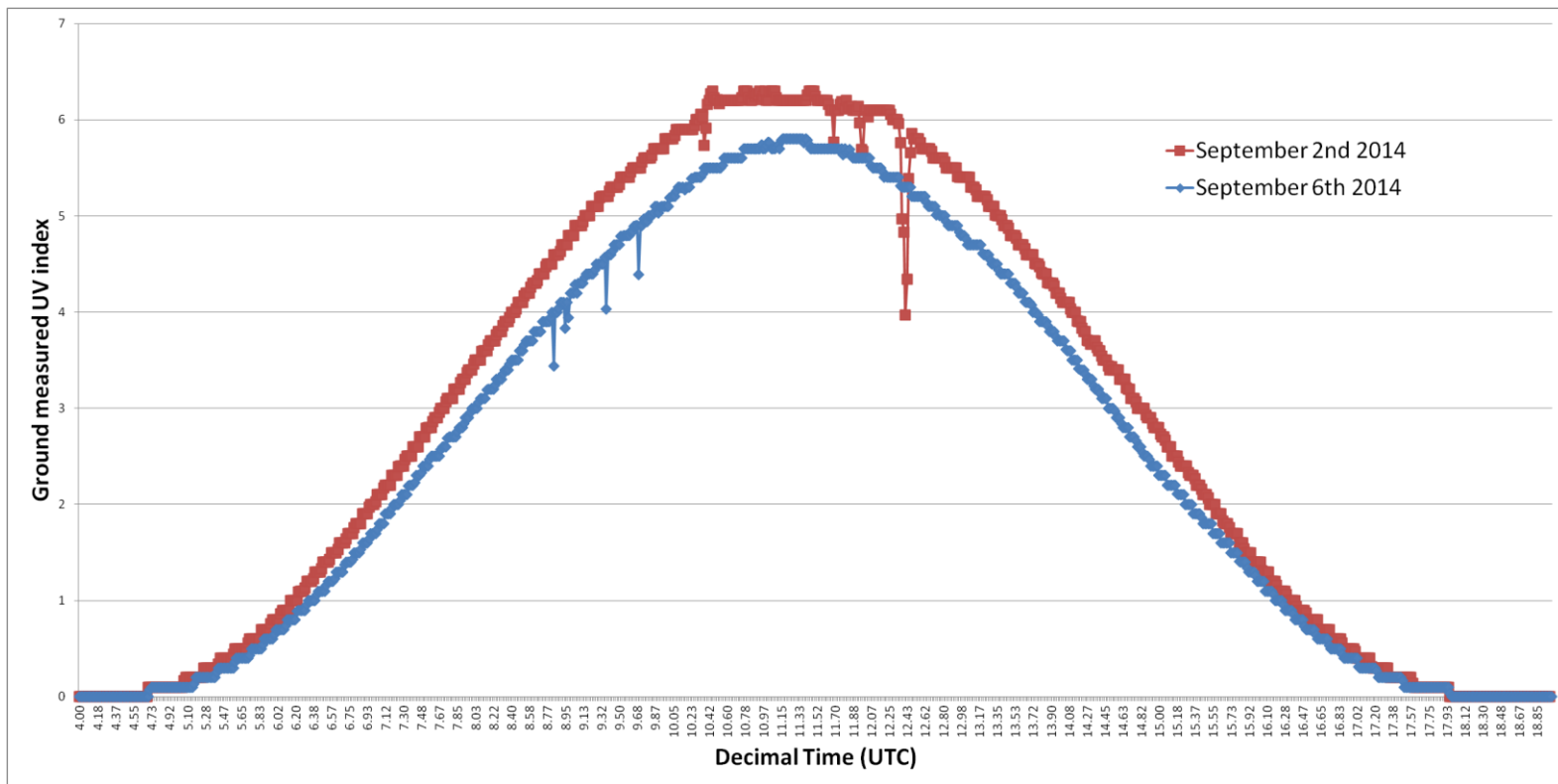


Figure 42: Comparison of the UV index on the horizontal plane measured at Flyby (Livorno, Italy) on September 2nd and on September 6th 2014. Data have been sampled every 1 minute from 4.00 UTC to 19.00 UTC. Source data are provided by Flyby.

3.2.1.2 At satellite sensor

Besides, we analyzed also the calibrated spectral radiance ($\text{mW}/\text{m}^2/\text{sr}/\text{cm}^{-1}$ units) observed by the SEVIRI sensor on the MSG satellite for the same site (i.e. Flyby at Livorno, Italy) and the same two days of September 2014.

In particular we focused on two infrared channels with central wavelengths $1.6 \mu\text{m}$ and $3.9 \mu\text{m}$: indeed these channels have been designed also to detect aerosols in absence of clouds (EUMETSAT 2005). Moreover the SEVIRI channel at $1.6 \mu\text{m}$ has already been found useful for aerosols detection (by simulations) as described in (Carboni, et al. 2007).

We actually found a difference in the radiance observed by SEVIRI in these two channels: this difference can be linked to aerosols presence, as shown also by our RTM simulations described in Section 3.2.2.2 .

We reported, as example, the source full-disk satellite optical images observed by SEVIRI at both $1.6 \mu\text{m}$ and $3.9 \mu\text{m}$ on September 2nd and September 6th (at 12.00 UTC) in Figure 43, Figure 44, Figure 45 and Figure 46.

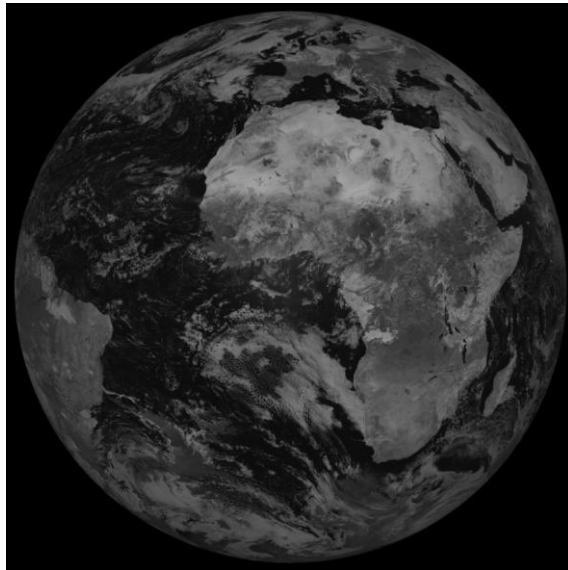


Figure 43: Full-disk image observed by the SEVIRI sensor on the MSG satellite in the $1.6 \mu\text{m}$ infrared channel on September 2nd 2014 at 12.00 UTC. Source data are provided by EUMETSAT.

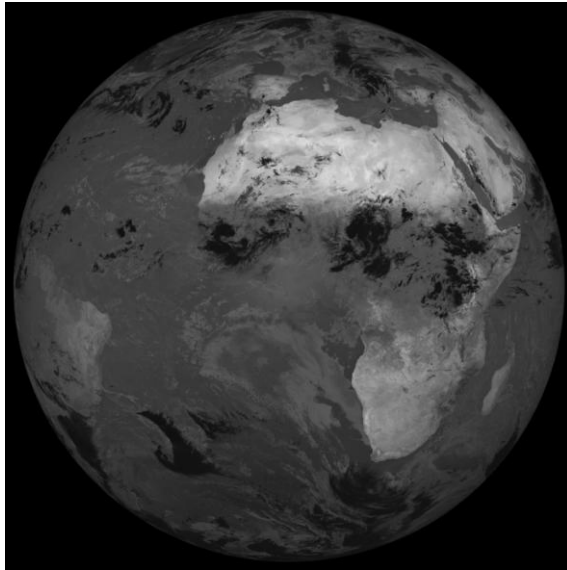


Figure 44: Full-disk image observed by the SEVIRI sensor on the MSG satellite in the 3.9 μm infrared channel on September 2nd 2014 at 12.00 UTC. Source data are provided by EUMETSAT.

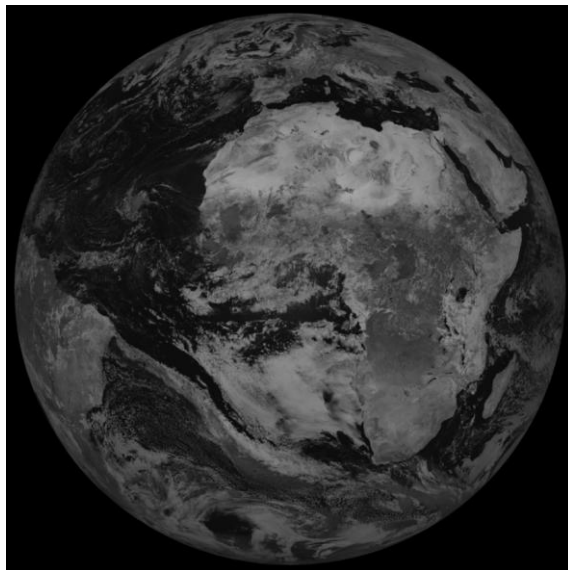


Figure 45: Full-disk image observed by the SEVIRI sensor on the MSG satellite in the 1.6 μm infrared channel on September 6th 2014 at 12.00 UTC. Source data are provided by EUMETSAT.

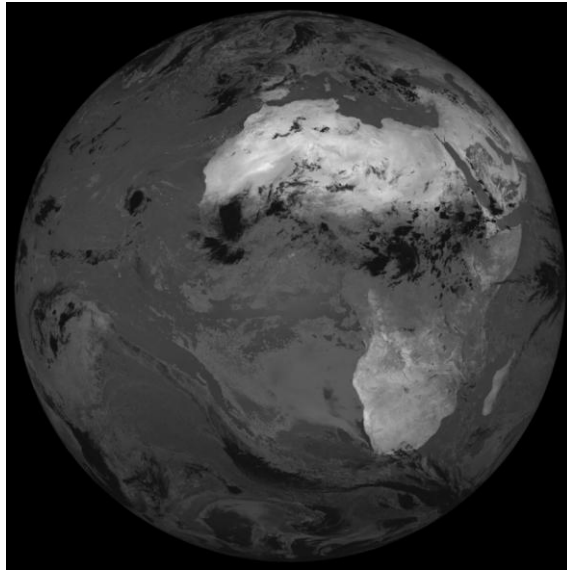


Figure 46: Full-disk image observed by the SEVIRI sensor on the MSG satellite in the 3.9 μm infrared channel on September 6th 2014 at 12.00 UTC. Source data are provided by EUMETSAT.

The comparison graph for the radiance observed by the SEVIRI channel at 1.6 μm on September 2nd and on September 6th is reported in Figure 47. The calibrated spectral radiance observed on September 6th is 0.1184 $\text{mW}/\text{m}^2/\text{sr}/\text{cm}^{-1}$ greater with respect to the one measured on September 2nd on average.

Instead the comparison graph for the radiance observed by the SEVIRI channel at 3.9 μm in the same two days is reported in Figure 48. In this case the calibrated spectral radiance observed on September 6th results 0.0312 $\text{mW}/\text{m}^2/\text{sr}/\text{cm}^{-1}$ greater with respect to the one measured on September 2nd on average.

Both the differences in radiance observed could be explained by an increase of the amount of aerosols in the atmosphere from September 2nd to September 6th, as shown by the RTM simulations described in Section 3.2.2.2.

As said, this difference in aerosols presence has been also directly observed by comparing both UV index and photovoltaic power production measured at ground in the two considered days (Section 3.2.1.1).

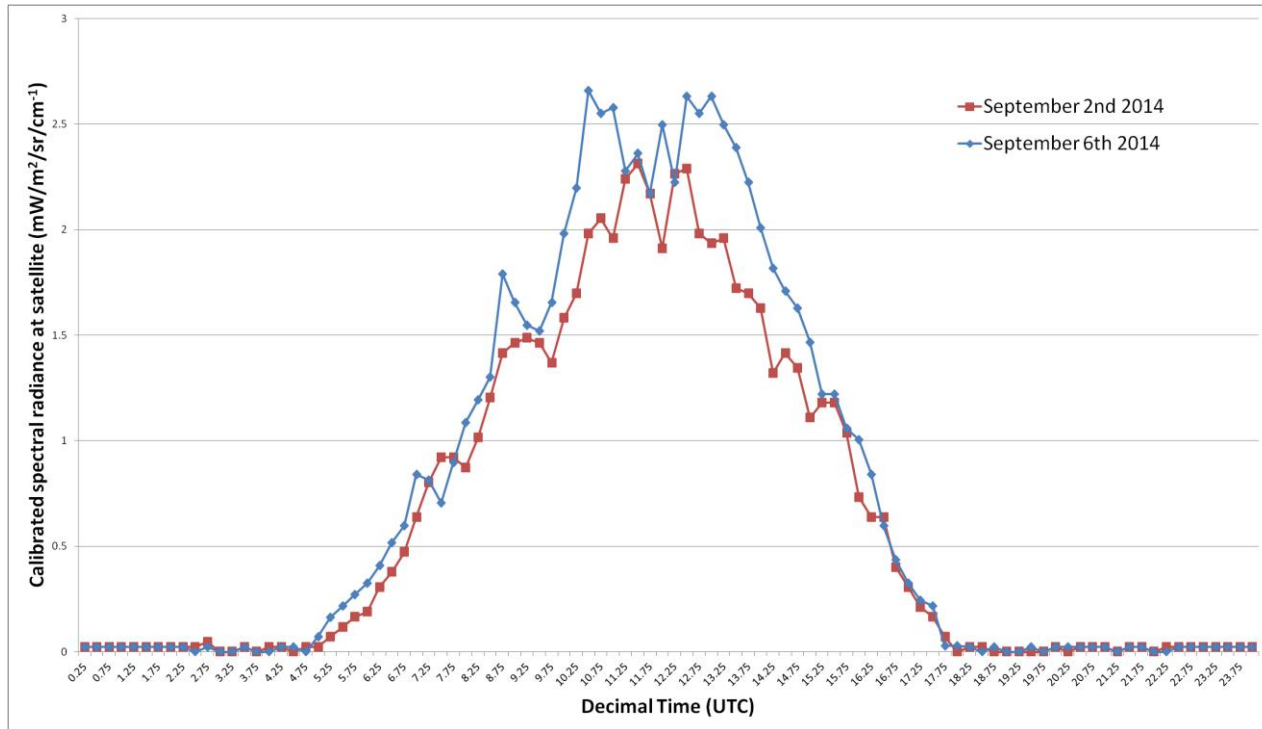


Figure 47: Comparison of the spectral radiance observed by the SEVIRI sensor on the MSG satellite in the 1.6 μm infrared channel for the Flyby site (Livorno, Italy) on September 2nd and on September 6th 2014. Data have been sampled every 15 minutes from 4.00 UTC to 19.00 UTC. Source data are provided by EUMETSAT.

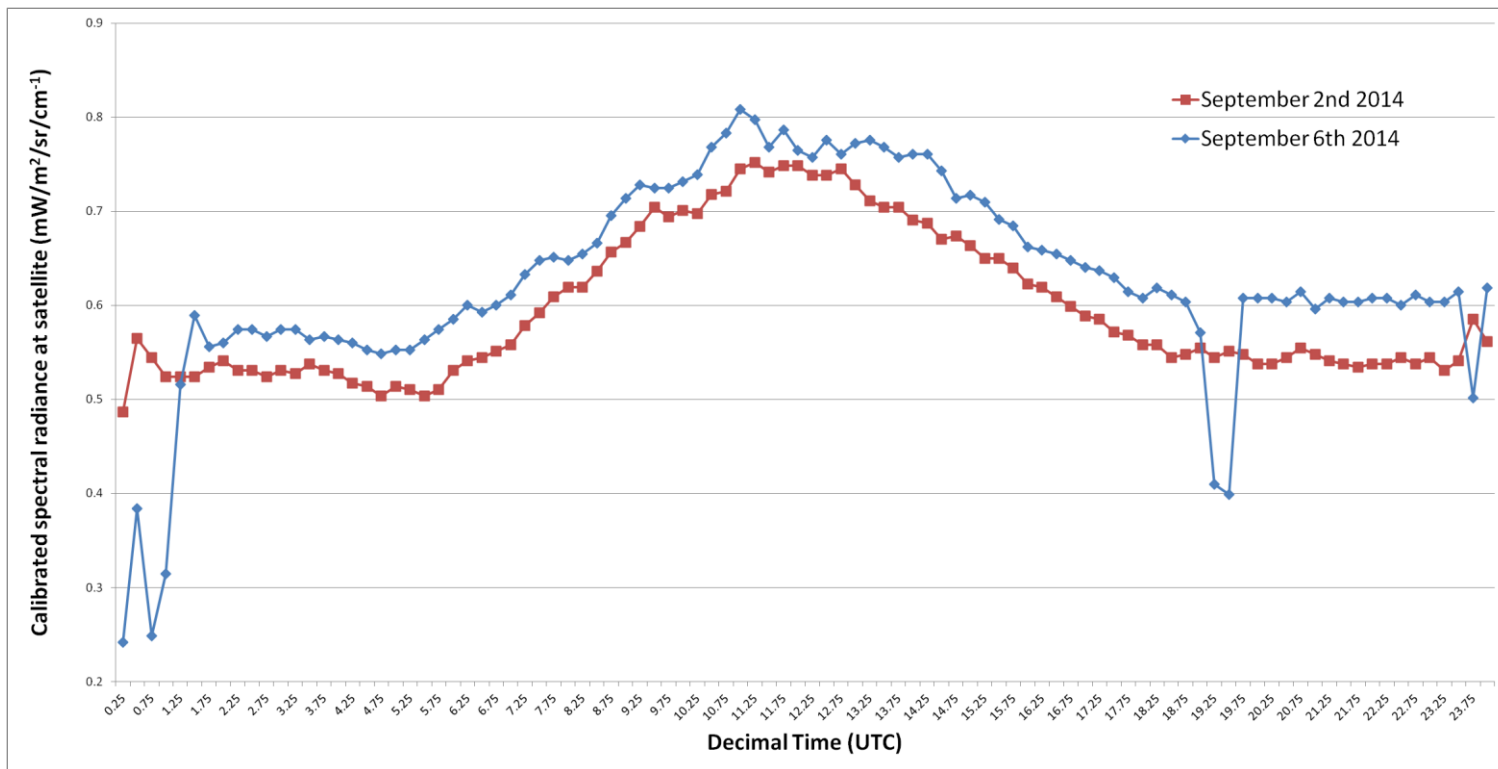


Figure 48: Comparison of the spectral radiance observed by the SEVIRI sensor on the MSG satellite in the 3.9 μm infrared channel for the Flyby site (Livorno, Italy) on September 2nd and on September 6th 2014. Data have been sampled every 15 minutes from 4.00 UTC to 19.00 UTC. Source data are provided by EUMETSAT.

3.2.2 Simulations

In Section 3.2.1 we described the observations performed on September 2nd and September 6th 2014 for the Flyby site (Livorno, Italy).

These observations reveal that there is an increase of aerosols presence in the atmosphere from September 2nd to September 6th, as shown by the ground measurements of both UV index and of the AC power produced by a photovoltaic plant.

This difference in the atmospheric composition of the two days can be observed also by satellite optical imagery, in particular comparing the radiances observed in the infrared channels 1.6 μm and 3.9 μm by the SEVIRI sensor on MSG. Indeed we observed a global increase of the radiance observed in both these channels that could be related to the increase in aerosols presence into the atmosphere.

But we still need radiative transfer simulations to confirm that:

- the effects observed at surface are really attributable to aerosols impact on solar radiative transfer;
- the increase in the radiances observed by the satellite channels can be actually related to the increase in aerosols presence (as supposed).

In this Section we present the results obtained from the simulations of the quantities measured both at ground and at satellite level (already described in Section 3.2.1). These simulations have been performed through a Radiative Transfer Model (RTM) for a typical atmospheric profile for Livorno (coastal type) in September, varying only the amount of aerosols in the atmosphere (i.e. the parameter “aerosols visibility”) in order to study its impact on the measured radiation values (both at ground and at satellite). The ground albedo value has been derived from (Baldrige, et al. 2009).

We decided to adopt one of the RTMs mostly used by the scientific community: libRadtran, that is an open source software containing a very accurate RTM (Kylling and Mayer 2005). In the last year libRadtran has been upgraded with the possibility to include also the simulation of the radiation observed in different spectral bands by EO geostationary satellite sensors (such as SEVIRI on MSG) in addition to the usual simulations of radiation at ground level (Gasteiger, et al. 2014).

3.2.2.1 At surface

First we consider the spectral solar irradiance incident at ground level at Flyby site on September 2nd and on September 6th for a typical value of aerosols visibility (10 km). The result of its simulation is reported in Figure 49. The graph shows that there is no substantial variation in the solar irradiance at ground with the same atmosphere for the two days considered, implying that the observed variations (Section 3.2.1) should be related to variations in the atmospheric composition itself.

Then we compared the simulated spectral solar irradiance at ground for different values of the aerosols visibility (i.e. amount of aerosols in the atmosphere) on September 2nd at 12.00 UTC (we didn't report the simulation of September 6th because it's very similar). We considered the following values for aerosols visibility: 0.1 km, 1 km, 10 km and 100 km. The resulting graph is shown in Figure 50. The most typical situation is represented by the 10 km visibility case, while

the 0.1 km is a quite impossible case (there is a quite complete darkness at noon only caused by aerosols).

The simulations always show that the impact of aerosols on solar irradiance at ground can be relatively very high.

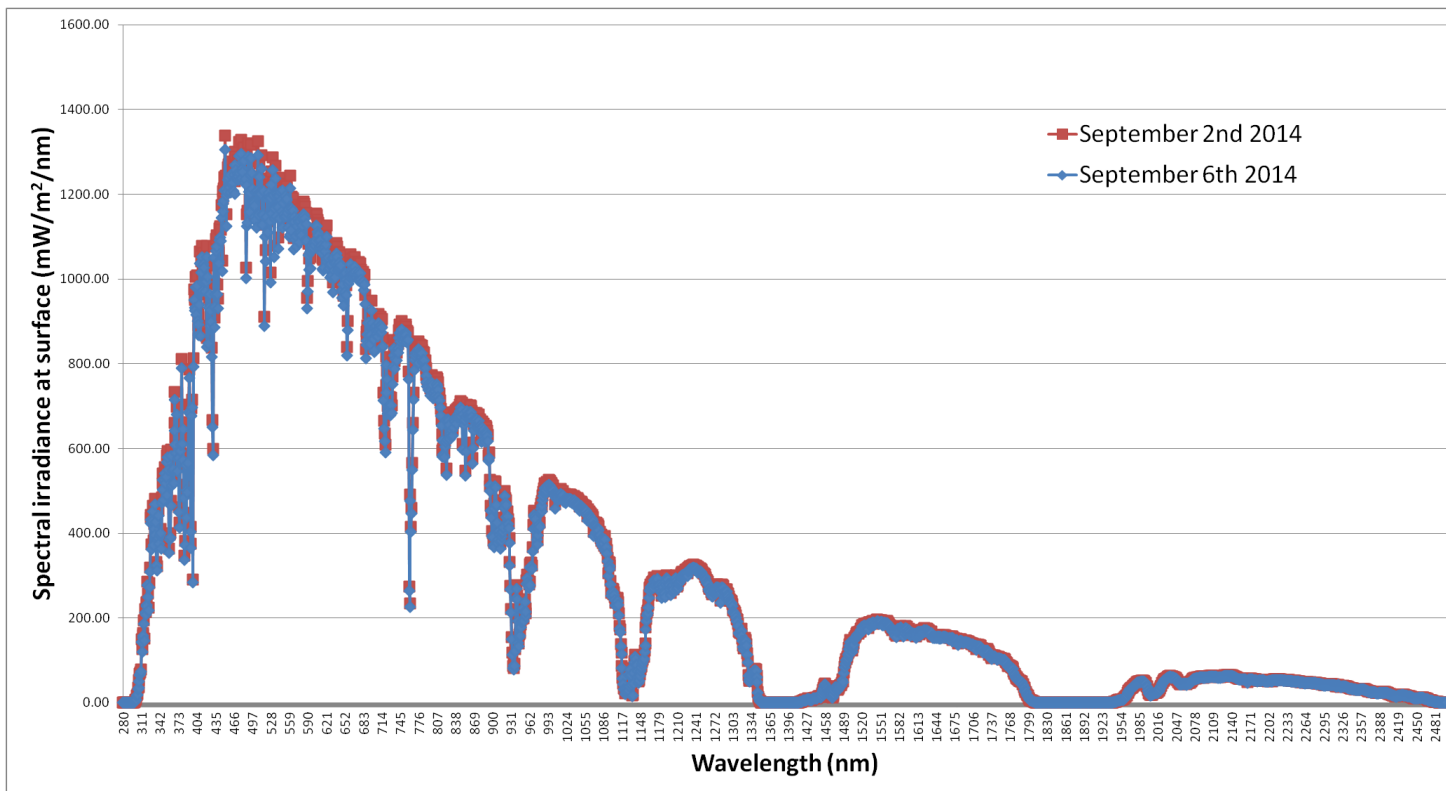


Figure 49: Comparison of the simulated spectral solar (shortwave) irradiance at Flyby (Livorno, Italy) on September 2nd and on September 6th 2014. Data have been obtained exploiting the libRadtran RTM.

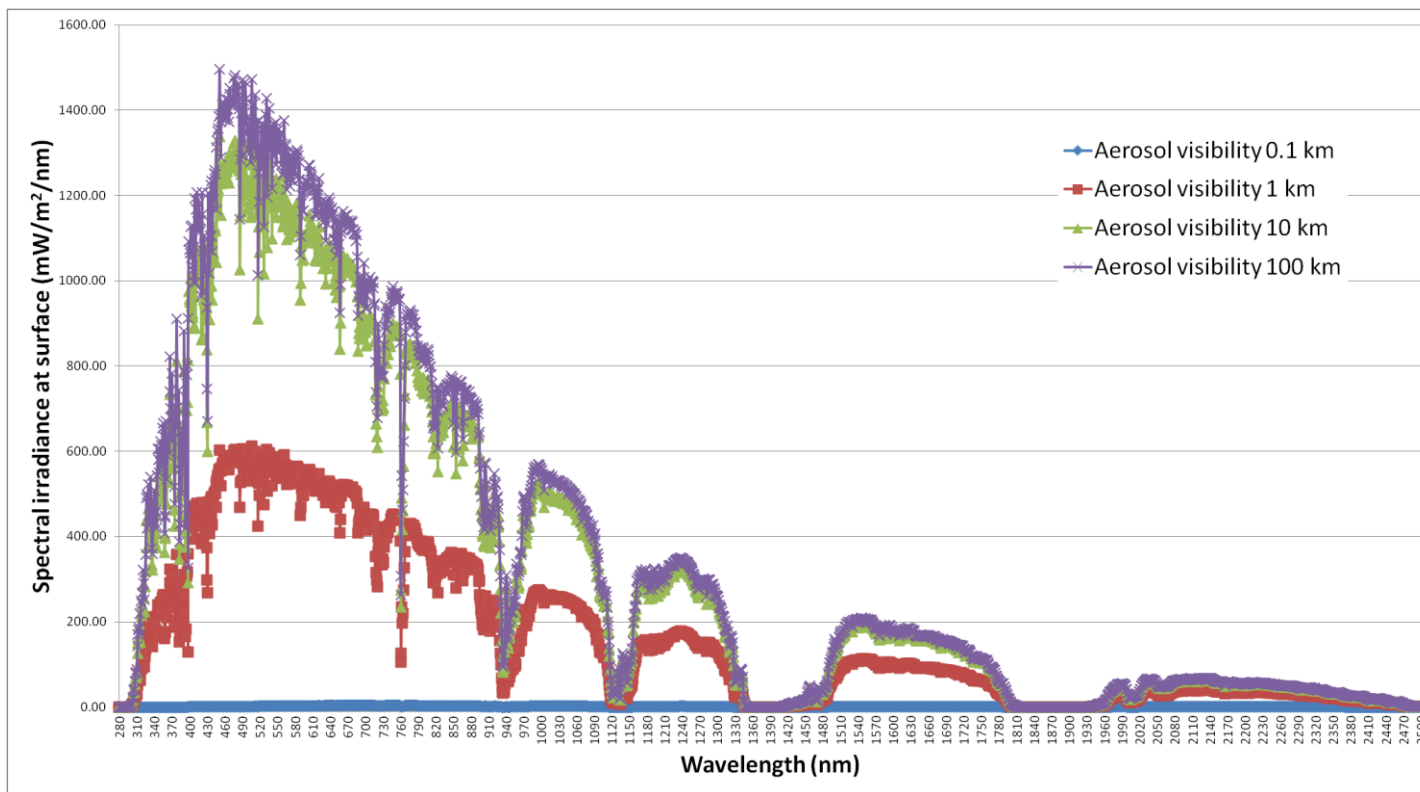


Figure 50: Simulated spectral solar (shortwave) irradiance at Flyby (Livorno, Italy) on September 2nd for different values of aerosols visibility. Data have been obtained exploiting the libRadtran RTM.

The same comparison for different values of aerosols visibility has been performed also for both the simulated shortwave solar irradiance at ground and the simulated UV index at ground. Results are shown in Figure 51 and Figure 52.

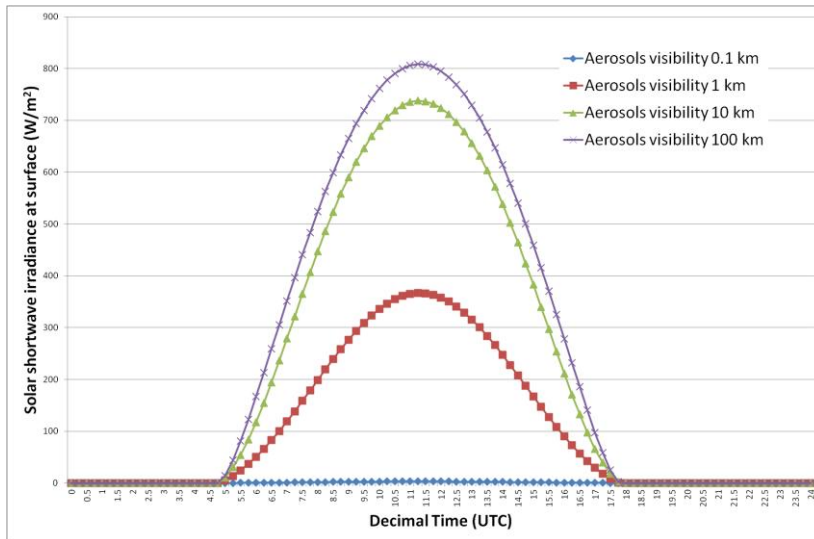


Figure 51: Simulated solar shortwave irradiance at Flyby (Livorno, Italy) on September 2nd (0 UTC - 24 UTC) for different values of aerosols visibility. Data have been obtained exploiting the libRadtran RTM.

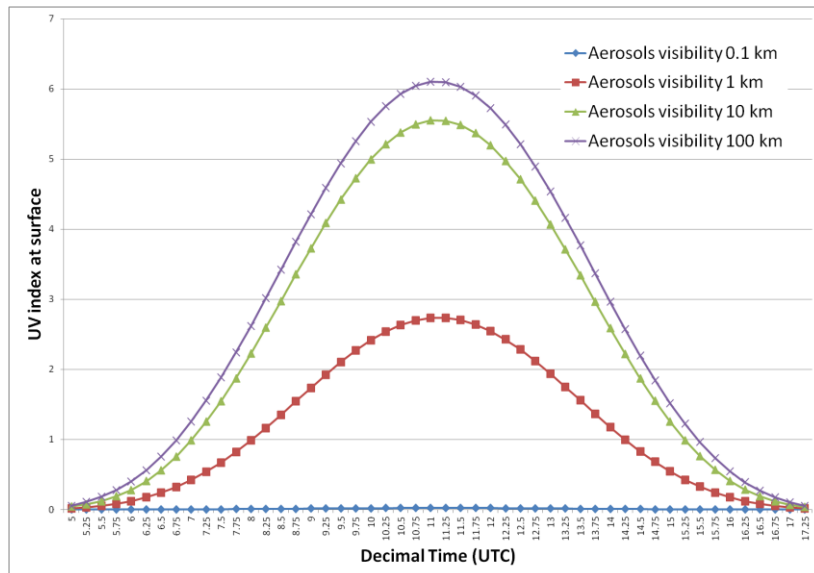


Figure 52: Simulated UV index at Flyby (Livorno, Italy) on September 2nd (5 UTC - 17.30 UTC) for different values of aerosols visibility. Data have been obtained exploiting the libRadtran RTM.

3.2.2.2 At satellite sensor

The same simulated atmosphere exploited in the previous Section has been used also to simulate the radiances to be observed by the SEVIRI sensor on the MSG satellite in the 1.6 μm and 3.9 μm infrared channels for different values of aerosols visibility. It's important to highlight that we changed only the aerosols visibility parameter in the different simulations, in order to emphasize its effects only.

Simulation results are reported in Figure 53 and Figure 54, clearly showing an inverse proportionality between radiance at satellite sensor and aerosols visibility in both channels.

The results obtained confirm our hypothesis described at the end of Section 3.2.1: actually the simulated radiances in both channels result inversely proportional to aerosols visibility on average, i.e. the radiances increase with the aerosols amount in the atmosphere (that is inversely proportional to visibility).

So the radiance observed in these two infrared channels can be correlated to aerosols impact on solar radiation at ground, possibly paving the way for the development of an innovative methodology for the satellite-based near real-time detection of aerosols impact on solar radiation at ground (Section 3.2.3).

The comparison of the spectral radiances observed by the satellite sensor (reported in Figure 47 and Figure 48) with the related simulated radiances (reported in Figure 53 and Figure 54) could also allow a satellite-based guess on the aerosols visibility on September 2nd and on September 6th at Livorno. Indeed the observed radiances (particularly for the 1.6 μm case) agree with the simulated radiances in the range 1 km – 100 km of aerosols visibility, compatibly also with Capraia island visibility/invisibility on the horizon in the two days (supposing the same aerosols visibility also in the troposphere between Livorno and Capraia, i.e. above open sea).

In any case all these conclusions should be further studied and validated with more measured and simulated data, taking into account also different ground albedo and air temperature conditions (possibly influencing the infrared satellite channels).

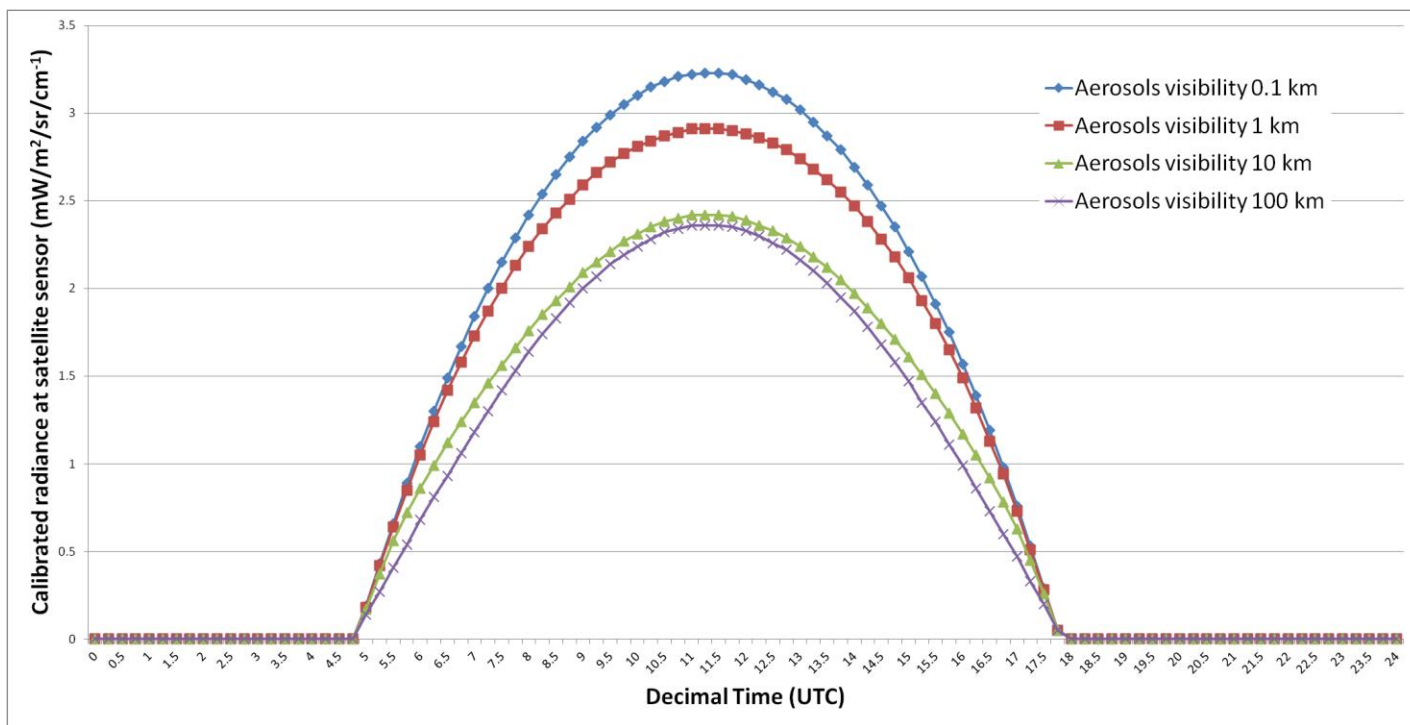


Figure 53: Simulation of the radiance observed by the SEVIRI sensor on the MSG satellite in the $1.6 \mu\text{m}$ channel for the Flyby site (Livorno, Italy) on September 2nd 2014 (0 UTC – 24 UTC). Data have been obtained exploiting the libRadtran RTM.

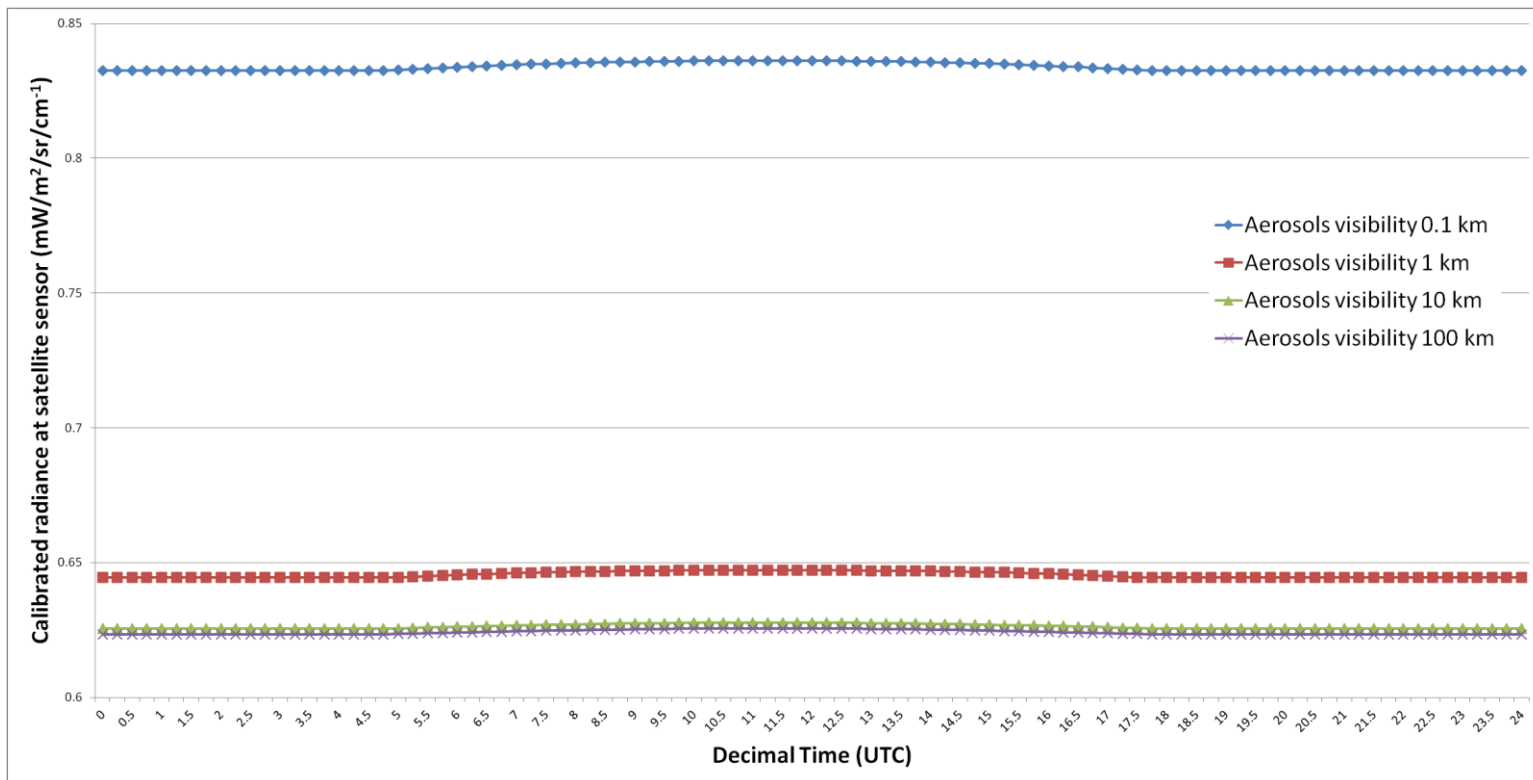


Figure 54: Simulation of the radiance observed by the SEVIRI sensor on the MSG satellite in the 3.9 μm channel for the Flyby site (Livorno, Italy) on September 2nd 2014 (0 UTC – 24 UTC). Data have been obtained exploiting the libRadtran RTM.

3.2.3 Innovative concepts for the near real-time assessment of aerosols impact

The results reported in Section 3.2.1 and Section 3.2.2 show that there is a correlation between the amount of aerosols in the atmosphere (aerosols visibility) and the spectral radiance observed by the SEVIRI sensor on the MSG satellite in the infrared channels at 1.6 μm and 3.9 μm . And aerosols visibility has an evident impact on solar radiative transfer and, consequently, on the solar radiation incident at ground level.

These facts can be exploited to develop an innovative satellite-based technique for the near real-time detection of aerosols impact on solar radiation at ground.

Indeed combining these results with the technique for cloudiness monitoring presented in Section 3.1, a novel method could be developed taking into account also aerosols impact in cloudless-sky conditions and further increasing the accuracy of current methods for satellite-based near real-time monitoring of solar radiation.

A possible scheme of the envisaged method is reported in Figure 55.

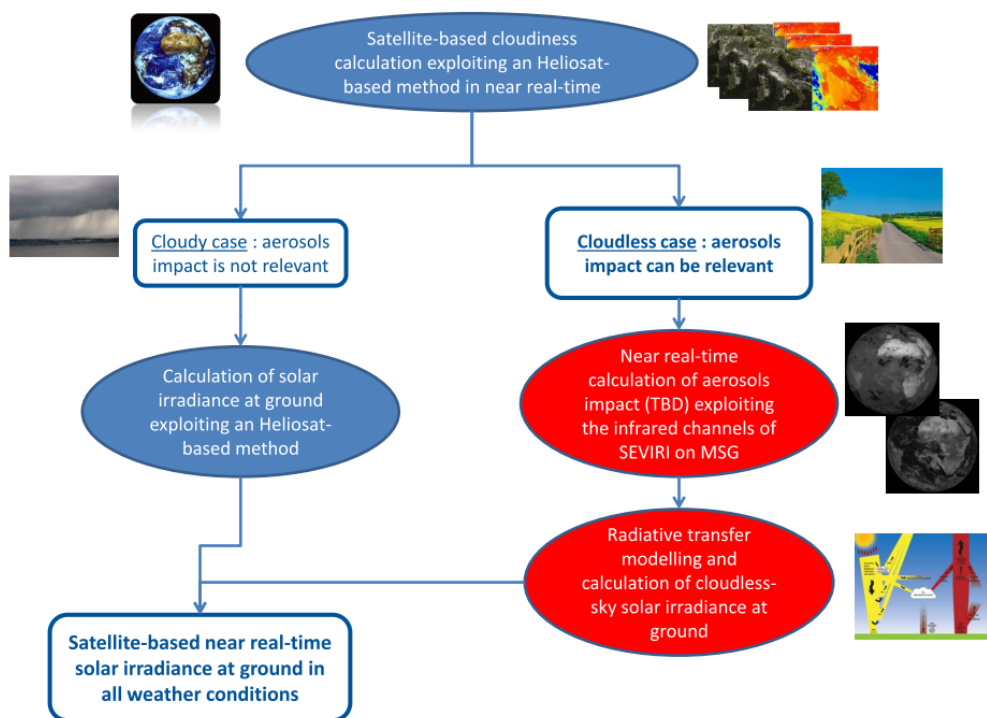


Figure 55: Scheme of a possible innovative method for the satellite-based near real-time monitoring of solar radiation at ground that takes into account also aerosols impact in cloudless-sky conditions.

4 APPLICATIONS

In Europe about half a million skin cancer cases occur per year. This is strongly associated with personal habits in exposing to sun with poor protection against its ultraviolet (UV) component. The need to protect oneself depends mainly on the local UV index which can be derived in near real time from satellite data.

Another challenge is the monitoring of solar plants. An early detection of the decline in energy production due to any malfunction can avoid a significant loss of income, especially for big plants. This can be done by comparing the actual energy production with the expected one, which can be estimated by means of satellite data.

These two challenges have been engaged by developing two different satellite-based applications, one dedicated to near-real time monitoring of the performances of solar energy plants (Section 4.1) and the other one that provides a near real-time monitoring of UV dose (Section 4.2). The applications rely on the scientific results presented in Chapter 3 and already showed a good level of accuracy in their first versions.

All the results presented hereby have already been published in (Morelli, Masini and Ruffini, et al. 2015 - in press) and in (Morelli, Masini and Diémoz, et al. 2014).

4.1 Solar energy: near real-time monitoring of solar plants

4.1.1 Concept

Our modelling technique, schematically shown in Figure 56, firstly models the global tilted irradiance incident on each PV module following the approach described by (Perez, Ineichen, et al., Modeling daylight availability and irradiance components from direct and global irradiance 1990) and starting from the satellite-based solar shortwave irradiance data derived exploiting the techniques described in Chapter 3.

Then the solar energy plant is modelled in order to calculate the AC power yield. The PV modules have been modelled using an equivalent circuit with a (photovoltaic) current

generator, connected in series with a resistance and in parallel with a diode and another resistance. This opto-electronic model of each PV cell has been taken from (De Soto, Klein and Beckman 2006) and has been schematically represented in Figure 57.

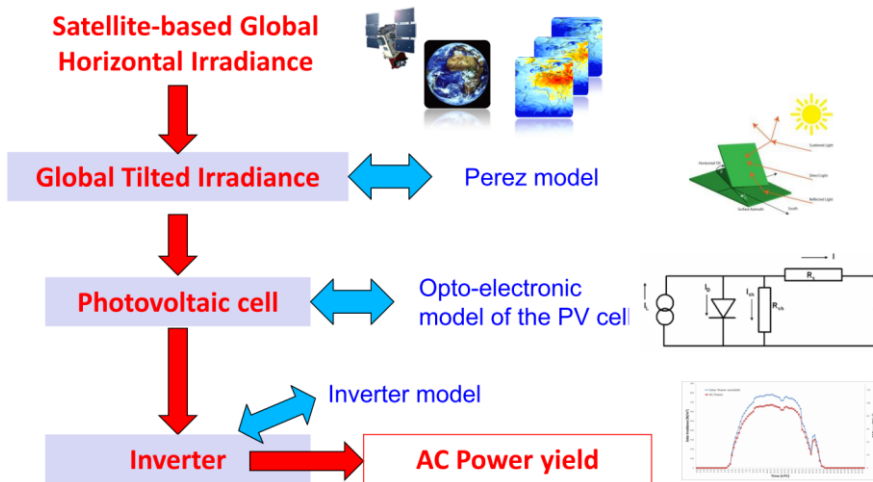


Figure 56: Scheme of our modelling technique for the satellite-based near real-time monitoring of solar energy photovoltaic plants.

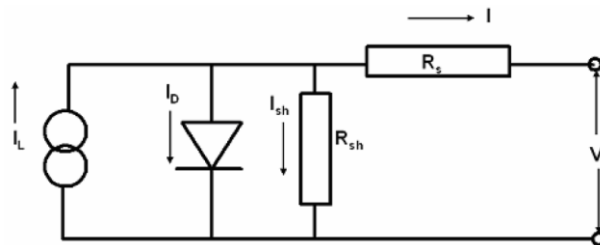


Figure 57: Equivalent circuit of a PV cell exploited in the opto-electronic model. Taken from (De Soto, Klein and Beckman 2006).

4.1.2 Results

We compared the hourly AC power (i.e. the hourly averaged AC power produced by the solar energy plant) calculated using our satellite-based methodology and the in-situ measured one for three PV solar energy plant, respectively located in Veneto (North Italy), in Lazio (Centre Italy) and in Sicily (South Italy). We considered the hourly AC power data from 05:00 UTC to 20:00 UTC for November 2013, January 2014, March 2014, May 2014, July 2014 and September 2014 (considering all-seasons data). Since we have some lacks of data, we considered a total of 5383 time instants.

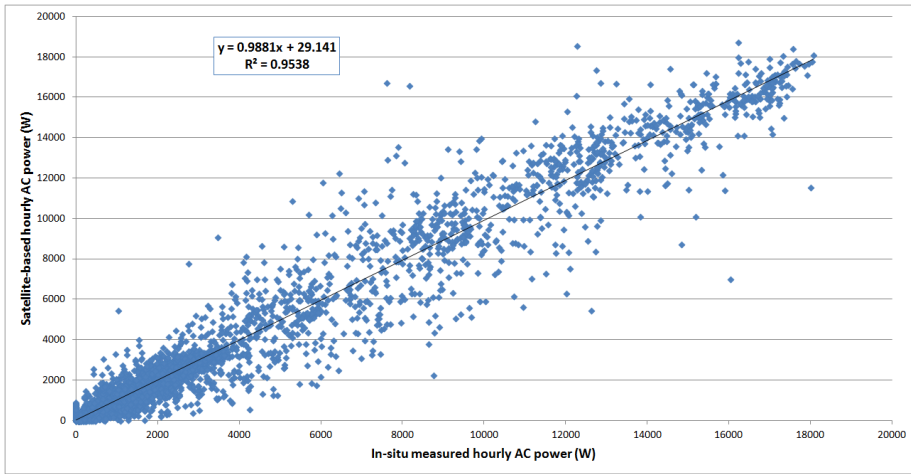


Figure 58: Scatter plot comparing the hourly AC power produced by three different PV plants as calculated by the satellite-based method and as obtained from in-situ measured data. Source data are referred to a 4.86 kWp plant in Veneto (North Italy), a 3.89 kWp plant in Lazio (Centre Italy) and a 20.0 kWp plant in Sicily (South Italy). The considered periods are November 2013, January 2014, March 2014, May 2014, July 2014 and September 2014, for a total of 5383 time instants that range from 05:00 UTC to 20:00 UTC. Taken from (Morelli, Masini and Ruffini, et al. 2015 - in press).

The results obtained are shown in the scatter plot graph presented in Figure 58. In Figure 59 and Figure 60 the results for one month for the Veneto plant has been reported, showing the comparison between the monthly behaviours of satellite-based and in-situ measured hourly AC power data (Figure 5) and the related behaviour of the NMAE (Figure 6) respectively.

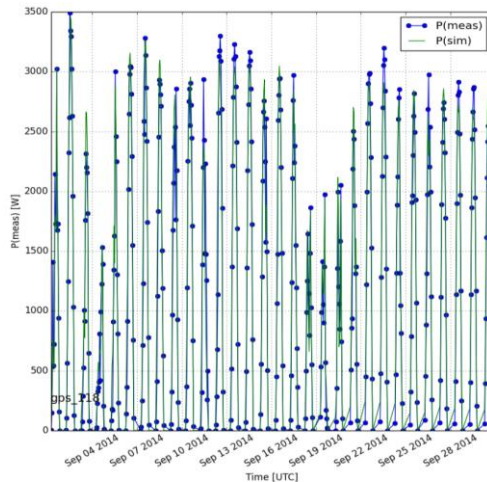


Figure 59: Comparison between the behaviour of the satellite-based hourly AC power and the in-situ measured one. Data are referred to a single month (September 2014) for the PV plant in Veneto. Taken from (Morelli, Masini and Ruffini, et al. 2015 - in press).

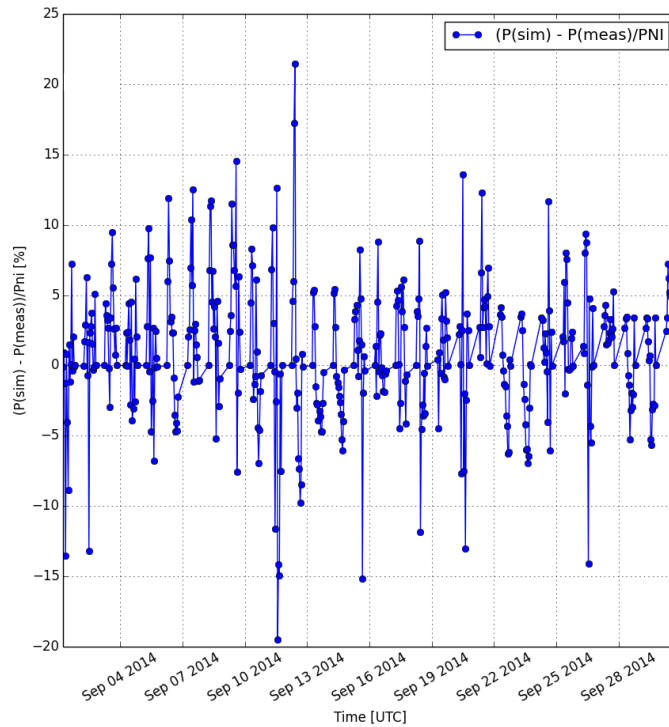


Figure 60: An example of the behaviour of the NMAE resulting from the comparison between satellite-based and in-situ measured hourly AC power. Data are referred to a single month (September 2014) for the PV plant in Veneto. Taken from (Morelli, Masini and Ruffini, et al. 2015 - in press).

The results show a good accuracy: the overall Normalized Bias (NB) is -0.41 %, the overall Normalized Mean Absolute Error (NMAE) is 4.90 %, the Normalized Root Mean Square Error (NRMSE) is 7.66 %. “Normalized” means that the statistical quantities reported here have been normalized with respect to the nominal power of each plant, i.e. 4.86 kWp, 3.98 kWp and 20.0 kWp respectively. The overall Correlation Coefficient (CC) is 0.9538. The maximum value of the Normalized Absolute Error (NAE) is about 30% and occurs for time periods with highly variable meteorological conditions.

4.2 Healthcare: satellite-based UV dosimetry

4.2.1 Concept

The satellite-based methodologies presented in Chapter 3 have been also exploited to calculate in near real-time the solar irradiance in the UV part of the spectrum only. This quantity can be converted in UV index units by applying the Erythemal Action Spectrum defined in (McKinlay and Diffey 1987). Then also the UV irradiance incident on the plane normal to sun rays is modelled (usually the maximum possible UV irradiance absorbed by the skin) is modelled by

exploiting the model described in (Perez, Ineichen, et al., Modeling daylight availability and irradiance components from direct and global irradiance 1990) and the related UV dose is calculated.

This idea is the base of the satellite-based UV dosimeter that we developed and that showed good accuracy with respect to in-situ measured UV dose data.

4.2.2 Results

The performances of our satellite-based UV dosimeter have been validated thanks to the collaboration with the Environmental Protection Agency of the Valle d'Aosta Italian region (ARPA Valle d'Aosta). So far we compared only data of UV dose on the horizontal plane.

The instrument used by ARPA has been the high-quality Kipp&Zonen UVS-AE-T radiometer installed at Saint Christophe (Aosta, Italy) at about 540 meters above sea level.

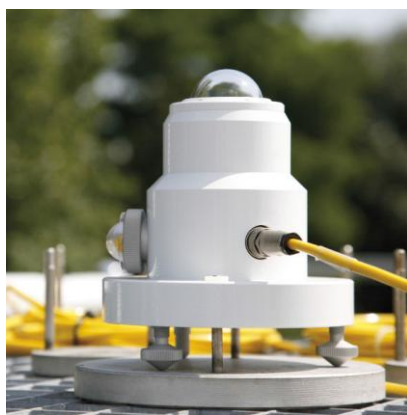


Figure 61: Photo of the UVS-AE-T radiometer exploited for the validation of the satellite-based UV dosimeter. Courtesy of Kipp&Zonen.

We obtained a good agreement between satellite based and in-situ measured UV dose data. In particular the agreement is very good for days with stable weather conditions, while in unstable or broken-clouds days we obtained lower accuracy probably due to multiple scattering processes in the clouds layer and low spatial resolution of the source satellite image (about 3-4 Km for Valle D'Aosta).

In the case of stable weather conditions we obtained the following results from the comparison of satellite-based and in-situ measured data (see also Figure 62): the correlation coefficient is 99.23 %, the bias is 4.98 %, the Mean Absolute Error (MAE) is 7.07 % and the Root Mean Squared Error (RMSE) is 8.63 %.

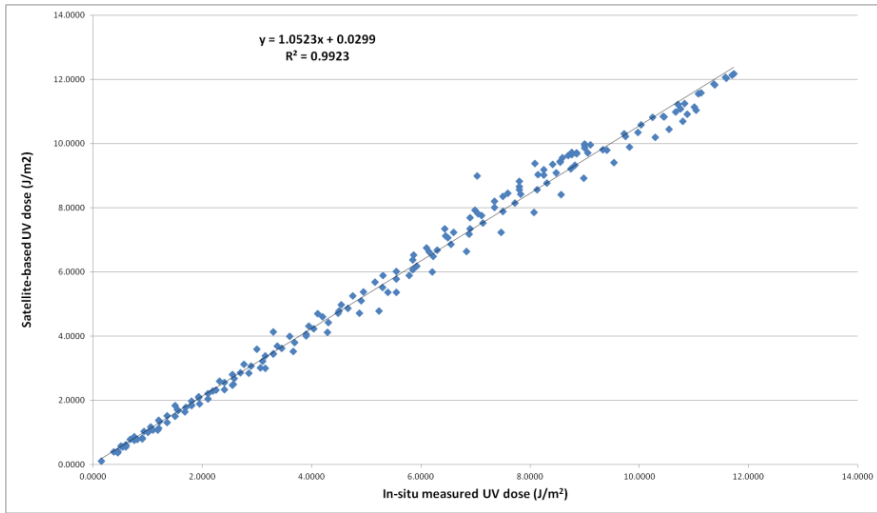


Figure 62: Comparison between the UV dose derived from the satellite-based dosimeter and the UV data provided by the in-situ measurements performed by ARPA Valle d’Aosta in stable weather conditions. Data are referred to the period June-July 2014. Taken from (Morelli, Masini and Diémoz, et al. 2014).

In Figure 63 we reported the behaviour of the maximum relative difference between satellite-based and in-situ measured UV dose data with respect to solar zenith angle (SZA) for stable weather conditions.

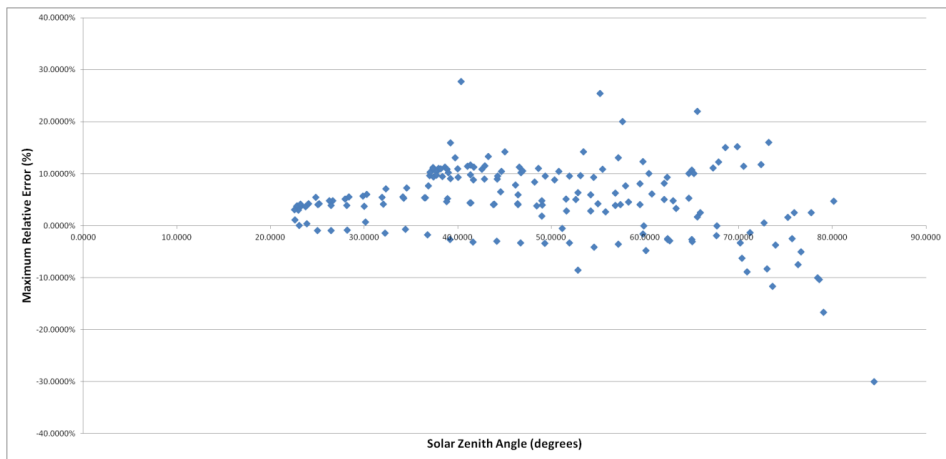


Figure 63: Maximum relative difference between satellite-based and in-situ measured UV dose data with respect to SZA in stable weather conditions. Data are referred to the Saint Christophe (Aosta, Italy) station in the period June-July 2014. Taken from (Morelli, Masini and Diémoz, et al. 2014).

The same comparisons have been performed also for the unstable weather conditions case. The results obtained are shown in Figure 64 and Figure 65.

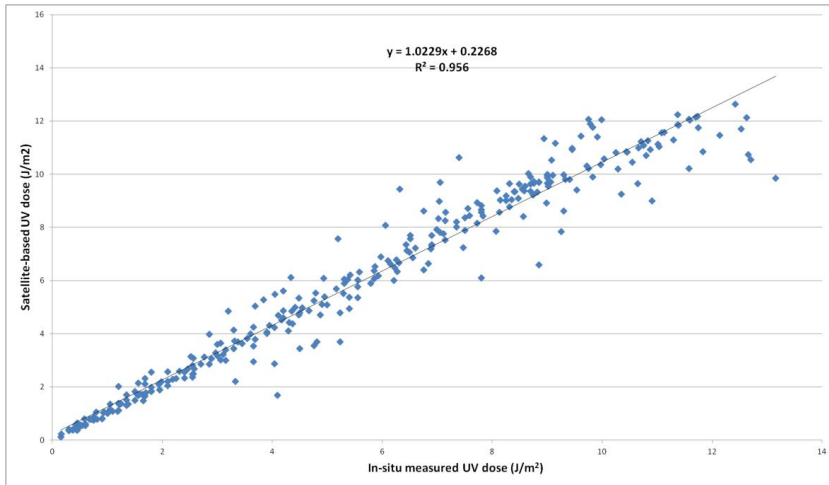


Figure 64: Comparison between the UV dose derived from the satellite-based dosimeter and the UV data provided by the in-situ measurements performed by ARPA Valle d'Aosta in unstable weather conditions. Data are referred to the period June-July 2014. Taken from (Morelli, Masini and Diémoz, et al. 2014).

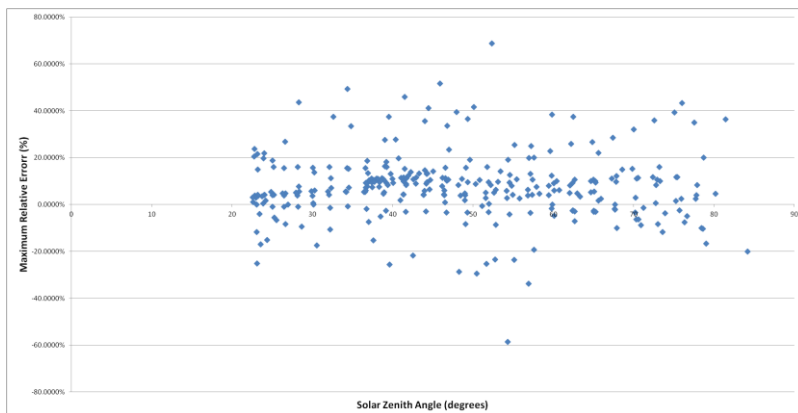


Figure 65: Maximum relative difference between satellite-based and in-situ measured UV dose data with respect to SZA in unstable weather conditions. Data are referred to the Saint Christophe (Aosta, Italy) station in the period June-July 2014. Taken from (Morelli, Masini and Diémoz, et al. 2014).

The following results have been obtained for the unstable weather conditions case: the correlation coefficient is 95.6 %, the bias is 7.61 %, the Mean Absolute Error (MAE) is 11.88 % and the Root Mean Squared Error (RMSE) is 16.08 %.

5 REPORT OF THE ACTIVITIES IN RESEARCH PROJECTS

5.1.1 FP7 “MACC” project

The MACC (Monitoring Atmospheric Composition and Climate) research project MACC was established under the European Union’s Seventh Framework Programme for Research and Technological Development to provide the pilot for the operational core GMES Atmosphere Monitoring Service. It built on the systems and prototype pre-operational services developed in the Sixth Framework Project GEMS, sustaining, improving and expanding the services and incorporating core elements of the ESA-funded GMES Service Element project PROMOTE.

MACC provided sets of graphical, data and documentary products that emanated from:

- Global service lines providing:
 - monitoring of key aspects of climate, climate forcing and sources and sinks of key species;
 - monitoring and forecasting of stratospheric ozone and UV radiation;
 - forecasts of reactive gases and aerosols;
 - boundary conditions for regional models.
- European service lines providing:
 - air-quality forecasts from an ensemble of high-resolution regional systems;
 - air-quality assessments based on retrospective running of the regional systems using validated
- Observational data;
- solar-energy resource assessment.

The consortium was composed by 39 partners (research institutes and companies) and led by the European Centre for Medium-Range Weather Forecasts (ECMWF).

In this framework the Author contributed to the development and assessment of a service dedicated to satellite-based solar radiation monitoring for applications in the renewable energies sector. In particular he has been involved in the project from September 2011 till the end (December 2011), being also the author of the deliverable D_R-RAD_3.1-1 "Service chain validation report for downstream test cases" in collaboration with DLR (Germany).

5.1.2 FP7 "ENDORSE" project

The three-year ENDORSE project (ENergy DOwnstReam SErVICES), co-funded by the European Commission from 2011 to 2013 in the frame of the Seventh Framework Programme, addressed the European Union's objective to providing 20% of Europe's energy from renewable sources by 2020. From this ten services have been developed that exploit Earth Observation data and models in five domains (wind, sun, electricity load balancing, biomass, and daylighting) with the aim to provide solutions at a regional scale.

The consortium was composed by ten partners, experts in energy or market analysis, which are research institutes or companies (SMEs):

- Transvalor (France)
- Flyby (Italy)
- ENTPE (France)
- DLR (Germany)
- University of Genova (Italy)
- iCons (Italy)
- 3E (Belgium)
- Hochschule Ulm (Germany)
- Armines (France, coordinator)
- JRC (Italy)

In this framework the Author contributed to the development and assessment of a service dedicated to satellite-based planning&monitoring of Concentrating Solar Power (CSP) plants (the so-called "S2 service"). In addition to this he has been the leader of the work package dedicated to products development (WP4), coordinating the development of the 10 ENDORSE services performed by the partners Transvalor (France), DLR (Germany), ENTPE(France), 3E (Belgium) and Hochschule Ulm (Germany). The Author participated to all the project meetings from September 2011 (when he was involved) till the end of the project (December 2013), having several oral presentations about the S2 service and about WP4 also for the European Commission representatives at the Review Meetings. He has been author and co-author of three deliverables.

5.1.3 ASI "SATENERG" project

The SATENERG project has been co-funded by the Italian Space Agency (ASI) from 2012 to 2014 for the development of innovative satellite-based services dedicated to planning&monitoring of solar energy plants (CSP and CPV) and off-shore wind plants. The consortium was composed by two Italian SMEs (Flyby and PXL) and led by Flyby, while the prime-user has been Enel Green Power.

In this frame the Author was the technical responsible of the project, coordinating the development of the services and in particular developing the services related to solar energy plants. He participated to all the project meetings, having several oral presentations and being author or co-author of 16 deliverables.

6 CONCLUSIONS

6.1 Achieved results

We presented the main innovative results obtained during the PhD, with a particular focus on the scientific results concerning with satellite-based characterization of the aerosols impact on solar radiative transfer in the atmosphere.

As explained in Chapter 3, the comparison of ground radiation measurements and satellite multispectral imagery led to find a correlation between the aerosols impact on solar radiation at ground in cloudless-sky conditions and the spectral radiance observed in near real-time by the SEVIRI sensor on the MSG satellite in two infrared channels. This could allow the development of an innovative technique for the near real-time assessment of aerosols impact on solar radiation at ground in cloudless-sky conditions starting from multispectral satellite imagery.

For what concerns applications, we described in Chapter 4 the satellite-based methodologies that we developed in the solar energy sector (solar energy plants monitoring) and in the healthcare sector (UV dosimeter) starting from the techniques described in Chapter 3. Both these applications have been already validated, showing a good agreement with ground-based measurements, as also described in (Morelli, Masini and Ruffini, et al. 2015 - in press) and in (Morelli, Masini and Diémoz, et al. 2014).

We can summarize the results achieved and described in this Thesis as follows:

- a satellite-based method for the near real-time monitoring of the performances of a solar energy plant has been developed and validated;
- a satellite-based UV dosimeter has been developed and validated;
- a correlation between multispectral (infrared) satellite imagery and aerosols impact on solar radiation at ground in cloudless-sky conditions has been demonstrated;
- a novel satellite-based methodology for the near real-time assessment of aerosols impact on solar radiation monitoring (and related applications) in cloudless-sky conditions has been envisaged.

These results have been developed also in the frame of national and international research project, as explained in Chapter 5.

6.2 Future developments

The scientific results on the satellite-based characterization of aerosols impact on solar radiative transfer in the atmosphere should be further validated. In particular the correlation found should be verified also for other locations (with different types of aerosols) and other seasons.

In case that this observed correlation will be confirmed by other data, the envisaged methodology for the near real-time assessment of aerosols impact should be actually developed. In particular an algorithm that relates the infrared spectral radiances observed by the satellite sensor and the actual solar radiation quantity at ground (i.e. solar shortwave irradiance or UV-index) should be developed and validated.

We could also exploit the aerosol optical depth (AOD) data provided by the AERONET network in order to find a possible relation of AOD with satellite optical data.

Other related scientific research activities could be also performed. For example the impact of aerosols shape on solar radiative transfer could be investigated. Aerosols are usually modelled (as in this Thesis) with a spherical shape, but real aerosols could have shapes very different from a sphere (as shown also in Chapter 2).

This could have important effects on atmospheric extinction processes, as shown also by (Dubovik, et al. 2000): the optical properties of non-spherical aerosols (ellipsoidal) and spherical aerosols resulted relevantly different, showing a possible great impact on atmospheric radiative transfer modelling.

This fact should be taken into account both at ground and at satellite level, because aerosols optical properties influence both the solar radiation incident at ground and the backscattered radiation observed by a satellite sensor. So aerosols shape could result a relevant factor to be assessed both in satellite-based aerosols impact detection and in the applications related to solar radiation at ground.

7 REFERENCES

- Baldrige, A. M., S. J. Hook, Grove C. I., and Rivera G. "The ASTER Spectral Library Version 2.0." *Remote Sensing of Environment* 113 (2009): 711-715.
- Butler, B. A., E. E. van Dyk, W. Okullo, M. K. Munji, and P. Booyesen. "Characterization of a low concentrator photovoltaics module." *Physica B* 407 (2012): 1501-1504.
- Cano, D., J. M. Monget, M. Albuisson, H. Guillard, N. Regas, and L. Wald. "A method for the determination of the global solar radiation from meteorological satellite data." *Solar Energy* 37 (1986): 31-39.
- Carboni, E., et al. "Retrieval of aerosol properties from SEVIRI using visible and infrared channels." *Proceedings of EUMETSAT/AMS conference 2007, Amsterdam (the Netherlands), September 24th - 28th 2007*, 2007.
- Chamaillard, K., et al. "Light backscattering and scattering by non-spherical sea-salt aerosols." *Journal of Quantitative Spectroscopy and Radiative Transfer*, 2003: 577-597.
- Chandrasekhar, S. *Radiative Transfer*. New York, USA: Dover, 1950.
- Clarke, A., et al. "Sea-salt size distributions from breaking waves: implications for marine aerosol production and optical extinction measurements during SEAS." *Journal of Atmospheric and Oceanic Technology* 20 (2003): 1362-1374.
- Dagestad, K. F., and J. A. Olseth. *An alternative algorithm for calculating the cloud index*. Bergen, Norway: Geophysical institute of the University of Bergen, 2005.
- Davis Instruments. "Specification sheet of the Vantage Pro UV Sensor." 2006.
- De Soto, W., S. A. Klein, and W. A. Beckman. "Improvement and validation of a model for photovoltaic array performance." *Solar Energy* 80 (2006): 78-88.
- Dubovik, O., et al. "Accuracy assessments of aerosol optical properties retrieved from Aerosol Robotic Network (AERONET): sun and sky radiance measurements." *Journal of Geophysical Research* 105 (2000): 9791-9806.

EUMETSAT. "CGMS 03 - Issue 2.6 - "LRIT/HRIT Global Specification - Coordination Group for Meteorological Satellites"." 1999.

EUMETSAT. "EUM/MSG/ICD/105 - "MSG Level 1.5 Image Data Format Description"." 2005.

EUMETSAT. "EUM/MSG/SPE/057 - "MSG Ground Segment LRIT/HRIT Mission Specific Implementation"." 2005.

EUMETSAT. "PDF_NWS_SEVERICHANS_0401_EN - "The 12 SEVIRI Imaging Channels"." 2005.

Forero, N., Hernandez J., and G. Gordillo. "Development of a monitoring system for a PV solar plant." *Energy Conversion and Management* 47 (2006): 2329–2336.

Gasteiger, J., C. Emde, B. Mayer, R. Buras, S. A. Buehler, and O. Lemke. "Representative wavelengths absorption parameterization applied to satellite channels and spectral bands." *Journal of Quantitative Spectroscopy and Radiative Transfer* 148 (2014): 99-115.

Hess, M., P. Koepke, and I. Schult. "Optical properties of aerosols and clouds: the software package OPAC." *Bulletin of the American Meteorological Society* 79 (1998): 831-844.

Hill, D., V. White, R. Marks, and R. Borland. "Changes in sun-related attitudes and behaviours, and reduced sunburn prevalence in a population at high risk of melanoma." *European Journal of Cancer Prevention* 2 (1993): 447-456.

IARC. "Solar and ultraviolet radiation." *IARC Monographs on the evaluation of carcinogenic risks to humans* 55 (1992): 1–316.

Iqbal, M. *An introduction to solar radiation*. Toronto, Canada: Academic Press, 1983.

Jaenicke, R. "Aerosol physics and chemistry." In *Numerical Data and Functional Relationships in Science*, by H Landolt and R. Bornstein. Berlin, Germany: Springer - FRG, 1988.

Kessner, A. L., J. Wang, Levy R., and P. Colarco. "Remote sensing of surface visibility from space: a look at the United States East Coast." *Atmospheric Environment* 81 (2013): 136-147.

Klashnikova, O. V., and I. N. Sokolik. "Modeling the radiative properties of nonspherical soil-derived mineral aerosols." *Journal of Quantitative Spectroscopy and Radiative Transfer* 87 (2004): 137-166.

Kokhanovsky, A. A. *Aerosol optics - Light Absorption and Scattering by Particles in the Atmosphere*. Chichester, UK: Springer-Praxis, 2008.

Kylling, B., and A. Mayer. "Technical Note: The libRadtran software package for radiative transfer calculations: Description and examples of use." *Atmospheric Chemistry and Physics* 5 (2005): 1855-1877.

Manins, P. *Australia State of the Environment Report 2001 (Theme Report)*. Sidney, Australia: CSIRO Atmospheric Research, 2001.

McCrone, W. C. *The particle atlas: a photomicrographic reference for the microscopical identification of particulate substances*. New York, USA: Ann Arbor Science Publishers, 1967.

McKinlay, A. F., and B. L. Diffey. "A reference action spectrum for ultraviolet induced erythema in human skin." *CIE Journal* 6 (1987): 17-22.

McNaught, A. D., and A. Wilkinson. *Compendium of Chemical Terminology: IUPAC Recommendations, 2nd Ed*. Hoboken, USA: Wiley-Blackwell, 1997.

Meehl, G. A., and C. Tebaldi. "More intense, more frequent and longer lasting heat waves in the 21st century." *Science* 305 (2004): 994-997.

Monfrecola, G., G. Fabbrocini, A. Del Sorbo, e E. Simeone. «Prevenzione del danno solare mediante dosimetria ultravioletta personalizzata: una nuova metodica con l'uso di telefonia cellulare.» *Annali Italiani di Dermatologia*, 2004.

Morelli, M., A. Masini, and M. A. C. Potenza. "Web tools concerning performance analysis and planning support for solar energy plants (PV, CSP, CPV) starting from remotely sensed optical images." *Proceedings of the "27th Enviroinfo Conference" – Hamburg, Germany*, 2013: 155-158.

Morelli, M., A. Masini, and M.A.C. Potenza. "A new method for the performance analysis of a concentrating solar power energy plant using remotely sensed optical images." *Proceedings of "ATMOS 2012 – Advances in Atmospheric Science and Applications" – Bruges, Belgium*, 2012: ESA SP-708.

Morelli, M., A. Masini, and M.A.C. Potenza. "Metodologie innovative per il support nella progettazione e l'analisi delle prestazioni di impianti ad energia solare a concentrazione ed eolici off-shore utilizzando immagini satellitari ottiche e SAR." *Bolletino della Associazione Italiana di Cartografia* 149 (2013): 103-115.

Morelli, M., A. Masini, and M.A.C. Potenza. "Metodologie innovative per il support nella progettazione e l'analisi delle prestazioni di impianti ad energia solare a concentrazione ed eolici off-shore utilizzando immagini satellitari ottiche e SAR." *Proceedings of the "16th Italian national conference ASITA 2012" - Vicenza, Italy*, 2012: 1001-1006.

Morelli, M., A. Masini, F. Ruffini, and M. A. C. Potenza. "Web tools concerning performance analysis and planning support for solar energy plants starting from remotely sensed optical images." *Environmental Impact Assessment Review* in press (2015 - in press).

Morelli, M., A. Masini, H. Diémoz, and M. A. C. Potenza. "Validazione di un sistema per il monitoraggio in quasi tempo reale e per la previsione a breve termine della radiazione UV a partire da immagini ottiche satellitari." *Proceedings of the "37th national meeting of the Italian National Association for Radioprotection" – Aosta, Italy*, 2014.

Morelli, M., and B. Canessa. "Nuovo teledosimetro UV mobile realizzato su periferiche Smartphone utilizzando dati di sensori ottici satellitari." *Proceedings of the "5th national meeting of the Italian Environmental Protection Agencies" – Novara, Italy*, 2012.

Morelli, M., and F. Flore. "Satellite data for solar ultraviolet and photovoltaic management services." *The growing use of GMES across Europe's Regions*, 2012: 120-121.

Mueller, R. W., C. Matsoukas, A. Gratzki, Behr H. D., and Hollmann R. "The CM-SAF operational scheme for the satellite based retrieval of solar surface irradiance — A LUT based eigenvector hybrid approach." *Remote Sensing of Environment* 113 (2009): 1012–1024.

NOAA. *U.S. Standard Atmosphere*. Washington D.C. (USA): U.S. Government Printing Office, 1976.

Oumbe, A., Z. Qu, P. Blanc, M. Lefèvre, L. Wald, e S. Cros. «Decoupling the effects of clear atmosphere and clouds to simplify calculations of the broadband solar irradiance at ground level.» *Geoscientific Model Development* 7 (2014): 1661-1669.

Papageorgas, P., D. Piromalis, K. Antonakoglou, G. Vokas, Tseles D., and K. G. Arvanitis. "Smart Solar Panels: In-situ monitoring of photovoltaic panels based on wired and wireless sensor networks." *Energy Procedia* 36 (2013): 535 – 545.

- Perez, R., P. Ineichen, R. Seals, J. Michalsky, and R. Stuart. "Modeling daylight availability and irradiance components from direct and global irradiance." *Solar Energy* 44 (1990): 271-289.
- Perez, R., P. Ineichen, R. Seals, Michalsky J., and Stuart R. "Modeling daylight availability and irradiance components from direct and global irradiance." *Solar Energy* 44 (1990): 271-289.
- Perez, R., R. Seals, P. Ineichen, Stewart R., e D. Menicucci. «A New Simplified Version of the Perez Diffuse Irradiance Model for Tilted Surfaces.» *1989* 44 (1989): 221-232.
- Powell, K. M., and T. F. Edgar. "Modeling and control of a solar thermal power plant with thermal energy storage." *Chemical Engineering Science* 71 (2012): 138-145.
- Qu, M., H. Yin, and D. H. Archer. "Experimental and Model Based Performance Analysis of a Linear Parabolic Trough Solar Collector in a High Temperature Solar Cooling and Heating System." *Solar Energy Engineering* 132 (2010): 021004.1-021004.12.
- Rigollier, C., O. Bauer, and L. Wald. "On the clear sky model of the 4th European Solar Radiation Atlas with respect to the Heliosat method." *Solar Energy* 68 (2000): 33-48.
- Seinfeld, J. H., and S. N. Pandis. *Atmospheric Chemistry and Physics*. New York, USA: Wiley, 1998.
- Shettle, E. P. "Models of aerosols, clouds and precipitation for atmospheric propagation studies, "Atmospheric Propagation in UV, Visible, IR and MM-Region and Related System Aspects." *AGARD Conference Proceedings* 454 (1989): 15-1 - 15-3.
- Stuetzle, T., N. Blair, J. Mitchell, and W. A. Beckman. "Automatic control of a 30 MWe SEGS VI parabolic trough plant." *Solar Energy* 76 (2004): 187-193.
- van de Hulst, H. C. *Light Scattering by Small Particles*. New York, USA: Wiley, 1957.
- Wallace, J. M., and P. Hobbs. *Atmospheric Science: an Introductory Survey*. London, UK: Academic Press, 1977.
- Wuttke, S., Verdebout J., and G. Seckmeyer. "An Improved Algorithm for Satellite-derived UV Radiation." *Photochemistry and Photobiology* 77 (2003): 52-57.
- Zerefos, C. S., and A. F. Bais. *Solar Ultraviolet Radiation: Modelling, Measurements and Effects*. Thessaloniki, Greece: Aristotle Univeristy of Thessaloniki, 1996.

8 APPENDICES

8.1 Appendix A: Publications

8.1.1 List of publications

8.1.1.1 Peer reviewed

- M. Morelli and F. Flore, *Satellite data for solar ultraviolet and photovoltaic management services*, ESA-NEREUS publication “The growing use of GMES across Europe’s Regions”, 120-121 (2012)
- M. Morelli, A. Masini, F. Ruffini and M. A. C. Potenza, *Metodologie innovative per il support nella progettazione e l’analisi delle prestazioni di impianti ad energia solare a concentrazione ed eolici off-shore utilizzando immagini satellitari ottiche e SAR*, Bolletino della Associazione Italiana di Cartografia **149**, 103-115 (2013)
- M. Morelli, A. Masini and M. A. C. Potenza, *Web tools concerning performance analysis and planning support for solar energy plants starting from remotely sensed optical images*, Environmental Impact Assessment Review - in press (2015)

8.1.1.2 Conference proceedings

- M. Morelli, A. Masini and M. A. C. Potenza, *A new method for the performance analysis of a concentrating solar power energy plant using remotely sensed optical images*, Proceedings of “ATMOS 2012 – Advances in Atmospheric Science and Applications” – Bruges, Belgium – **ESA SP-708** (2012)

- M. Morelli and B. Canessa, *Nuovo teledosimetro UV mobile realizzato su periferiche Smartphone utilizzando dati di sensori ottici satellitari*, Proceedings of the “5th national meeting of the Italian Environmental Protection Agencies” – Novara, Italy – ISBN: 978-88-7479-118-7 (2012)
- M. Morelli, A. Masini and M. A. C. Potenza, *Metodologie innovative per il support nella progettazione e l’analisi delle prestazioni di impianti ad energia solare a concentrazione ed eolici off-shore utilizzando immagini satellitari ottiche e SAR*, Proceedings of the “16th Italian national conference ASITA 2012” - Vicenza, Italy – 1001-1006 (2012)
- M. Morelli, A. Masini and M. A. C. Potenza, *Web tools concerning performance analysis and planning support for solar energy plants (PV, CSP, CPV) starting from remotely sensed optical images*, Proceedings of the “27th Enviroinfo Conference” – Hamburg, Germany – 155-158 (2013)
- M. Morelli, A. Masini, S. Venafra and M. A. C. Potenza, *New approaches to off-shore wind energy management exploiting satellite EO data*, Proceedings of “ESA Living Planet Symposium” – Edinburgh, UK – **ESA SP-722** (2013)
- M. Morelli, A. Masini and H. Diémoz and M. A. C. Potenza, *Validazione di un sistema per il monitoraggio in quasi tempo reale e per la previsione a breve termine della radiazione UV a partire da immagini ottiche satellitari*, Proceedings of the “37th national meeting of the Italian National Association for Radioprotection” – Aosta, Italy (2014)

8.1.2 Published peer-reviewed papers

8.1.2.1 In *ESA-NEREUS publication "The growing use of GMES across Europe's Regions"* (2012)



SATELLITE DATA FOR SOLAR ULTRAVIOLET AND PHOTOVOLTAIC MANAGEMENT SERVICES

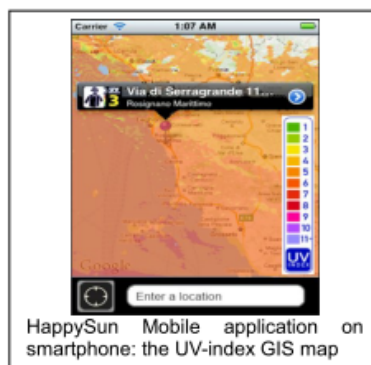
GMES-data are used for near-real-time services dedicated to sun exposure safety and to the analysis of solar plants' performance.

The challenge

In Europe about half a million skin cancer cases occur per year. This is strongly associated with personal habits in exposing to sun with poor protection against its ultraviolet (UV) component. The need to protect oneself depends mainly on the local UV index which can be derived in near real time from satellite data. Another challenge is the monitoring of solar plants. An early detection of the decline in energy production due to any malfunction can avoid a significant loss of income, especially for big plants. This can be done by comparing the actual energy production with the expected one, which can be estimated by means of satellite data.

Benefits to citizens

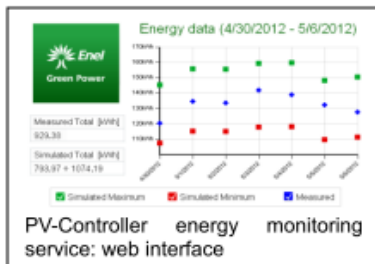
The UV information service 'HappySunMobile' was conceived for the



HappySun Mobile application on smartphone: the UV-index GIS map

Mediterranean area and has been delivered and continuously improved since 2006 to any interested regions.. Besides the UV-index, the 'Happysun Mobile' service provides sunburn times based on personal skin sensitivity and suggestions on the sunscreen protective factor to use. This information is delivered in near real time on the web or to smartphone users and is a valuable reference to reduce the risk of even mild skin damage. The 'PV-Controller' system provides the user with a continuous view of the energy production efficiency of his photovoltaic plant, thus allowing for timely interventions instead of periodic controls, with the benefit of achieving a fast payback and greatest income.

'PV-Controller is a very useful solution that makes us really confident in our solar plants' remote monitoring activity.' **Fabrizio Bizzarri, Enel Green Power**



The space-based solution

In 'HappySun Mobile', the UV index is calculated by a radiative transfer model which uses the ozone concentration and the cloud coverage retrieved from satellite sensors. The user's phototype and Minimum Erythral Dose (MED) are derived from a questionnaire regarding skin type and other meaningful user characteristics. The sunburn time is calculated correlating the MED, the UV index and the user choices regarding: sunscreen protection factor (SPF) and terrain type (to estimate the amount of UV radiation reflected towards the user). 'HappySun Mobile' has been validated by comparing the satellite UV-index with ground measurements by a spectroradiometer. The results showed an agreement better than 16% between UV -index derived from satellite and spectroradiometer in every meteorological condition. The 'PV-Controller' system uses solar radiation data based on MACC project core

Morelli, M. and Flore, F.

services. Using satellite based solar irradiance data and other parameters, like PV module temperature and ambient temperature, together with an accurate opto-electronic model of the PV plant, it evaluates the hourly producible energy and compares it to the produced energy. The plant efficiency is then presented on a website together with energy production, profitability and plant diagnostics. The typical error in the energy yield prediction (with respect to the real value) is always less than 10%, which is usually satisfactory for the customers

Outlook for the future

In the framework of the GMES project ENDORSE, the 'PV-Controller' system is currently being upgraded to also serve Concentrating Solar Plants. Both the UV and the solar plant monitoring services will be improved by taking into account the aerosol optical depth that is soon to be measured by TROPOMI on board the Sentinel-5 precursor and later by Sentinel-4 at an hourly rate.

Acknowledgements

'PV-Controller' and 'HappySun Mobile' services were developed by Flyby S.r.l. in the ESA-GSE project PROMOTE and the EC project MACC.

MACC: www.gmes-atmosphere.eu

PROMOTE: www.gse-promote.org

ENDORSE: www.endorse-fp7.eu



METODOLOGIE INNOVATIVE PER IL SUPPORTO ALLA
PROGETTAZIONE E ALL'ANALISI DELLE PRESTAZIONI DI
IMPIANTI AD ENERGIA SOLARE A CONCENTRAZIONE
ED EOLICI OFF-SHORE UTILIZZANDO IMMAGINI
SATELLITARI OTTICHE E SAR

*INNOVATIVE METHODOLOGIES TO SUPPORT THE DESIGN
AND PERFORMANCE ANALYSIS OF CONCENTRATED SOLAR
POWER PLANTS AND OFF-SHORE WIND POWER PLANTS
USING OPTICAL AND SAR SATELLITE IMAGERY*

Marco Morelli*, Andrea Masini, Marco Alberto Carlo Potenza***

Riassunto

In questo lavoro presentiamo delle nuove metodologie, sviluppate nell'ambito del progetto SATE-
NERG (Servizi sATEllitari per le ENergie Rinnovabili di nuova Generazione) finanziato dall'Agenzia
Spaziale Italiana, sia per il supporto alla progettazione/pianificazione che per il monitoraggio
quasi in tempo reale e l'analisi delle prestazioni degli impianti ad energia rinnovabile di nuova
generazione (CSP, CPV ed eolici *off-shore*) utilizzando immagini satellitari.

In particolare per quanto riguarda gli impianti solari a concentrazione (CSP e CPV), abbiamo
sviluppato un metodo per ricavare l'irradianza solare incidente al suolo (in particolare la sua
componente diretta normale rispetto ai raggi solari, fondamentale per questo tipo di impianti) da
immagini ottiche satellitari. Ciò, unito ad un modello di funzionamento di tali impianti e degli
inverter, ci ha resi in grado di poter sviluppare un servizio di supporto nella progettazione e piani-
ficazione di nuove costruzioni di impianti CSP e CPV (analizzando serie storiche di dati satellitari)
ed anche un servizio di monitoraggio e analisi delle prestazioni per quelli già esistenti (usando
invece immagini satellitari quasi in tempo reale).

In maniera simile, usando immagini SAR (*Synthetic Aperture Radar*), abbiamo sviluppato un me-
todo per ricavare l'intensità e la direzione del vento in aree marine da remoto che ci ha permesso,
utilizzando anche un modello di impianto eolico *off-shore* (turbina e *inverter*), di sviluppare sia
un servizio di supporto alla progettazione/pianificazione che un servizio di monitoraggio quasi
in tempo reale della produzione di un impianto eolico *off-shore*.

Le prime applicazioni di queste nuove metodologie hanno già portato ad avere ottimi risultati in
vari casi di prova sia per quanto concerne il monitoraggio dell'irradianza diretta su piano normale,
in cui l'irradianza misurata e quella ricavata da dato satellitare non si sono discostate più del 10%,

* Dipartimento di Fisica, Università degli Studi di Milano, Via Celoria 16, 20133 – Milano (Italia); marco.mo-
relli@unimi.it

** Flyby S.r.l., Via Puini 97, 57128 – Livorno (Italia)

sia per quanto riguarda il calcolo dell'intensità e direzione del vento da immagini SAR, in cui l'errore rispetto al dato misurato è rimasto al di sotto del 15%, fornendo quindi una buona base per il monitoraggio della energia AC prodotta dagli impianti.

Parole chiave: energie rinnovabili; monitoraggio da remoto; CSP; CPV; eolico *off-shore*; immagini satellitari ottiche; immagini satellitari SAR; Meteosat Second Generation; Cosmo-Skymed

Abstract

In this work we present new methodologies aimed to support both planning and near-real-time monitoring of new generation solar and wind energy plants (CSP, CPV and wind off-shore) using satellite imagery. Such methodologies are currently being developed in the scope of SATENERG, a project funded by ASI (Italian Space Agency).

In particular, for what concerns the concentrating solar energy plants (CSP and CPV) we developed a method to calculate solar irradiance at ground (and its direct normal component, that has primary importance in this type of plants) starting from satellite optical images. Then, using also detailed opto-electronic models of the plants and inverters, we are able to calculate the producible energy, which can be used to support either the design of potential plants (using historical series of satellite images) or the monitoring and performance analysis of existing plants (using near-real-time satellite imagery). Producible energy and other interesting parameters, like production efficiency, return on investment etc., are delivered through dedicated web services.

In a similar way, we developed also a method to calculate the intensity and the direction of off-shore wind from satellite SAR (Synthetic Aperture Radar) images that permitted us, together with detailed models of wind turbine and inverters, to develop a new service in support to both planning and near-real-time monitoring activities of off-shore wind plants.

The first applications of these methods gave successful results in several test cases: we obtained a maximum error of 10% for satellite retrieved direct normal solar irradiance and a maximum error of 15% for wind direction and intensity calculated from SAR images (with respect to in-situ measured data).

Keywords: renewable energies; remote monitoring; CSP; CPV; wind *off-shore*; optical satellite imagery; SAR satellite imagery; Meteosat Second Generation; Cosmo-Skymed

I. Introduzione

I.1 Contesto

L'incremento del consumo di energia, previsto per i prossimi anni è superiore al tasso di crescita delle fonti energetiche derivanti dai combustibili fossili (carbone, gas e petrolio), che rappresentano oggi all'incirca, l'80% dell'energia prodotta globalmente. Il problema di garantire un'abbondanza di disponibilità di fonti energetiche il cui uso abbia, al contempo, un impatto limitato sul sistema ambientale è una delle grandi sfide per prossimi decenni.

Un modo concreto per affrontare il problema energetico, che è stato adottato dall'Italia e da altri paesi, è quello di favorire, anche tramite l'introduzione di un'apposita legislazione, un uso sempre maggiore di energie rinnovabili. Le potenzialità dell'energia solare ed eolica, pur essendo note da anni, iniziano ad essere sfruttate solo oggi. Data la variabilità non facilmente prevedibile che caratterizza queste due fonti energetiche, l'installazione di nuovi impianti richiede un'attenta analisi in termini di pianificazione e operatività. Strumenti capaci di fornire un'accurata stima delle risorse sono quindi fortemente richiesti dagli investitori che hanno la necessità di pianificare il rientro degli investimenti necessari a finanziare la costruzione di nuovi impianti energetici. Prima di giungere ad un uso fattuale

dell'energia solare e di quella eolica, è fondamentale, quindi, valutare la loro disponibilità tramite il monitoraggio dei parametri ambientali significativi. Può accadere, però, come nel caso di impianti eolici *off-shore*, che le tecniche standard per il monitoraggio dei dati ambientali, basate sull'uso di sensori in situ, siano particolarmente onerose.

Una significativa riduzione dei costi può, allora, essere ottenuta impiegando metodi di monitoraggio che usano tecniche di misura satellitare per valutare la quantità di energia producibile in una certa località. Inoltre sin dall'inizio dell'attività produttiva dell'impianto energetico, è necessario uno strumento che consenta di monitorare e gestire in modo ottimale la produttività dell'impianto così da aumentarne l'efficienza e da garantire una riduzione dei costi operativi. Un metodo efficace ed economicamente sostenibile per questo scopo, è il controllo dell'impianto tramite il confronto tra la potenza prodotta e quella prevista da opportuni metodi di simulazione, che usano dati satellitari per la stima dei parametri ambientali coinvolti nella produzione.

1.2 Il progetto SATENERG

SATENERG è un progetto finanziato dall'Agenzia Spaziale Italiana (ASI) nell'ambito del 2° Bando Tematico P.M.I. "Osservazione della Terra" dedicato all'utilizzo di dati satellitari per servizi nell'ambito delle energie rinnovabili. I partner del progetto sono l'azienda Flyby S.r.l. di Livorno (*Prime Contractor*) e l'azienda PXL di Roma.

Al fine di orientare, il più possibile, lo sviluppo dei servizi verso le effettive richieste del mercato, è stato coinvolto come utente di riferimento del progetto ENEL Green Power S.p.a (ENEL GP), che ha formalmente espresso il suo interesse per le attività di SATENERG.

Il progetto mira a sviluppare servizi di pianificazione e monitoraggio della produzione energetica da fonti rinnovabili sfruttando dati satellitari EO (*Earth Observation*) e tecniche di modellizzazione. Gli impianti oggetto di tali servizi sono gli impianti eolici *off-shore*, solari termodinamici (CSP) e fotovoltaici a concentrazione (CPV).

Per offrire questo tipo di servizi si propone di stimare due principali entità fisiche:

- l'intensità e della direzione del vento in mare aperto;
- l'irradianza solare a terra.

La stima del vento è di fondamentale importanza per assistere la progettazione e il monitoraggio di impianti eolici *off-shore*. Il progetto SATENERG ha l'obiettivo di analizzare e sviluppare le metodologie satellitari per la stima dei venti, in particolare si pianifica di sviluppare una nuova metodologia per la stima dei venti in banda X (permettendo l'utilizzo dei dati COSMO/SKYMED per questa finalità) e di investigare altre possibilità come l'uso di scatterometri e SAR in banda C.

Per quanto riguarda invece la stima della quantità di energia solare che giunge a terra, essa è fondamentale per assistere l'industria energetica nella progettazione e nel monitoraggio di impianti solari termodinamici e di impianti fotovoltaici a concentrazione. Il progetto prevede di utilizzare i dati del satellite MSG (SEVIRI) e contemplare i sensori MIOSAT e PRISMA per un futuro utilizzo con questa applicazione.

I servizi di assistenza nella produzione energetica da fonti rinnovabili che saranno sviluppati all'interno del progetto SATENERG consistono in due aspetti:

- supporto alla progettazione dell'impianto;
- supporto per la gestione dell'impianto.

2. Stima del vento e dell'irradianza solare dai satelliti di osservazione della Terra

2.1 Stima del vento in ambiente marino

L'estrazione di informazioni ambientali da immagini SAR oceaniche è stata un'area di ricerca per molti anni, e molteplici approcci sono stati sviluppati per caratterizzare una vasta serie di parametri:

- onde;
- venti;
- correnti.

Nel progetto SATENERG l'attenzione si concentra maggiormente sull'uso di immagini SAR per la stima di vettori di vento in acque marine, costiere e non. Quasi tutte le metodologie di estrazione di informazioni oceaniche da immagini SAR si basano sulla teoria di *scattering* dell'oceano (*scattering* Bragg). Questa teoria, presuppone che le variazioni della luminosità (o intensità) delle immagini SAR siano proporzionali all'ampiezza delle onde superficiali oceaniche. Secondo questa teoria le onde che scatterano maggiormente hanno un numero d'onda K_b tale che:

$$K_b = 2K_{em} \sin(\vartheta) \quad [1]$$

dove K_{em} è il numero d'onda della radiazione elettromagnetica incidente e ϑ l'angolo con cui incide. Ciò significa che si avrà maggiore evidenza dello *scattering* da onde di piccola scala.

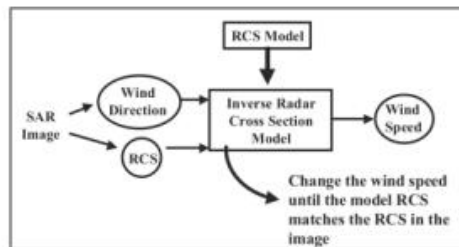


Fig. 1 – Schema dell'algoritmo per la stima del vento da immagini SAR
Fonte: Staffelen, 1997.

Considerando che il responsabile delle onde di piccola scala è proprio il vento locale, è da queste considerazioni che derivano i vari approcci, presentati in letteratura, per stimarlo. Questo fatto, infatti implica, che la RCS (*Radar Cross Section*) dell'immagine SAR possa essere collegata alla velocità e alla direzione del vento locale. L'approccio generale per la stima del vento è illustrato nella Figura 1. Alla base di tutto viene utilizzato un modello che metta in relazione la RCS con la velocità e la direzione del vento (Nirchio, 2010). La procedura generale è quella di stimare inizialmente la direzione del vento e successivamente trovare la velocità del vento che riproduce la RCS osservata. Ciò che differenzia i diversi approcci sono il modello di RCS utilizzati e il modo con cui viene stimata la direzione del vento.

Per la Missione ESA ERS-1/2 (sensori SAR in banda C che operano in polarizzazione VV) alcuni modelli di RCS sono stati presentati e validati. Per la missione canadese RADARSAT-1 (sensore SAR in banda C che opera in polarizzazione HH), in letteratura sono stati presentati due diversi approcci. Il primo è quello di modificare empiricamente i modelli VV per adattarli alla polarizzazione HH. Il secondo approccio è quello di analizzare nuovi modelli direttamente per la polarizzazione HH.

Per la missione ENVISAT (sensore SAR in banda C) sono due i modelli, derivanti dagli approcci seguiti per la missione ERS 1/2, che hanno portato ai migliori risultati:

- CMOD4 sviluppato dall'Agenzia Spaziale Europea;
- CMOD_IFR2.

Vari approcci sono stati sviluppati anche per stimare la direzione del vento. Una classe di metodologie sfrutta l'immagine SAR anche per stimare questo parametro osservando che ci sono caratteristiche nelle immagini che tendono ad essere allineate con il vento locale. Il vantaggio di questa classe di approcci è stimare il vettore di vento dal solo dato SAR senza riferimento ad altre sorgenti. Lo svantaggio è che la direzione del vento risultante ha ambiguità di 180° e che le caratteristiche che vengono utilizzate non sempre sono presenti nell'immagine SAR.

La seconda classe di approcci utilizza contemporaneamente altri satelliti (ad esempio scatterometri) o fa uso di modelli atmosferici da cui derivare questo parametro. La recente possibilità di poter usufruire di nuove costellazioni in banda X (COSMO/SKYMED, TerraSARX) sta focalizzando l'interesse del mondo accademico verso lo sviluppo di metodologie (XMOD) per la stima di parametri utilizzando queste nuove sorgenti di dati.

Se per l'utilizzo di dati della missione TerraSAR-X in letteratura è possibile trovare alcuni risultati, sono molto poche ad oggi le metodologie che sfruttino la costellazione Cosmo/SkyMed e la definizione di nuove metodologie per la stima del vento utilizzando questa costellazione garantirebbe lo sfruttamento di nuovi dati per applicazioni facilmente sfruttabili commercialmente.

2.2 Stima dell'irradianza solare al suolo

Lo sfruttamento dei dati di osservazione della Terra per la stima della radiazione solare che giunge al suolo è stata oggetto di molte ricerche che hanno portato alla definizione della metodologia denominata Heliosat. La tecnica Heliosat per l'analisi di immagini satellitari fu introdotta per la prima volta da Cano (Cano, 1986) e nel corso degli anni è stata più volte validata ed oggetto di studi migliorativi (Rigollier, 2000) che hanno introdotto nuove metodologie per calcolare l'indice di nuvolosità, di cielo sereno e l'irradianza globale orizzontale nel caso di cielo sereno. Tale tecnica è pertanto ad oggi una metodologia standard e affidabile.

Heliosat è uno dei metodi più usati per ottenere da dati ambientali rilevati con tecniche di misura satellitare, l'irradianza globale orizzontale sulla superficie terrestre. I suoi aspetti chiave sono:

- la conversione dell'immagine satellitare in una matrice di "indici di nuvolosità";
- la conversione dell'indice di nuvolosità in "indice di cielo sereno";
- il modello per il calcolo dell'irradianza globale orizzontale in condizioni di cielo sereno.

L'indice di nuvolosità rappresenta una sorta di attenuazione della radiazione dovuta all'atmosfera. Per il suo calcolo è anche necessario una serie temporale di immagini satellitari, insieme con la corrispondente informazione (*Cloud Mask*) sulla presenza o meno di nuvole al momento della rilevazione della radiazione da parte dei pixel del sensore. L'indice di nuvolosità è quindi collegato, da una rela-

zione lineare, all'indice di cielo sereno che rappresenta il rapporto tra l'irradianza globale orizzontale (la grandezza che si vuole calcolare) e l'irradianza globale orizzontale in condizioni di cielo sereno. Stimando quest'ultima per mezzo di un modello di atmosfera priva di nubi (Rigollier, 2000), si può infine ricavare l'irradianza globale orizzontale.

Questo metodo è applicato a immagini acquisite da satelliti meteorologici geostazionari, quali Meteosat (EUMETSAT), GOES (NASA) e GMS (NASDA). La metodologia appena descritta potrà essere adattata ai dati che verranno raccolti dal sistema PRISMA, che avrà anche un sensore iperspettrale che rileverà la radiazione nell'intervallo $0.4-2.5 \mu\text{m}$, avrà una risoluzione spaziale di 20-30 metri e annovererà tra i prodotti di livello I la *Cloud Mask*. Si potrà valutare l'applicazione di questa metodologia anche ai dati raccolti con il sensore MIOSAT.

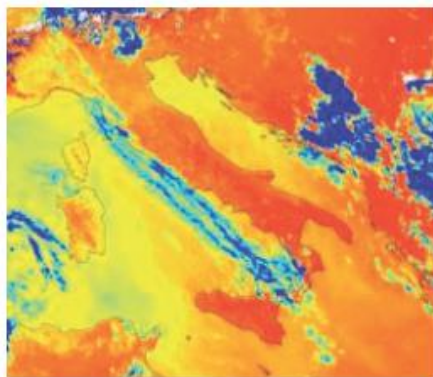


Fig. 2 – Mappa di irradiazione solare ricavata usando il modello Heliosat ed immagini del satellite MSG
Fonte: elaborazione dati MSG effettuata da Flyby, 2013.

3. La modellizzazione degli impianti

Partendo dai parametri ambientali stimabili sfruttando i dati satellitari è possibile, utilizzando opportuni modelli che descrivono il comportamento degli impianti, calcolare la potenza producibile dall'impianto e confrontarla con quella effettivamente prodotta ai fini di un monitoraggio delle prestazioni.

3.1 Gli impianti eolici *off-shore*

Il modello di impianto eolico *off-shore* che sarà considerato include due elementi:

- il campo di vento;
- le turbine eoliche.

La turbina eolica è un trasformatore di energia con, in ingresso, l'energia eolica e, in uscita, la potenza prodotta. Quando il vento attraversa le pale della turbina parte della sua energia cinetica è trasferita al rotore. La frazione di potenza che è estratta dalla potenza eolica (stimabile dalla velocità del vento, dalla densità dell'aria e dal raggio delle pale della turbina) può essere calcolata tramite un coefficiente che dipende, esso stesso, dalla velocità del vento e dall'angolo di beccheggio della pala eolica.

3.2 Gli impianti CSP

Gli impianti solari termodinamici sfruttano la radiazione solare diretta su superficie normale per produrre energia. La conoscenza di questa quantità è essenziale, sia nella fase di pianificazione, per valutare la fattibilità finanziaria di un nuovo impianto produttivo, che nella fase operativa, per un'accurata analisi delle prestazioni del sistema.

I principali dati necessari per la modellizzazione di un campo solare sono:

- la temperatura e la portata del fluido termovettore;
- l'irradianza solare diretta su superficie normale;
- la temperatura ambiente;
- la velocità del vento.

In uscita dal campo solare, il modello, tramite l'analisi del bilancio energetico tra la potenza assorbita dal fluido termovettore e quella ceduta all'ambiente circostante, fornirà i seguenti risultati:

- la temperatura del fluido termovettore;
- la potenza assorbita;
- la potenza ceduta all'ambiente;
- l'efficienza istantanea del campo.

Altri aspetti significativi della modellizzazione del campo solare riguardano:

- l'ottica degli specchi (caratteristiche quali la forma e le proprietà riflettenti);
- la pellicola sulla superficie del tubo ricevitore).

3.3 Gli impianti CPV

I sistemi fotovoltaici a concentrazione sono generalmente costituiti da:

- un sistema ottico di specchi riflettenti o di lenti refrattive che concentrano la radiazione solare su dei moduli fotovoltaici;
- un sistema di inseguimento del sole.

I sistemi fotovoltaici concentrati sono usualmente classificati in sistemi a bassa, media e alta concentrazione, a secondo del rapporto tra l'area della superficie effettiva su cui incide la radiazione solare e l'area della superficie dei moduli su cui la radiazione viene concentrata.

I sistemi fotovoltaici a bassa concentrazione sono i più diffusi.

Come nel caso dei sistemi CSP, l'unica componente della radiazione solare che può essere concentrata è quella diretta su superficie normale, la cui conoscenza è fondamentale sia al momento di pianificare l'installazione di un nuovo impianto, per la valutare la fattibilità finanziaria, sia durante la fase operativa dell'impianto, per analizzarne accuratamente le prestazioni.

Gli altri due aspetti significativi della modellizzazione degli impianti CPV sono:

- la geometria degli specchi riflettenti;
- i moduli fotovoltaici.

I moduli, essendo quelli utilizzati nei sistemi fotovoltaici tradizionali, possono essere modellizzati tramite delle tecniche ben collaudate. Una di queste prevede la rappresentazione del modulo fotovol-

taico tramite un circuito equivalente costituito da un generatore di corrente (fotovoltaica), collegato in serie con una resistenza e in parallelo con un diodo ed un'altra resistenza.

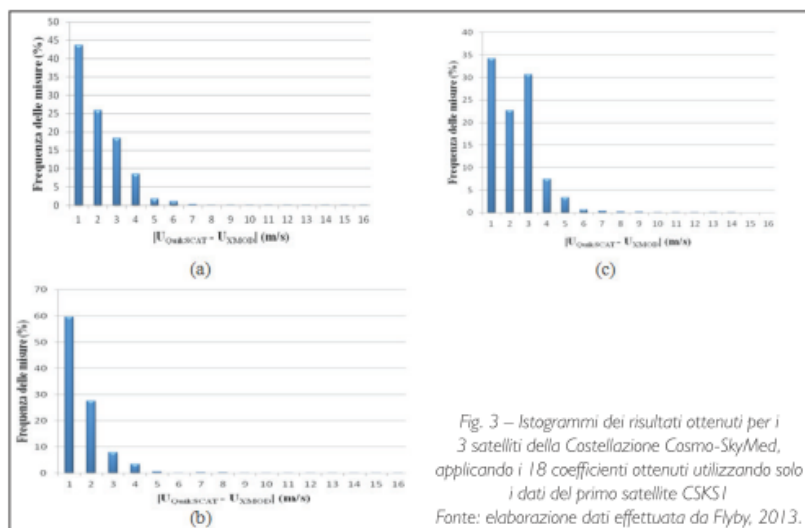
4. Risultati

Le prime applicazioni di questi metodi hanno già portato ad avere ottimi risultati in vari casi di test sia per quanto concerne il monitoraggio dell'irradianza diretta su piano normale, in cui l'irradianza misurata e quella ricavata da dato satellitare non si sono discostate più del 10%, sia per quanto riguarda il calcolo dell'intensità e direzione del vento da immagini SAR, in cui l'errore rispetto al dato misurato è rimasto al di sotto del 15%, fornendo quindi una buona base per il monitoraggio della energia AC prodotta dagli impianti e per i servizi web.

4.1 Impianti eolici *off-shore*

Il confronto dell'intensità di vento stimata dall'XMOD e i valori di riferimento è stato effettuato su un data set costituito dalle stesse immagini utilizzate per il calcolo dei parametri del modello usato in (Nirchio, 2010), validando i risultati con l'integrazione di immagini acquisite sul Mar Mediterraneo per le quali fossero disponibili i dati QuikSCAT e quelli di ECMWF.

Per ognuno dei 3 satelliti della Costellazione Cosmo-SkyMed allora in orbita, si è verificata l'accuratezza dell'intensità di vento stimata. Per CSKS1 (1° satellite della Costellazione) si è misurata una RMS di circa 1.55 m/s con una deviazione standard di 1.26 m/s (Figura 3a). Per CSKS2, RMS=1 m/s con deviazione standard pari a 1.2 m/s (Figura 3b). Infine per CSKS3 i risultati non sono dei migliori in quanto solo il 57% delle misure disponibili ha una RMS con QuikSCAT compresa tra 1 e 2 m/s (Figura 3c), forse giustificato dal fatto che tali misure si discostano evidentemente da quelle degli altri due sensori, rendendo il terzo sensore indipendente dagli altri due, dal punto di vista delle misure, come si evince dalla Figura 4.



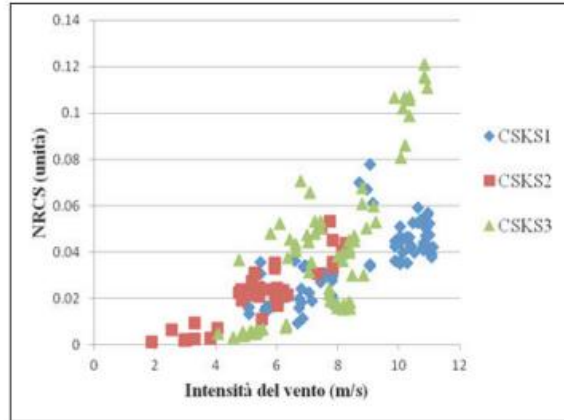


Fig. 4 – Distribuzione della $\sigma_0 \sigma_0$ in funzione dell'intensità del vento fissato l'angolo d'incidenza tra 30° e 35° per tutti e 3 i sensori della Costellazione Cosmo-SkyMed.
Fonte: elaborazione dati effettuata da Flyby, 2013.

Analizzando i risultati ottenuti si può affermare che l'implementazione dell'XMOD possa considerarsi abbastanza soddisfacente. Tali misure forniscono un ottimo punto di riferimento per le previsioni meteorologiche, la navigazione, le variazioni climatiche, le previsioni di disastri naturali e/o pericoli ambientali, per il monitoraggio del vento in prossimità di impianti eolici offshore, etc. a livello mondiale. Esso rappresenta un modello preliminare per la stima del vento sul mare da dati SAR in banda X: un aspetto che richiederà ulteriori approfondimenti è quello che riguarda il range dei dati usati nello sviluppo del modello che, nella presente sperimentazione, copre venti d'intensità compresa tra i 2 e gli 8 m/s. In futuro sarà necessario estendere questo range a venti che raggiungano i 25 m/s. In secondo luogo si vorrebbe anche comprendere le motivazioni per cui c'è un miglior accordo tra i risultati ottenuti confrontando CSKS1 e CSKS2 con QuikSCAT, rispetto a quelli ottenuti tra CSKS3 e QuikSCAT.

Come già accennato precedentemente, una miglioria apportabile all'XMOD [RD1] è stata realizzata con l'implementazione dell'XMOD2 (sviluppato precedentemente al progetto SATENERG e in attesa di essere pubblicato). Similmente a ciò che è stato fatto in banda C con il CMOD4, anche in banda X si è pensato di separare l'intensità del vento in due range e di determinare due diversi set di coefficienti, uno per i venti bassi e l'altro per i venti alti. È stato quindi necessario acquisire nuovi dati Cosmo-SkyMed in zone in cui è nota una ventosità alta (al largo dell'Islanda, del Regno Unito, dell'Alaska e del Canada nell'Oceano Atlantico). Il confronto tra i dati calcolati con l'XMOD2 e i dati di verità a terra (QuikSCAT, NCEP, etc.) ha fornito una RMS pari a 0.8 m/s per i venti di bassa intensità (Figura 5a) e uguale a circa 2 m/s per i venti alti (Figura 5b).

Nella Figura 6 è possibile visualizzare direttamente il confronto tra i dati di vento XMOD2 e quelli di riferimento (QuikSCAT ed NCEP) sia per i venti di bassa intensità che per quelli ad elevata intensità.

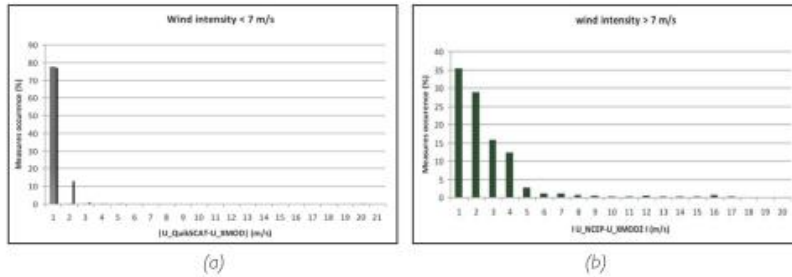


Fig. 5 – Istogrammi dei risultati ottenuti per il primo satellite della Costellazione Cosmo-SkyMed CSKS1 con XMOD2, rispettivamente per venti bassi (a) e per venti alti (b)
 Fonte: elaborazione dati effettuata da Flyby, 2013.

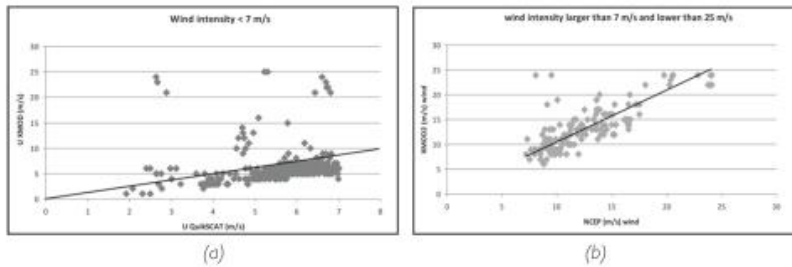


Fig. 6 – Scatter Plot dei risultati ottenuti con XMOD2, rispettivamente per venti bassi (a) e per venti alti (b)
 Fonte: elaborazione dati effettuata da Flyby, 2013.

A differenza dei risultati ottenuti con l'XMOD, anche le misure relative ai sensori CSKS2 (Figura 7a – 7b) e CSKS3 (Figura 8a – 8b), hanno prodotto un buon accordo in termini di intensità di vento se confrontate coi dati di riferimento. Si potrebbe pensare di migliorare ulteriormente l'XMOD2 cercando di ottenere un set di dati più completo soprattutto nei range in cui il data set precedente era carente.

La validazione dell'algoritmo per la stima del vento in banda C (Stoffelen, 1997), ovvero il CMOD4, ha invece prodotto un'accuratezza pari a ± 1.2 m/s in mare aperto con una deviazione standard di circa 0.5-1 m/s.

A partire dalla stima del vento effettuata è poi possibile calcolare la potenza AC prodotta da un impianto eolico *off-shore* localizzato in tale sito usando una modellizzazione matematica delle prestazioni di una o più turbine eoliche e degli inverter collegati (Powell, 1981).

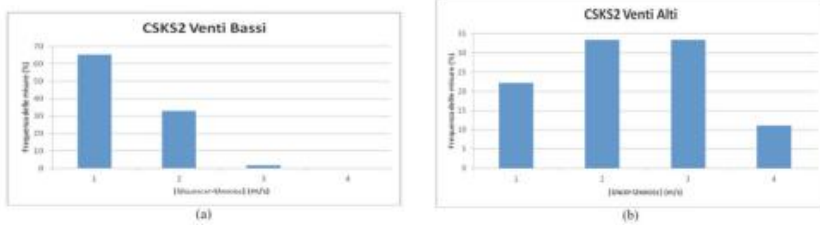


Fig. 7 – Istogrammi dei risultati ottenuti per CSKS2 con XMOD2, rispettivamente per venti bassi (a) con una RMS pari a 0.7 m/s e per venti alti (b) con RMS uguale a 1.7 m/s
Fonte: elaborazione effettuata da Flyby, 2013.

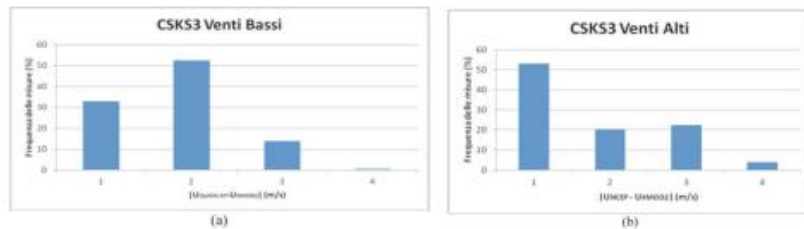


Fig. 8 – Istogrammi dei risultati ottenuti per CSKS3 con XMOD2, rispettivamente per venti bassi (a) con una RMS pari a 1.27 m/s e per venti alti (b) con RMS uguale a 1.3 m/s
Fonte: elaborazione dati effettuata da Flyby, 2013.

4.2 Impianti ad energia solare

Nel caso degli impianti ad energia solare è stato ottenuto un ottimo riscontro fra l'irradianza calcolata da satellite e quella misurata *in-situ*: in generale l'accordo fra i dati rientra nella soglia del 15% per condizioni meteorologiche nuvolose e sotto il 5-10% in condizioni di cielo sereno.

Allo stesso modo anche il test di utilizzo del nuovo metodo nel processo di monitoraggio della produzione di impianti fotovoltaici (pre-esistente) ha condotto ad ottimi risultati, confermando un accordo compreso tra il 5% ed il 10% fra la produzione di potenza AC ricavata a partire da immagini satellitari e quella invece misurata al contatore *in-situ*. Infatti utilizzando i dati di irradianza solare incidente a terra ricavati da satellite è stato possibile ricavare la produzione di potenza AC attesa utilizzando un modello opto-elettronico dell'impianto solare (Eicker, 2003).

Ad esempio nel caso di un impianto test in cui sono state effettuate misurazioni per un periodo di circa otto mesi (aprile – dicembre 2012), il confronto fra la potenza AC oraria misurata e quella calcolata a partire da dati satellitari ha portato ad ottenere un coefficiente di correlazione pari a 0.9075 ed una RMS del 2.06% (come mostrato in Figura 9).

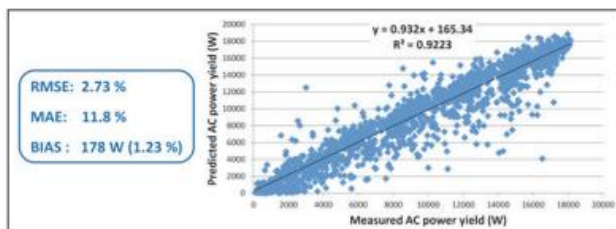


Fig. 9 – Confronto nel caso di un impianto fotovoltaico di 20 kWp installato presso Baucina, Sicilia (periodo aprile-dicembre 2012) fra la produzione di potenza AC misurata e quella calcolata a partire da dati satellitari
Fonte: elaborazione dati effettuata da Flyby, 2012.

Utilizzando la nuova metodologia sviluppata è stata anche prodotta una mappa dell'irradiazione diretta annuale media incidente su di un piano ad inseguimento solare in Italia. A tal fine sono state elaborate le immagini MSG relative agli ultimi 5 anni ed il risultato (riportato su mappa GIS) è raffigurato in Figura 10.

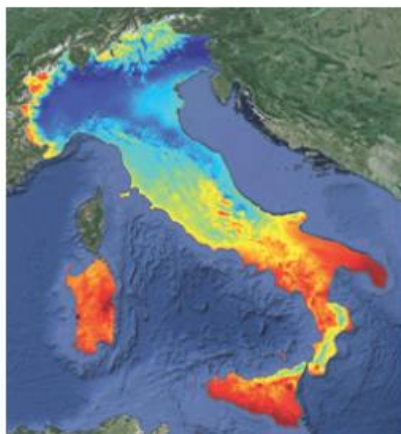


Fig. 10 – Esempio di mappa GIS dell'irradiazione annuale media incidente su di un piano ad inseguimento solare in Italia ricavata dall'applicazione della nuova metodologia EO ad una serie di immagini satellitari MSG di archivio
Fonte: elaborazione dati effettuata da Flyby, 2013.

È attualmente in corso di messa a punto la parte di modellizzazione degli impianti CSP e CPV, a cui sarà applicata la stessa metodologia sopra descritta per poterne monitorare le prestazioni partendo dal calcolo dell'irradianza solare incidente a terra da immagini ottiche satellitari.

I test saranno effettuati utilizzando i dati di produzione di alcuni impianti CSP e CPV messi a disposizione dall'utente di riferimento Enel Green Power.

Bibliografia

- CANO D., MONGET J.M., ALBUSSON M., GUILLARD H., REGAS N., e WALD L. (1986), A method for the determination of the global solar radiation from meteorological satellite data, "Solar Energy", 37, pp. 31-39.
- EICKER U. (2003), Solar technologies for buildings, John Wiley & Son Ltd, Chichester (UK).
- NIRCHIO F. e VENAFA S. (2010), *Preliminary model for wind estimation from Cosmo/SkyMed X band SAR data*, in *Conference Proceedings: Proceedings of 2010 IEEE International Geoscience and Remote Sensing Symposium (IGARSS)*, Institute of Electrical and Electronics Engineers (IEEE), Honolulu (USA), pp. 3462 –3465.
- POWELL W. R. (1981), An Analytical Expression for the Average Output Power of a Wind Machine, "Solar Energy", 26, pp. 77-80.
- RIGOLIER C., BAUER O. e WALD L. (2000), On the clear sky model of the 4th European Solar Radiation Atlas with respect to the Heliosat method, "Solar Energy", 68, pp. 33-48.
- STOFFELEN A. e ANDERSON D. (1997), Scatterometer Data Interpretation: Measurement and inversion, "Journal of Atmospheric and Oceanic Technology", 14, pp. 1298-1313.

8.1.2.1 In *Environmental Impact Assessment Review* (2015 – in press)

ARTICLE IN PRESS

EIR-05931; No of Pages 6

Environmental Impact Assessment Review xxx (2014) xxx–xxx

Contents lists available at ScienceDirect

Environmental Impact Assessment Review

journal homepage: www.elsevier.com/locate/eiar



Web tools concerning performance analysis and planning support for solar energy plants starting from remotely sensed optical images

Marco Morelli ^{a,*}, Andrea Masini ^b, Fabrizio Ruffini ^c, Marco Alberto Carlo Potenza ^a

^a Department of Physics, University of Milano, Via Celoria 16, 20133 Milano, Italy

^b Fbyby S.r.l. Via Paitini 97, 57128 Livorno, Italy

^c I-EM S.r.l. Via Lampredi 45, 57121 Livorno, Italy

ARTICLE INFO

Available online xxxxx

Keywords:
Satellite optical imagery
Web tools
Near real-time performance analysis
Planning support
Solar energy plants

ABSTRACT

We present innovative web tools, developed also in the frame of the FP7 ENDORSE (ENergy DDownstReam Services) project, for the performance analysis and the support in planning of solar energy plants (PV, CSP, CPV). These services are based on the combination between the detailed physical model of each part of the plants and the near real-time satellite remote sensing of incident solar irradiance.

Starting from the solar Global Horizontal Irradiance (GHI) data provided by the Monitoring Atmospheric Composition and Climate (GMES-MACC) Core Service and based on the elaboration of Meteosat Second Generation (MSG) satellite optical imagery, the Global Tilted Irradiance (GTI) or the Beam Normal Irradiance (BNI) incident on plant's solar PV panels (or solar receivers for CSP or CPV) is calculated. Combining these parameters with the model of the solar power plant, using also air temperature values, we can assess in near-real-time the daily evolution of the alternate current (AC) power produced by the plant. We are therefore able to compare this satellite-based AC power yield with the actually measured one and, consequently, to readily detect any possible malfunctions and to evaluate the performances of the plant (so-called "Controller" service). Besides, the same method can be applied to satellite-based averaged environmental data (solar irradiance and air temperature) in order to provide a Return on Investment analysis in support to the planning of new solar energy plants (so-called "Planner" service).

This method has been successfully applied to three test solar plants (in North, Centre and South Italy respectively) and it has been validated by comparing satellite-based and in-situ measured hourly AC power data for several months in 2013 and 2014. The results show a good accuracy: the overall Normalized Bias (NB) is -0.41% , the overall Normalized Mean Absolute Error (NMAE) is 4.90% , the Normalized Root Mean Square Error (NRMSE) is 7.66% and the overall Correlation Coefficient (CC) is 0.9538 . The maximum value of the Normalized Absolute Error (NAE) is about 30% and occurs for time periods with highly variable meteorological conditions.

© 2014 Elsevier Inc. All rights reserved.

Introduction

Context

One of the major global challenges in the near future is how to provide energy in abundance, and to be able to provide this energy from sources with a limited impact on the environment. The electricity consumption in the European Union has been estimated to rise by 50% from 2000 to 2020 (Eicker, 2003) and the exploitation of renewable energy in an efficient as possible way is fundamental to face the energy demand avoiding a strong increase of air pollution.

An effective and tangible approach to solve the energy production problem, used in Italy and in other countries, involves an improvement of the use of the solar energy solution. This could be also favoured by the introduction of specific laws. The solar energy production potentialities are well known, but they have begun to be fully developed only in recent years. Given the large variability, non-easily predictable, of the solar source, the planning and installation of new power plants require a careful a priori analysis. Therefore, the presence of services able to provide an accurate estimation of available energy sources is extremely important for the investors, that are given the possibility to evaluate the repayment plan when planning new plants. A service providing this kind of information can use standard techniques, such as in-situ measurements of the solar energy available in a certain location, but this kind of approach can be significantly expensive. On the contrary, cost reductions can be the strength of alternative approaches, such as planning support systems using data remotely sensed by satellites (Mueller et al., 2009).

* Corresponding author. Tel.: +39 0586 505016.
E-mail addresses: marco.morelli1@unimi.it (M. Morelli), andrea.masini@fbyby.it (A. Masini), fabrizio.ruffini@i-em.eu (F. Ruffini), marco.potenza@unimi.it (M.A.C. Potenza).

<http://dx.doi.org/10.1016/j.eiar.2014.10.003>
0195-9255/© 2014 Elsevier Inc. All rights reserved.

Please cite this article as: Morelli M, et al, Web tools concerning performance analysis and planning support for solar energy plants starting from remotely sensed optical images, Environ Impact Asses Rev (2014), <http://dx.doi.org/10.1016/j.eiar.2014.10.003>

Furthermore, when the energy plant begins its activity, a service able to monitor the productivity of the plant so to improve it and increase the efficiency is necessary for cost reductions. An effective and low-cost approach is to use a service able to compare the power actual produced with the power predicted by a model. The model uses data from satellite to evaluate the environmental parameters needed to calculate the expected power production in well-functioning conditions.

"Planner" and "Controller" web tools

In order to face the problems related to planning and monitoring of solar energy plants described before, we developed two innovative web tools based on Earth Observation (EO) optical imagery: the "Planner" and the "Controller" services.

Both the services start from temporal series of solar GHI provided by the MACC Core Service, that is calculated from Meteosat Second Generation (MSG) optical imagery by means of the Heliosat-2 algorithm (Cano et al., 1986) and the ESRA model for clear-sky solar irradiance (Rigollier, 2000).

The "Planner" service consists of a web-GIS map showing average solar irradiance (Beam Normal Irradiance for CSP or CPV plants; Global Horizontal Irradiance for PV plants) and average air temperature, both obtained from historical satellite optical imagery archive (air temperature data lacks are filled by a spatial interpolation of the data provided by the meteorological stations of the Italian AirForce). The service shows the monthly averaged expected energy yield starting from site selection and planned plant technical features, providing also an estimate of the Return on Investment (break-even point and cumulative cash-flow).

The "Controller" service, instead, is in practice of an active solar plant production monitoring web-service that, starting from the near real-time calculation of the expected energy yield based on satellite-based incident solar irradiance, can provide a malfunctioning daily detection with an embedded email/SMS alerting system.

These services are currently available for PV, CSP and CPV plants. The spatial coverage comprises Italy, North-Africa and Brazil but it's going to be extended also to other regions (such as Brazil).

Methods

Both the "Planner" and the "Controller" web services are based on a similar scheme (as shown in Fig. 1); satellite-based irradiance data and air temperature data are set as inputs to a detailed physical model of the solar energy plant (PV, CPV or CSP) and of the inverters to calculate the expected AC power yield. The solar irradiance data have 4 km spatial resolution (in Italy) and 15 minute time resolution (following the MSG satellite resolution), whilst the air temperature data could have the same resolution if obtained from MSG or 30 km of spatial resolution and 3-hourly temporal resolution if obtained from Italian AirForce measured data.

The same scheme can be applied in the frame of the "Planner" service by using environmental data retrieved from historical long time-series of satellite imagery, whilst in the "Controller" service case the satellite-based data are elaborated in near real-time (i.e. with a maximum 24 hour delay and 15-min temporal resolution) to calculate the plant's performances for monitoring purposes. The plant's modelling part of the method, of course, is different depending on the type of solar energy plant of interest.

The interfaces of both services are based on web-GIS standards (such as GeoTIFF) and data are elaborated using also the PostgreSQL database with PostGIS extension.

CSP plants

A thermodynamic solar plant uses the direct solar radiation by reflecting it towards a concentrating point where a fluid is heated. The radiation intensity is hence a fundamental parameter for the plant planning and for its financial evaluation, but it is also a critical information in the operational mode of the plant, since it allows an accurate analysis of the plant performances.

The model has been developed in the frame of the FP7-ENDORSE project (Morelli et al., 2012) adapting existing approaches both for the modelling of the irradiance incident in the one-axis sun-tracking solar receivers (Perez et al., 1990) and for the performance analysis of CSP parabolic-trough plants (Qu et al., 2010; Powell and Edgar, 2012).

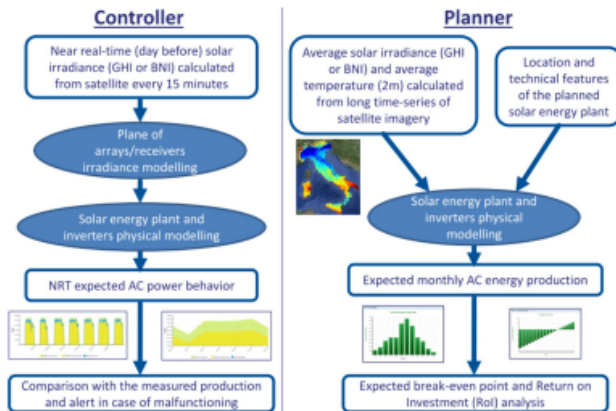


Fig. 1. General scheme of the "Controller" and "Planner" services dedicated to solar energy plants.

Please cite this article as: Morelli M, et al, Web tools concerning performance analysis and planning support for solar energy plants starting from remotely sensed optical images, Environ Impact Asses Rev (2014), <http://dx.doi.org/10.1016/j.eiar.2014.10.003>

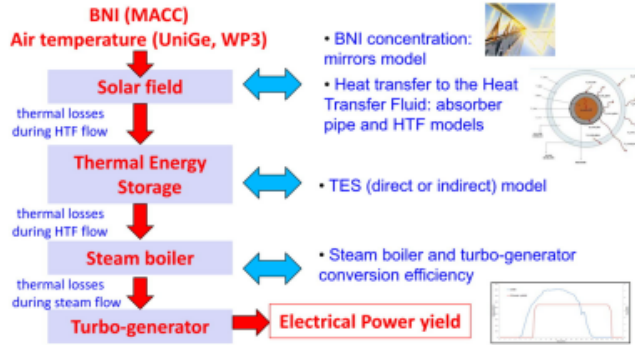


Fig. 2. Scheme of the model of parabolic-trough Concentrated Solar Power (CSP) plants used in the developed services.

The main parameters involved in the model are:

- the temperature and the flow rate of the heat-transfer fluid;
- the direct solar irradiance incident on the plane normal to sun rays (BNI) at ground level;
- the air temperature.

The algorithm (described schematically in Fig. 2) analyses the balance between the power absorbed by the fluid and the overall power losses, so the outputs of the whole modelling will be the following:

- The fluid temperature;
- The absorbed power;
- The power losses
- The instantaneous efficiency.

Other important aspects in the model are:

- Mirrors' optical characteristics (shape, reflecting properties);
- The film applied to the surface of the heat-concentrating pipe.

PV and CPV plants

The PV plants are typically composed by:

- Photovoltaic modules;
- Inverters.

The CPV plants are similar to the PV plants with the addition of:

- Reflecting mirrors or lenses concentrating the solar radiation on photovoltaic modules;
- Sun-tracking system to correctly orientate the reflecting mirrors.

In the case of these systems the environmental variable that mainly affects plant's performances is the solar irradiance absorbed by each PV module, that is proportional to the Global Tilted Irradiance incident on its plane.

Concentrating photovoltaic systems, instead, are usually divided into three categories: low, medium and high concentrations, based on the ratio between the effective area of the surface absorbing the solar radiation and the area of the modules where the radiation is concentrated. The photovoltaic systems with low concentration are the most used ones.

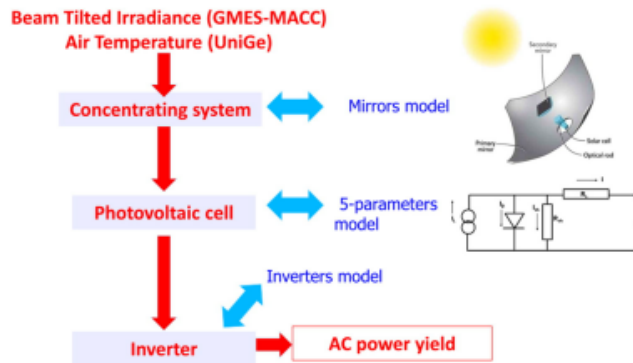


Fig. 3. Scheme of the model of Concentrating Photovoltaic (CPV) plants or Photovoltaic (PV) plants (avoiding the first part dedicated to concentrating system modelling) used in the developed services.

Please cite this article as: Morelli M, et al, Web tools concerning performance analysis and planning support for solar energy plants starting from remotely sensed optical images, Environ Impact Asses Rev (2014), <http://dx.doi.org/10.1016/j.eiar.2014.10.003>

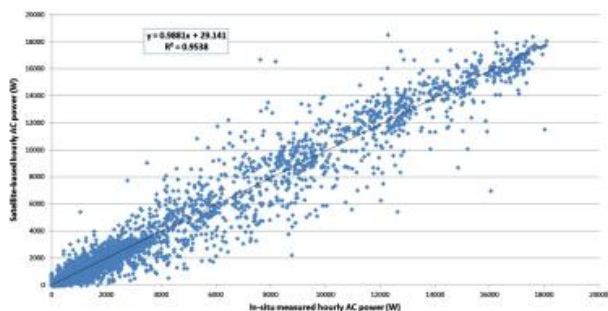


Fig. 4. Scatter plot comparing the hourly AC power produced by three different PV plants as calculated by the satellite-based method and as obtained from in-situ measured data. Source data are referred to a 4.86 kWp plant in Veneto (North Italy), a 3.89 kWp plant in Lazio (Centre Italy) and a 20.0 kWp plant in Sicily (South Italy). The considered periods are November 2013, January 2014, March 2014, May 2014, July 2014 and September 2014, for a total of 5383 time instants that range from 05:00 UTC to 20:00 UTC.

Similar to the CSP systems, the only solar radiation components that can be concentrated is the component direct incident on the plane normal to sun rays (BNI); the knowledge of this quantity is fundamental for planning and for financial evaluation of the costs, but is also a critical information in the operational mode of the plant, since it allows an accurate analysis of the plant performances.

The other two important aspects in the CPV plants are:

- the mirrors' shape;
- the photovoltaic modules.

Our modelling technique (schematically shown in Fig. 3) firstly models the Global Tilted Irradiance incident on the PV modules (PV case) or the Beam Normal Irradiance incident on the reflecting mirrors (CPV case) is following the approach described by (Perez et al., 1990) as above.

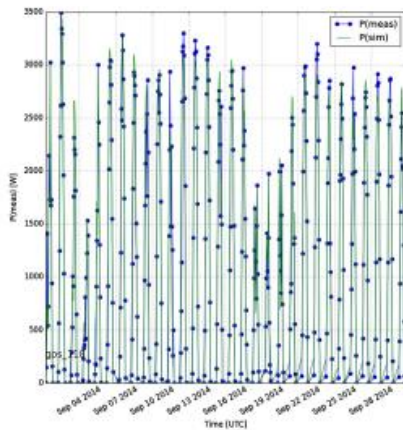


Fig. 5. Comparison between the behaviour of the satellite-based hourly AC power and the in-situ measured one. Data are referred to a single month (September 2014) for the PV plant in Veneto.

Then the solar energy plant is modelled in order to calculate the AC power yield. The PV modules used in the CPV plants are typically the same as the ones used in traditional PV systems and they have been modelled using an equivalent circuit with a (photovoltaic) current generator, connected in series with a resistance and in parallel with a diode and another resistance. This opto-electronic model of each PV cell has been taken from De Soto et al. (2006), whilst the modelling part concerning with the concentrating mirrors in the CPV case has been taken from Butler et al. (2012).

Results and discussion

We compared the hourly AC power (i.e. the hourly averaged AC power produced by the solar energy plant) calculated using the satellite-based methodology presented above and the in-situ measured one for three PV solar energy plants, respectively located in Veneto

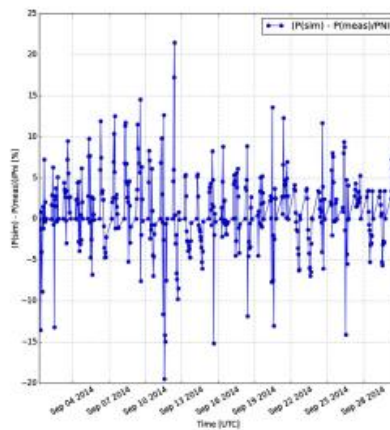


Fig. 6. An example of the behaviour of the NMAE resulting from the comparison between satellite-based and in-situ measured hourly AC power. Data are referred to a single month (September 2014) for the PV plant in Veneto.

Please cite this article as: Morelli M, et al, Web tools concerning performance analysis and planning support for solar energy plants starting from remotely sensed optical images, Environ Impact Asses Rev (2014), <http://dx.doi.org/10.1016/j.eiar.2014.10.003>

(North Italy), in Lazio (Centre Italy) and in Sicily (South Italy). We considered the hourly AC power data from 05:00 UTC to 20:00 UTC for November 2013, January 2014, March 2014, May 2014, July 2014 and September 2014 (considering all-seasons data). Since we have some lack of data, we considered a total of 5383 time instants.

The results obtained are shown in the scatter plot graph presented in Fig. 4. In Figs. 5 and 6 the results for one month for the Veneto plant have been reported, showing the comparison between the monthly behaviours of satellite-based and in-situ measured hourly AC power data (Fig. 5) and the related behaviour of the NMAE (Fig. 6) respectively.

The results show a good accuracy: the overall Normalized Bias (NB) is -0.41% , the overall Normalized Mean Absolute Error (NMAE) is 4.90% , and the Normalized Root Mean Square Error (NRMSE) is 7.66% . "Normalized" means that the statistical quantities reported here have been normalized with respect to the nominal power of each plant, i.e. 4.86 kWp , 3.98 kWp and 20.0 kWp respectively. The overall Correlation Coefficient (CC) is 0.9538 . The maximum value of the Normalized Absolute Error (NAE) is about 30% and occurs for time periods with highly variable meteorological conditions.

The services are currently available online (an example of the web interface is shown in Fig. 7) and, in particular for PV plants, they have been already used satisfactorily by several customers (e.g. Enel Green Power, Martifer Solar, Global Power Service) in the last years.

Conclusions

The downstream services presented herein can be really useful for a great number of end-users like solar energy designers, building designers and solar energy plant installers and designers. Indeed the exploitation of satellite-based data could represent an optimal solution with lower costs and an only slightly lower accuracy with respect to solutions based on in-situ solar irradiance sensors (Forero et al., 2006; Papageorgas et al., 2013), avoiding also possible problems related to unpredictable malfunctions or dirtiness of sensors.

In particular the "PV-Planner" and "PV-Controller" services plants have been widely used and satisfied the end-users, whilst the web services dedicated to CSP and CPV are currently being provided in pre-market versions and will be launched on the market most probably in 2015.

Almost half hundred power plants in Europe have been constructed with the assistance of the PV-Planner (that in year 2011 has been used by more than 50,000 users) and currently more than 300 solar energy plants in Italy, Greece and South-Africa are being monitored by the PV-Controller system.

We found a great interest for these services, especially from the solar energy installers and designers, and we received generally good feedbacks. We received also a few suggestions for developing them further and to improve their usefulness.

The performances of these services could be further increased:

- improving the accuracy of the satellite-based irradiance data, in particular in highly variable meteorological conditions (e.g. forecasting the short-term cloud motion);
- including a ground albedo map with high accuracy and high spatial resolution;
- integrating a near-real-time map of air temperature (at surface) with high spatial and high temporal resolutions;
- knowing the intensity of each spectral component of the incoming solar radiation to modelling better the irradiance actually absorbed by the energy plant's solar panels/receivers.

Acknowledgments

The R&D activities leading to those results have partly received funding from the European Union's Seventh Framework Programme (FP7/2007–2013) under Grant Agreement no. 262892 (ENDORSE project). The authors would like to thank Transvalor S.A. for providing the solar radiation data via the SoDa Service (MACC Core Service), the University of Genoa for providing the satellite-based air temperature

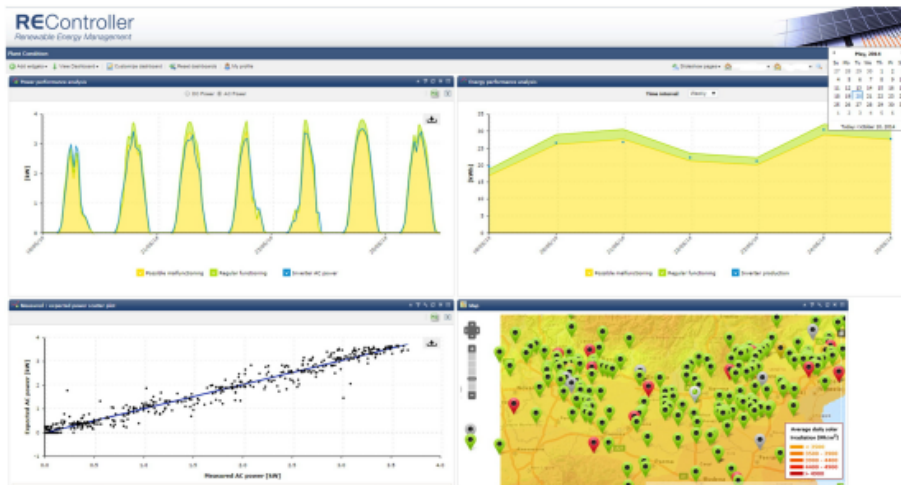


Fig. 7. An example of the web interface (dashboard) of the "Controller" service.

Please cite this article as: Morelli M, et al, Web tools concerning performance analysis and planning support for solar energy plants starting from remotely sensed optical images, Environ Impact Asses Rev (2014), <http://dx.doi.org/10.1016/j.eiar.2014.10.003>

data for east Sicily and the Italian AirForce (Aeronautica Italiana) for providing the air temperature data for the other regions covered by the service.

References

- Butler BA, van Dyk EE, Olullo W, Murji MK, Booyens P. Characterization of a low concentrator photovoltaics module. *Physica B* 2012;407:1501–4.
- Cano D, Monget JM, Albuissou M, Guillard H, Regas N, Wald L. A method for the determination of the global solar radiation from meteorological satellite data. *Sol Energy* 1986;37:31–9.
- De Soto W, Klein SA, Beckman WA. Improvement and validation of a model for photovoltaic array performance. *Sol Energy* 2006;80:78–88.
- Eicker U. *Solar technologies for buildings*. Chichester (UK): John Wiley & Son Ltd; 2003.
- Forero N, Hernandez J, Gordillo G. Development of a monitoring system for a PV solar plant. *Energy Convers Manag* 2006;47:2329–36.
- Morelli M, Masini A, Potenza MAC. A new method for the performance analysis of a Concentrating Solar Power energy plant using remotely sensed optical images. *Proceedings of "AIMOS 2012 – Advances in Atmospheric Science and Applications" – Brugis (Belgium)* 2012; ESA SP-708; 2012.
- Mueller RW, Matsoukas C, Gratzki A, Behr HD, Hollmann R. The CM-SAF operational scheme for the satellite based retrieval of solar surface irradiance – a IJIT based eigenvector hybrid approach. *Remote Sens Environ* 2009;113:1012–24.
- Papageorgas P, Piromalis D, Antonakoglou K, Voikas G, Tselis D, Arvanitis KG. Smart Solar Panels: in-situ monitoring of photovoltaic panels based on wired and wireless sensor networks. *Energy Procedia* 2013;36:535–45.
- Perez R, Ineichen P, Seals R, Michalsky J, Stuart R. Modeling daylight availability and irradiance components from direct and global irradiance. *Sol Energy* 1990;44:271–89.
- Powell KM, Edgar TF. Modeling and control of a solar thermal power plant with thermal energy storage. *Chem Eng Sci* 2012;71:136–45.
- Qin M, Yin H, Archer DH. Experimental and model based performance analysis of a linear parabolic trough solar collector in a high temperature solar cooling and heating system. *Sol Energy Eng* 2010;132:021004.1–021004.12.
- Rigollier C, Bauer O, Wald L. On the clear sky model of the 4th European Solar Radiation Atlas with respect to the Heliosat method. *Sol Energy* 2000;68:33–48.
- Dr. Marco Morelli** received the Laurea degree (M.S.) in Physics from the University of Pisa (Italy) in 2011. Since 2011 he is doing research activities at Flyby S.r.l. (Livorno, Italy) in the fields of satellite remote sensing and renewable energy plants modelling. He worked in the frame of the FP7-MACC project, being the author of the deliverable D_R-RAD_3.1.1, and he has been the Project Manager for Flyby in the FP7-ENDORSE project, being the author of several deliverables and the leader of one of the five work packages, the WP4 "Products Development". He is currently attending Ph.D. studies at the Physics Department of the University of Milano (Milano, Italy) with a particular interest on atmospheric radiative transfer modelling and its applications.
- Dr. Andrea Masini** received his Laurea (M.S.) degree in Telecommunications Engineering and his Ph.D. degree in remote sensing from the University of Pisa (Pisa, Italy) in 2004 and 2008, respectively. He is now working as the head of the remote sensing department at Flyby S.r.l. (Livorno, Italy). His current research interests concern image processing, in particular environmental monitoring from remotely sensed images, pattern recognition and information fusion. He has been the Project Manager of several international and national projects. He is the author or co-author of more than 20 scientific papers in journals and conferences.
- Dr. Fabrizio Ruffini** received his Master's Degree (Laurea specialistica in Scienze Fisiche) in March 2009 at the University of Pisa (Pisa, Italy). Dr. Ruffini defended his Ph.D. thesis on "First evidence of B0s → pi pi decay modes at CDF II" in June, 2013, at the University of Siena (Siena, Italy). The results of the thesis were published in *Phys. Rev. Lett.* 108, 211803 (2012). Since 2013 he is working at i-EM S.r.l. (Livorno, Italy) in the fields of data mining and data fusion for renewable energy plant models. Also, he was the teaching assistant of the course Laboratory of Physics III on digital and analogical electronics for the undergraduate degree course in Physics of the University of Pisa, in the academic years 2011–2012 and 2010–2011.
- Marco Alberto Carlo Potenza** Department of Physics, University of Milano, Via Celoria 16, 20133 – Milano, Italy. Dr. Marco A.C. Potenza, Ph.D., is currently an Assistant Professor at the Physics Department of the University of Milano (Milano, Italy). His research activities concern with instrumental optics, light scattering for metrological applications, image analysis, and holography. He has also experiences of statistical optics, non-linear optics and X-ray optics.

8.2 Appendix B: Presentations at conferences

8.2.1 International

In the following list we report the 10 presentations had by the Author at international scientific conferences.

- Poster presentation with title “A new method for the performance analysis of a Concentrating Solar Power energy plant using remotely sensed optical images” at the “ATMOS – Atmospheric Science Conference” organized by the European Space Agency (ESA) at Bruges (Belgium) in June 2012

Some preliminary results obtained in the frame of the FP7 ENDORSE project have been presented. These results concerned with the development of a satellite-based monitoring and planning system for Concentrating Solar Power plants based on the integration of satellite-based irradiance measurements with a model of CSP plants. A performance analysis can be carried out by comparing the actual power production with the satellite-based (estimated) one in near real-time with a good accuracy.

ATMOS 2012
Advances in Atmospheric Science and Applications

A new method for the performance analysis of a Concentrating Solar Power energy plant using remotely sensed optical images

Marco Morelli¹, Andrea Masini² and Marco Alberto Carlo Potenza³

¹Department of Fisica, Università degli Studi di Milano, via Celeste 15, 20121 Milano, Italy
²Flyby S.r.l., via Pavia 17 (ex. 26), 07101 - L'Aquila, Italy
³Gmes

INTRODUCTION
In the framework of the FP7 project ENDORSE (Energy Observation Services), we developed a new method for the performance analysis of a Concentrating Solar Power (CSP) energy plant and the related service.
We use a detailed model of a CSP parabolic trough plant (with direct energy storage system) and the solar radiation values at ground level derived in near real-time from satellite imagery. This information, together with in-situ measured or temperature-based to calculate every 15 minutes the expected power yield of the plant and, comparing it to the actual one measured, readily assess a possible malfunctioning and perform an overall plant performance analysis.
To calculate the electric power yield we developed a model containing the technical features of a CSP plant and the air temperature values (measured in-situ). Then by feeding it with satellite based solar radiation, we could monitor in near-real-time the daily behaviour of the alternate current produced by the plant and finally, using a temporal integration, obtain the expected daily energy yield by the CSP plant.

PLANT MODELING
Starting from satellite based values of solar radiation incident on a CSP plant every 15 minutes, we can calculate the Direct Normal Irradiance incident on the plant solar collector and the related thermal energy that is dissipated by the Heat Transfer Fluid (HTF) that flows in the pipes located at the focus of the parabolic mirrors [1].
Then we are able to calculate the HTF temperature at the outlet of the solar collector. Starting from it and using a heat exchange and mass flow equations for modeling thermal losses, Thermal Storage System (TSS) effects, queue boiler and turbo-generator [2] [3], we derive the expected power yield by the plant.
Finally, using the AC power values calculated every 15 minutes, we obtain the expected daily energy yield of the plant using a temporal integration. Comparing it to the measured production, possible loss of performance can be detected.

RESULTS
This method was firstly applied for a 1 MW CSP parabolic plant with direct thermal storage located in Sicily (Italy). HTF outlet temperature, hot tank temperature and power yield was simulated for several days and meteorological conditions. The results showed good agreement with the same quantities measured for similar plants [1].
HTF outlet temperature and power yield resulting from a 1 MW CSP energy plant of Sicily (Italy) for the 14th and 15th of June 2012. The HTF values are retrieved from satellite every 15 min.

MONITORING SERVICE
Using the CSP plant production remote sensing method reported, we developed also a web-service for CSP plants planning and monitoring.
Planner sub-service
• Keep all data showing the DNI averaged data (derived from 5 years historical satellite images archive)
• Monthly averaged expected energy yield starting from the selection and planned plant technical features
Control sub-service
• Active CSP plant production monitoring web-service
• Multifunctioning daily detection with email/DMS alerting system

CONCLUSIONS
The results of this method for CSP plant production assessment showed a good agreement with measured data retrieved from literature. They will be further validated using in-situ production data retrieved from a CSP active energy plant located at Prato Gargallo (Sicily, Italy).

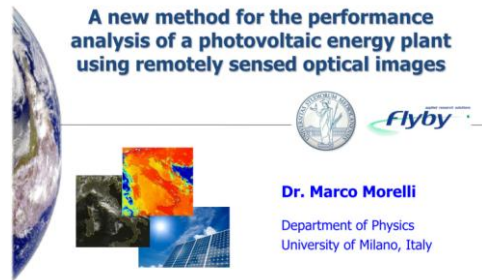
REFERENCES
[1] Masini, A., Morelli, M., and Potenza, M., "Assessment of an FP7 project of satellite-based plant", Solar Energy 96, 307-319 (2012).
[2] Masini, A., Morelli, M., and Potenza, M., "Thermal simulation of a solar thermal power plant with thermal energy storage", Conference Proceedings of the 12th International Conference on Energy Storage, 108-114 (2011).
[3] Masini, A., Morelli, M., and Potenza, M., "Thermal simulation of a solar thermal power plant with thermal energy storage", Conference Proceedings of the 12th International Conference on Energy Storage, 108-114 (2011).

18-22 June 2012 | Bruges, Belgium
European Space Agency

- Oral presentation with title “A new method for the performance analysis of a photovoltaic energy plant using remotely sensed optical images” at the “EUMETSAT

Meteorological Satellite Conference” organized by the EUMETSAT at Sopot (Poland) in September 2012

A method for the near real-time monitoring of the performances of a photovoltaic plant has been presented. This method integrates a satellite-based assessment of the shortwave solar radiation incident on each PV cell (with some improvements with respect to the original Heliosat method) and an opto-electronic model of the PV plant.



- Poster presentation with title “The SATENERG project: satellite services for new generation renewable energies” at the conference “Renewable Energy: the added value of satellite solutions for SMEs” organized by the EURISY at Graz (Austria) in September 2012

Presentation of some web-services developed in the frame of the SATENERG project. In particular a satellite-based monitoring/planning support system for solar energy plants (PV, CPV, CSP) and off-shore wind plants (based on SAR imagery) has been presented.

The SATENERG project
Satellite services for new generation renewable energies

Partners: Flyby, OVI

THE PROJECT
 The SATENERG project ("Satellite services for new Generation Renewable Energies") is funded by the Italian Space Agency (ASI). It aims at:

- satellite data exploitation and modeling for the development of services to support Renewable energy plants; to provide a solution on the planning and monitoring of new generation plants like Concentrating Solar Power (CSP), Concentrating Photovoltaics (CPV) and Off-shore wind.
- satellite radiation ground reception; the data acquired by the optical sensor (SIRIS) on the MSG (Meteosat Second Generation) satellite and using the Heliosat algorithm.

THE PRODUCTS
 The main SATENERG products, derived from satellite based solar irradiance and wind data, are:

- near real-time expected power yield for a CSP (CPV or Off-shore wind plant).
- near real-time wind speed (10 m) from space or ground satellite data.
- possible energy yield for a virtual CSP (CPV or Off-shore wind plant) using the above solar irradiance and wind data.

CPV and CSP energy plants monitoring service
 Includes intelligence applied to new generation plants permits a greater efficiency in the production of renewable energy, preventing significant energy losses and ensuring the costs for energy managers and clients.

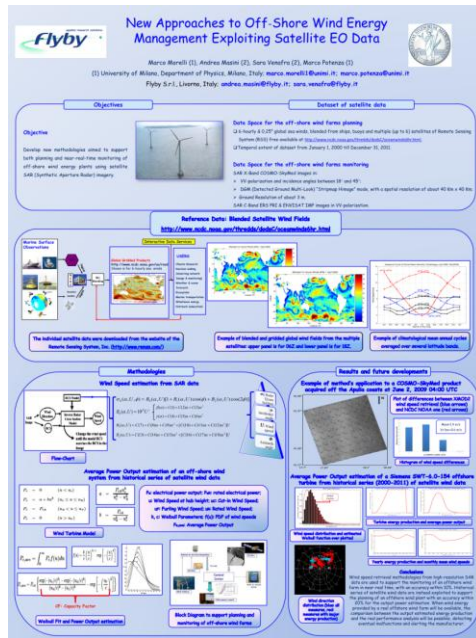
Off-shore wind plants monitoring service
 Includes intelligence applied to new generation plants permits a greater efficiency in the production of renewable energy, preventing significant energy losses and ensuring the costs for energy managers and clients.

INTENDED RESULTS
 The main intended results of the SATENERG project are:

- to provide a solution on the planning and monitoring of new generation plants like Concentrating Solar Power (CSP), Concentrating Photovoltaics (CPV) and Off-shore wind.
- to provide a solution on the satellite radiation ground reception; the data acquired by the optical sensor (SIRIS) on the MSG (Meteosat Second Generation) satellite and using the Heliosat algorithm.

Partners involved in the project
 Flyby, OVI, ASI, and other partners.

September 13th 2012 | EURISY Conference "Renewable energy: the added value of satellite solutions for SMEs" | Graz, Austria



- Oral presentation with title “Web tools for performance analysis and planning support for solar energy plants starting from remotely sensed optical images” at the 27th “EnviroInfo” conference organized by the University of Hamburg at Hamburg (Germany) in September 2013

Presentation of the results obtained in the frame of the FP7 ENDORSE project about satellite-based monitoring of solar energy plants (PV, CPV, CSP) and the related web-services.

Web tools for performance analysis and planning support for solar energy plants starting from remotely sensed optical images



Dr. Marco Morelli
University of Milano – Department of Physics
Flyby S.r.l. – R&D Department





- Poster presentation with title “Sentinel-2 Imagery for the Development of Innovative Decision Support Systems Dedicated to Sustainable Forest Management” at the “Sentinel-2 for Science Workshop” organized by the European Space Agency (ESA) at Frascati (Italy) in May 2014

Presentation of some innovative concepts aimed to support intelligent forestry management based on satellite imagery and in particular on the (future) features of the ESA’s Sentinel-2 satellite.

Sentinel-2 Imagery for the Development of Innovative Decision Support Systems Dedicated to Sustainable Forest Management

Marco Morelli and Andrea Masini
Flyby S.r.l., via Pirelli 97 (ex. 26), 57128 - Livorno, Italy
Contact: marco.morelli@flyby.it

SATELLITE-BASED DECISION SUPPORT SYSTEMS FOR FOREST MANAGEMENT

Satellite high resolution optical imagery could be exploited for the development of innovative services providing highly accurate information on forests status. Moreover these remotely sensed data, synergistically combined with terrain morphology data (DEM - Digital Elevation Model), can feed **Innovative Decision Support Systems (DSS)** dedicated to sustainable forest management, e.g. supporting the optimal planning of both harvesting and reforestation practices.

THE FP7 SLOPE PROJECT

We are currently developing in the frame of the EU funded FP7 SLOPE project (Integrated processing and control systems for sustainable forest production in mountain areas) a new service that automatically elaborates RapidEye satellite imagery in order to provide forest classification maps and forest health maps. In particular these data are being integrated into a new decision support system dedicated to forestry in mountain areas.

The SLOPE project (2014-2017) will integrate information from remote sensing, Unmanned Aerial Vehicles (UAV) and on-field surveying systems, to support macro and local analysis to characterize forest resources. Spatial information will be integrated with multi-sensor data in a model for Sustainable Forest Management and for optimization of logistics during forest operations. The integration and post-processing of data collected by SLOPE will be used for further optimization of the “mountain forest models” and finally silviculture routines.

PARTNERS INVOLVED IN THE SLOPE PROJECT

CHESSELLA, KESLA, COASTAL, MHG, Flyby, GLOBETECH, ITIS

CONTRIBUTION OF SENTINEL-2 IMAGERY

The DSS dedicated to intelligent forest management could be greatly improved by means of the Sentinel-2 satellite imagery. Indeed the combined availability of more spectral bands and a greater swath width (maintaining a similar high spatial resolution) with respect to currently available satellite imagers, could allow the development of a cheaper and quicker solution based on both a more accurate plants classification and a more accurate elaboration of fundamental parameters such as Normalized Difference Vegetation Index (NDVI), Leaf Chlorophyll Concentration (LCC), Leaf Water Concentration (LWC), Leaf Area Index (LAI).

May 20th – 22nd 2014 ESA SENTINEL-2 for Science Workshop ESA-ESRIN
Frascati (RM), Italy

- Poster presentation with title “Satellite-based ultraviolet and shortwave direct-diffuse solar radiation data validated through ground-measured BSRN data in support of downstream services dedicated to health prevention and solar energy” at the “13th Baseline Surface Radiation Network Scientific Review and Workshop” organized by BSRN at Bologna (Italy) in September 2014

Presentation of the solar radiation measurement station installed at Livorno, Italy (by a team led by the Author) and of the satellite-based applications that can be validated by exploiting its high-quality measurements.

Satellite-based ultraviolet and shortwave direct-diffuse solar radiation data validated through ground-measured BSRN data in support of downstream services dedicated to health prevention and solar energy

Flyby
Marco Morelli and Andrea Masini
Flyby S.r.l. via Pavesi 04, 20132, Lissone, Italy
Contact: masini@flyby.it

INTRODUCTION

The quality of satellite downstream services strongly depends on the accuracy of the satellite-based data they exploit. So one of the most important phases in the development of such services is the scientific validation of the satellite-based data elaborated. The validation process is completely based on the reliability (i.e. completeness, accuracy, etc.) of the ground measured data taken as reference. This affects both the assessment of the service quality itself and also the possibility to plan and realize further developments.

Therefore all the downstream services concerning with solar radiation strongly need high quality ground-based measurements: the Baseline Solar Radiation Network (BSRN) is currently the best possible way to freely retrieve such high quality measurements as needed, providing data acquired with instruments of the highest available accuracy and with high time resolution.

Current BSRN network in Europe (December 2014)

SATELLITE-BASED SOLAR RADIATION DATA BEING VALIDATED WITH BSRN DATA

In particular Flyby is involved into the solar energy and the healthcare sectors, providing a solution for the near real-time monitoring of solar energy plants and an innovation system providing real-time personalized recommendations for safe sun exposure.

In the first case (SolarAT service) the satellite remote sensing of short-wave solar irradiances has a fundamental importance. Indeed the performance monitoring of solar energy plants is based on the near real-time calculation of the incident global horizontal short-wave irradiance (GHI) and its beam and diffuse components (DNI and DHI).

In the second case (HappySun service), instead, the fundamental quantity is the UV spectral irradiance (i.e. the UV irradiance weighted with the erythemal action spectrum - EAS) that also acts as a highly accurate near real-time remote sensing of both the UVA (315-400 nm) and the UVB (280-315 nm) irradiances.

So far the GHI, DNI and DHI satellite-based data have been validated exploiting the BSRN's European (ESA) station data, while the UVA and UVB data have been validated thanks to the BSRN's Gulev (USA) station measurements. The validation resulted in a good agreement between ground-based and satellite based data and it's the starting point for further developments of Flyby's elaboration processes.

DOWNSTREAM SERVICES THAT CURRENTLY BENEFIT FROM BSRN DATA

SolarAT service

Using satellite based solar irradiance data together with an accurate atmospheric model of a solar energy plant (photovoltaic, CSP or CHT), SolarAT evaluates the production energy and compares it to the production one. The plant efficiency is then presented in a multi-touch interface together with energy production, profitability and plant response to near real-time.

HappySun service

HappySun is an innovative mobile App that provides real-time personalized recommendations for safe sun exposure. Starting from the user's latitude, erythemal dose (EAS) and the UV radiation calculator in near real-time elaborating satellite imagery, HappySun calculates the personal safe exposure time. Along the way, it also provides the necessary applied knowledge to simple and reliable solar photoprotection solutions, allowing a continuous satellite monitoring of the UV radiation incident on the skin.

PERSPECTIVES

- BSRN data are essential for the R&D activities of the industries involved in the solar radiation field: further new BSRN stations monitoring solar radiation (both conventional GHI and spectral UV) could be really important in a global scale.
- Flyby is interested in collaborating with BSRN station operators (or users) to provide joint scientific R&D activities (e.g. research impact on solar energy production or UV exposure) or in the frame of EU/ESA funded projects.
- Flyby could be interested in ground-based solar radiation data sharing, since also Flyby has a (partial) proprietary meteorological station in Lissone on its headquarters' roof with UV sensor and pyranometer.
- Please feel free to contact Flyby if you could be interested in possible collaborations.

- Oral presentation with title “Combining satellite optical remote sensing and radiative transfer simulation of spherical and non-spherical atmospheric aerosols to increase the performances of downstream applications in the fields of renewable energy and healthcare” at the “SPIE Remote Sensing 2014” conference organized by the International Society for Optics and Photonics (SPIE) at Amsterdam (the Netherlands) in September 2014

Presentation of the first results obtained by comparing spherical and non-spherical shapes of the aerosols in the atmosphere and their effects on solar radiation transfer.

Combining satellite optical remote sensing and radiative transfer simulation of spherical and non-spherical atmospheric aerosols to increase the performances of downstream applications in the fields of renewable energy and healthcare

Dr. Marco Morelli
Department of Physics
University of Milano, Italy

SPIE. REMOTE SENSING

SPIE Remote Sensing 2014
Conference 9242A "Remote Sensing of Clouds and the Atmosphere"

September 24th 2014
Amsterdam, Netherlands

- Oral presentation with title “Monitoring the performance of solar energy plants from satellite remote sensing of air temperature and ground solar irradiance through an accurate modelling of the effects of aerosol optical properties” at the 14th European Meteorological Society (EMS) Conference organized by EMS at Prague (Czech Republic) in October 2014

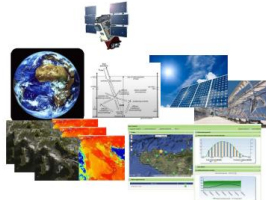
Presentation of the first results obtained by comparing spherical and non-spherical shapes of the aerosols in the atmosphere and their effects on solar energy plants monitoring by taking into account also satellite-based air temperature values (starting from the product developed in collaboration with the University of Genoa in the frame of the FP7 ENDORSE project).




Monitoring the performance of solar energy plants from satellite remote sensing of air temperature and ground solar irradiance through an accurate modelling of the effects of aerosol optical properties







Dr. Marco Morelli
 Department of Physics, University of Milano (Italy)
 Recipient of EMS's 2014 YST Award - Fee Waiver



14th EMS & 10th ECAC Conference
 Session ASI13 “Energy Meteorology”, Presentation EMS2014-32

October 7th 2014
 Prague, Czech Republic

8.2.2 National

In the following list we report the 4 presentations had by the Author at national (Italian) scientific conferences.

- Oral presentation with title “Nuovo teledosimetro UV mobile realizzato su periferiche Smartphone utilizzando dati di sensori ottici satellitari” (New mobile UV teledosimeter realized on Smarthphone devices exploiting satellite optical data) at the 5th national meeting of the Italian Environmental Protection Agencies held at Novara (Italy) in June 2012

Presentation of the first results obtained with the satellite-based UV dosimeter and of the related smartphone application (first version).



**Nuovo teledosimetro UV mobile
realizzato su periferiche
Smartphone utilizzando dati di
sensori ottici satellitari**

Dr. Marco Morelli Dipartimento di Fisica, Università degli Studi di Milano
Dr. Bruno Canessa Software&GIS Department, Flyby S.r.l.



Quinto Convegno Nazionale Agenti Fisici – ARPA Piemonte
"Il controllo degli agenti fisici: ambiente, salute e qualità della vita"
8 giugno 2012, Novara

- Oral presentation with title “Metodologie innovative per il supporto nella progettazione e l’analisi delle prestazioni di impianti ad energia solare a concentrazione ed eolici off-shore utilizzando immagini satellitari ottiche e SAR” (Innovative methodologies in support to the planning and the performance monitoring of concentrating solar energy plants and off-shore wind plants by exploiting satellite optical and SAR images) at the 16th ASITA conference at Vicenza (Italy) in November 2012

Presentation of the first results obtained in the frame of the ASI SATENERG project about satellite-based monitoring of solar energy plants and off-shore wind plants.



Metodologie innovative per il supporto nella progettazione e l'analisi delle prestazioni di impianti ad energia solare a concentrazione ed eolici off-shore utilizzando immagini satellitari ottiche e SAR

Dr. Marco Morelli Dipartimento di Fisica, Università degli Studi di Milano
Ing. Andrea Masini Dipartimento R&D, Flyby S.r.l.
Dr. Marco A.C. Potenza Dipartimento di Fisica, Università degli Studi di Milano



16° Conferenza Nazionale ASITA
8 novembre 2012, Vicenza

- Oral presentation with title “Monitoraggio in quasi tempo reale e previsione a breve termine della radiazione UV su piano normale basati sull’elaborazione di immagini ottiche satellitari e sulla modellizzazione del trasferimento radiativo in atmosfera” (Near real-time monitoring and short-term prediction of UV radiation on normal plane based both on the elaboration of satellite optical images and on atmospheric radiative transfer modelling) at the 100th national meeting of the Italian Physical Society (SIF) organized by SIF at Pisa (Italy) in September 2014

Presentation of the satellite-based UV dosimeter and of the results obtained in predicting sunburn timings (in collaboration with ARPA Valle d’Aosta and ARPA Toscana).



Monitoraggio in quasi tempo reale e previsione a breve termine della radiazione UV su piano normale basati sull’elaborazione di immagini ottiche satellitari e sulla modellizzazione del trasferimento radiativo in atmosfera



Dr. Marco Morelli
Dipartimento di Fisica, Università degli Studi di Milano
Socio della Società Italiana di Fisica



100° Congresso Nazionale della Società Italiana di Fisica
Pisa, 22 settembre 2014



- Poster presentation with title “Validazione di un sistema per il monitoraggio in quasi tempo reale e per la previsione a breve termine della radiazione UV a partire da immagini ottiche satellitari” (Validation of a system for the near real-time monitoring and the short-term prediction of the UV radiation starting from satellite optical images) at the 37th national meeting of the Italian Association for RadioProtection (AIRP) organized by AIRP at Aosta (Italy) in October 2014

Results of the validation of satellite-based UV dosimeter performed thanks to the UV data provided by ARPA-Valle d'Aosta (measured at the ARPA's meteorological station involved in the World Ozone and UV Data Center – WOUDC - project).

Validazione di un sistema per il monitoraggio in quasi tempo reale e per la previsione a breve termine della radiazione UV a partire da immagini ottiche satellitari



Marco Morelli¹, Andrea Masini², Henri Diemoz³, Marco Alberto Carlo Potenza⁴

¹ Dipartimento di Fisica, Università degli Studi di Milano (Milano), marco.morelli1@unimi.it

² Flyby S.r.l. (Livorno), andrea.masini@flyby.it

³ Arpa Valle d'Aosta (Aosta), henri.diemoz@arpa.vda.it



INTRODUZIONE

In questo lavoro viene presentato un metodo innovativo per il calcolo in quasi tempo reale e per la previsione a breve termine della dose UV incidente a terra a partire da immagini ottiche satellitari (dosimetro satellitare). Tale metodologia è basata sull'elaborazione di immagini ottiche del satellite geostazionario Meteosat Second Generation (MSG) e sull'analisi del trasferimento radiativo in atmosfera, oltre che sul calcolo della radiazione UV incidente sul piano normale rispetto ai raggi solari tenendo conto anche dell'albedo del terreno circostante.

METODOLOGIA

Applicando la metodologia Heliosat (Cano, 1986) alle immagini ottiche del satellite MSG è possibile ottenere in quasi tempo reale un indice di nuvolosità. Da ciò, tramite un'opportuna modellizzazione dell'irradianza globale nello spettro UV ed alla conversione in indice UV basata sullo spettro d'azione eritemico, viene calcolato il valore dell'indice UV a terra su piano orizzontale e la dose UV su piano orizzontale. Inoltre, applicando poi un metodo per la stima dell'irradianza su piano inclinato basata sulla scomposizione in componenti diretta e diffusa della radiazione e sull'albedo del terreno circostante (Perez, 1989), viene infine ricavato il valore dell'indice UV su piano normale rispetto ai raggi solari e la dose UV incidente su piano normale.

La previsione a breve termine della radiazione UV è invece effettuata tramite una modellizzazione della relazione tra radiazione UV incidente e angolo solare zenitale.

APPLICAZIONE: APP "HAPPYSUN"

A partire da ciò è stata sviluppata una nuova applicazione (App) per Smartphones, HappySun, dedicata alla dosimetria UV in tempo reale che, grazie ad un metodo per la previsione a breve termine della radiazione UV incidente, consente anche di avere una stima dell'esposizione cumulata al sole in base alla dose eritemica minima (Minimum Erythmal Dose – MED) personale dell'utente. L'App è attualmente disponibile gratuitamente per piattaforme Android e iOS.

PROSPETTIVE

Attualmente viene utilizzato un modello uni-dimensionale di nubi (non è stato ancora considerato lo scattering orizzontale dei fotoni) e la parte dedicata al trasferimento radiativo in condizioni di cielo sereno è in fase di ulteriore sviluppo grazie all'implementazione di un metodo per la caratterizzazione ottica di nanno- e micro- aerosol basato su dati ricavati dalla rete AERONET e da altre stazioni di misura a terra. Oltre a ciò anche la correlazione tra indice di nuvolosità e indice UV nel caso di condizioni meteo instabili sarà oggetto di ulteriore sviluppo.

BIBLIOGRAFIA

Cano, D., Mingot, JM., Albusson, M., Guilard, H., Rogoz, N., Wild, L., "A method for the determination of the global solar radiation from meteorological satellite data", *Solar Energy* 37:31-39, 1986.

Diemoz, H., Scar, M., Casale, G.P., Di Domenico, A., Scatena, B., Pellegrino, B., Barro, A., Fazio, S., Fieschi, F., Gilibert, D., Venz, L., Zapp, G., "First national intercomparison of solar irradiance measurements in Italy", *Atmospheric Measurement Techniques* 4: 1885-1703, 2011.

Monteleone, G., Fabozzi, G., Del Sorbo, A., Senatore, E., "Previsione del danno solare mediante rilevamento ultravioletto personalizzato: una nuova metodica con l'uso di telecamere satellite", *Annali Italiani di Dermatologia*, 2004.

Morelli, M., Casassa, B., "Nuovo ambizzionato UV mobile realizzato su periferiche Smartphone utilizzando dati di sensori ottici satellitari", Atti del V Convegno Nazionale Agenti Fisici "Il controllo degli agenti fisici: ambiente, salute e qualità della vita" - Novembre 2012.

Perez, R., H. Seale, P. Incewan, B. Stewart, D. Maricucci, "A New Simplified Version of the Perez Diffuse Irradiance Model for Tilted Surfaces", *Solar Energy* 20: 221-232, 1988.



37° Convegno Nazionale di Radioprotezione

"Le radiazioni: valori, conoscenza scientifica e aspetti operativi"

Aosta, 15-17 ottobre 2014



8.3 Appendix C: Presentations at project meetings

8.3.1 International

In the following list we report the 8 oral presentations had by the Author at international research projects meetings.

- “WP402 – Product S2: “Design CSPS” Development status and first version availability”
– 3rd Meeting of the FP7 ENDORSE project – Paris (France) - 14/12/2011



- “ENDORSE WP4 activities and results” – 3rd Meeting of the FP7 ENDORSE project – Paris (France) - 15/12/2011



- “WP402 – Product S2: “Design CSPS” - Development status and complete version availability” – 4th Meeting of the FP7 ENDORSE project – Wessling (Germany) - 04/07/2012

WP402 – Product S2: “Design CSPS”
Development status and complete version availability

Marco Morelli
 Flyby S.r.l.



ENDORSE (Energy DOWnstReam SErvices)
 Providing energy components for GMES

Meeting #4 ENDORSE – Wessling, Germany





- “WP602 – Service S2: “Design CSPS – Wessling (Germany) - 05/07/2012” – 4th Meeting of the FP7 ENDORSE project

WP602 – Service S2: “Design CSPS
Preparation and development plan

Marco Morelli
 Flyby S.r.l.



ENDORSE (Energy DOWnstReam SErvices)
 Providing energy components for GMES

Meeting #4 ENDORSE – Wessling, Germany





- “WP 602 – Service S2 “Design CSPS” Development status” – 5th Meeting of the FP7 ENDORSE project – Brussels (Belgium) - 05/03/2013

**WP 602 – Service S2 “Design CSPS”
Development status**

Marco Morelli
Flyby S.r.l.



ENDORSE (Energy DOWNstReam SERVICES)
Providing energy components for GMES

Services Session (WP6) – ENDORSE Meeting #5
Brussels, 5th March 2013



- “WP 4 “Product Development” - Current status” - 5th Meeting of the FP7 ENDORSE project – Brussels (Belgium) - 06/03/2013

**WP 4 “Product Development”
Current status**

Marco Morelli
Flyby S.r.l.



ENDORSE (Energy DOWNstReam SERVICES)
Providing energy components for GMES

General Assembly – ENDORSE Meeting #5
Brussels, 6th March 2013



- “WP 4 “Product Development” - Activities done in 2012 and perspectives” – 5th Meeting of the FP7 ENDORSE project – Brussels (Belgium) - 07/03/2013

WP 4 “Product Development” ***Activities done in 2012 and perspectives***

Marco Morelli
Flyby S.r.l.



ENDORSE (Energy DOWnstReam SERVICES)
Providing energy components for GMES

Annual Review #2 – ENDORSE Meeting #5
Brussels, 7th March 2013



- “WP 602 – Service S2 “Design CSPS” Service demonstration” - Final Meeting of the FP7 ENDORSE project – Paris (France) - 11/12/2013

WP 602 – Service S2 “Design CSPS” ***Service demonstration***

Marco Morelli
Flyby S.r.l.



ENDORSE (Energy DOWnstReam SERVICES)
Providing energy components for GMES

Review Session – ENDORSE Final Meeting
Paris, 11th December 2013



8.3.2 National

In the following list we report the 5 oral presentations had by the Author at national (Italian) research projects meetings.

- “Presentazione dei requisiti utente” (User requirements presentation) – 2nd Meeting of the ASI SATENERG project – Livorno (Italy) - 08/05/2012



- “Presentazione dei requisiti tecnici per i servizi Earth Observation” (Technical requirements for Earth Observation services) - 2nd Meeting of the ASI SATENERG project – Livorno (Italy) - 08/05/2012



- “Stato dell’arte delle metodologie EO per le energie rinnovabili” (State of art of EO methodologies for renewable energies) – 3rd Meeting of the ASI SATENERG project – Roma (Italy) - 07/11/2012



SATENERG

**STATO DELL'ARTE DELLE
METODOLOGIE EO PER LE
ENERGIE RINNOVABILI**

Flyby small research solutions

Dr.ssa Sara Venafra
Responsabile tecnico dei
Servizi EO - parte Eolica

Dr. Marco Morelli
Responsabile tecnico dei
Servizi EO - parte Solare

Progetti Finanziati 2° Bando Tematico P.M.I.
"Osservazione della Terra"
07 Novembre 2012 - H3 Meeting

- “Algoritmo per la stima dell’irradianza solare a terra” (Algorithm for the estimate of solar irradiance at ground)- 3rd Meeting of the ASI SATENERG project – Roma (Italy) - 07/11/2012



SATENERG

**ALGORITMO PER LA STIMA
DELL’IRRADIANZA SOLARE A
TERRA**

Flyby small research solutions

Dr. Marco Morelli
Responsabile tecnico dei
Servizi EO - parte Solare

Progetti Finanziati 2° Bando Tematico P.M.I.
"Osservazione della Terra"
07 Novembre 2012 - H3 Meeting

- “Metodologie innovative di elaborazione dei dati EO per le energie rinnovabili” (Innovative methodologies for EO data elaboration for renewable energies)- 3rd Meeting of the ASI SATENERG project – Roma (Italy) - 07/11/2012



SATENERG

**METODOLOGIE INNOVATIVE DI
ELABORAZIONE DEI DATI EO
PER LE ENERGIE RINNOVABILI**

Flyby small research solutions

Dr.ssa Sara Venafra
Responsabile tecnico dei
Servizi EO - parte Eolica

Dr. Marco Morelli
Responsabile tecnico dei
Servizi EO - parte Solare

Progetti Finanziati 2° Bando Tematico P.M.I.
"Osservazione della Terra"
07 Novembre 2012 - H3 Meeting

8.4 Appendix D: Awards

8.4.1 EMS Young Scientist Travel Awards (YSTAs) – Fee Waiver

The “EMS Young Scientist Travel Awards (YSTAs) 2014 – registration fee waiver” prize has been awarded in September 2014 to the Author by the European Meteorological Society for the participation to the conference “14th EMS Annual Meeting & 10th European Conference on Applications of Meteorology” (held in October 2014 in Prague - Czech Republic) in recognition to his oral contribution “Monitoring the performance of solar energy plants from satellite remote sensing of air temperature and ground solar irradiance through an accurate modelling of the effects of aerosol optical properties”.

8.5 Appendix E: other relevant activities performed during the PhD

8.5.1 Attended courses

8.5.1.1 Courses at the University of Milan

- Laboratory of Optical Instrumentation with applications to Atmospheric Physics (Dr. Roberta Vecchi)
- Methodologies of Data Analysis (Prof. Fernando Palombo)

8.5.1.2 ESA Earth Observation Summer School

Flyby fully funded the participation of the Author to the international Summer School on Earth Observation with title “Earth System Monitoring & Modelling”, organized by the European Space Agency (ESA) at Frascati (Rome, Italy) on August 4th – 14th 2014.

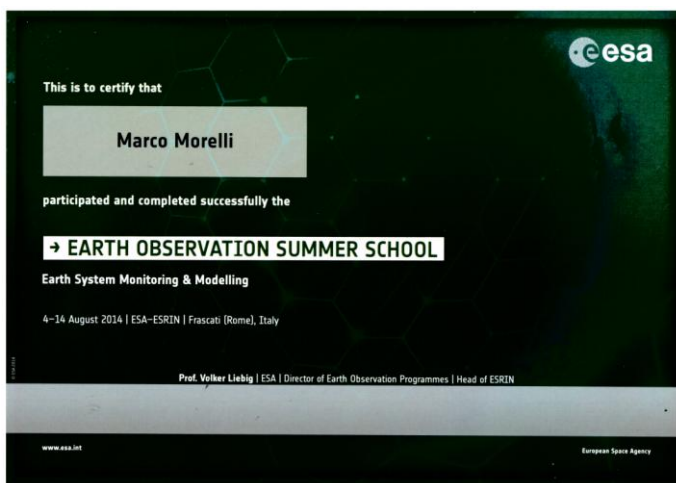


Figure 66: Copy of the Diploma released to the Author for the participation to the ESA EO Summer School in August 2014 at Frascati (Rome, Italy)

8.5.2 BSRN “Spectral measurements” expert group

BSRN is a project of the Data and Assessment Panel from the Global Energy and Water Cycle Experiment (GEWEX) under the umbrella of the World Climate Research Programme (WCRP) proposed by the World Meteorological Organization (WMO). It is the global baseline network for surface radiation for the Global Climate Observing System (GCOS), contributing to the

Global Atmospheric Watch (GAW), and forming a cooperative network with the Network for the Detection of Atmospheric Composition Change (NDACC).

The Author has been included in September 2014 in the expert group on spectral measurements of the Baseline Surface Radiation Network (BSRN) for his contributions in the field of UV radiation measurements.

8.5.3 Teaching activities

The Author contributed during his PhD to two courses of the University of Pisa (Italy):

- Course on “Quantum Optics” at the Department of Physics (Prof. Danilo Giulietti);
- Course on “Home Automation” at the Department of Electrical Engineering (Dr. Emanuele Crisostomi).

In the first case he had a two-hours lecture (courtesy of Prof. Giulietti) on solar radiation measurement at ground level and by satellite optical sensors (and its possible applications), while in the second case he had a one-hour lecture on the possible applications of satellite-based monitoring of solar radiation in the energy efficiency field (courtesy of Dr. Crisostomi).

8.5.4 Reviewer activities

The Author has been asked, in view of his expertise, to make a review of the paper ENSY-D-13-00129 “Study on the performance enhancement of the filled-type solar collector with U-tube” submitted to the Energy Systems journal (ISSN: 1868-3975) edited by Springer.

The abstract of the paper was the following:

The enhancement on the efficiency of solar collector will affect the application of solar heating and cooling systems, and the solar collector with high thermal performance has become a hot topic for research. In order to increase the efficiency of solar collector, this paper proposes a methodology based on the analysis of the influencing factors such as thermal conductivity of filled layer, structure forms of filled layer and heat loss coefficient. The analysis results show that the heat transfer between pipes in evacuated tube is one of the most important factors, which can lead to the decrease the outlet temperature of working fluid. In order to eliminate the negative influence of the heat transfer between pipes, the hollow filled-type evacuated tube with U-tube (HUFET) has been developed in this study, and the heat transfer characteristic of HUFET has been analyzed by theoretical and experimental studies. The results show that the thermal resistances decrease

*with the increasing of the thermal conductivity of filled layer. When the thermal conductivity is over 10 W/(m*K), the change of thermal resistances is very little. Furthermore, the larger thermal conductivity of filled layer, the less rate of the energy transfer between the two pipes to the total energy transfer between the absorber tube and the working fluid. There is a little difference between the efficiency of HUFET and UFET, with the efficiency of HUFET is higher 2.4% than that of UFET. Meanwhile, the validation of the model developed has been confirmed by the experimental investigation in this study.*

A complete review of the paper has been done by the Author in February 2014.

8.5.5 Thesis supervision

The Author has been involved in 2013 as co-Supervisor in a Master Thesis at the Department of Electrical Engineering of the University of Pisa (in collaboration with Dr. Mauro Tucci - Supervisor of the Thesis - and Flyby S.r.l.). The topic of the Thesis was the realization of a satellite-based system for the remote diagnostics of photovoltaic energy plants.

Moreover the Author is currently involved in the co-Supervision of a Master Thesis at the Department of Physics of the University of Pisa (in collaboration with Prof. Danilo Giulietti - Supervisor of the Thesis - and Flyby S.r.l.). The topic of the Thesis is the ground-based measurement of solar radiation and the characterization of aerosols impact.

8.6 Appendix F: Project deliverables

8.6.1 Non-public

In the following list we report the 16 non-public research project deliverables where the Author is an author or a co-author.

- “Requisiti tecnici per i servizi di EO” (Technical requirements for the EO services)- M2 deliverable of the ASI SATENERG project - 17/04/2012



- “User requirements” (Technical requirements for the EO services)- M2 deliverable of the ASI SATENERG project - 16/04/2012



- “Algoritmo per la stima dell’irradianza solare a terra utilizzando diverse fonti di dati satellitari” (Algorithm for the estimate of the solar irradiance at ground exploiting different satellite sources)- M3 deliverable of the ASI SATENERG project - 06/11/2012



- “Metodologie di elaborazione dati EO satellitari per le energie rinnovabili” (Methodologies for the elaboration of EO satellite data for the renewable energies)- M3 deliverable of the ASI SATENERG project - 18/09/2012



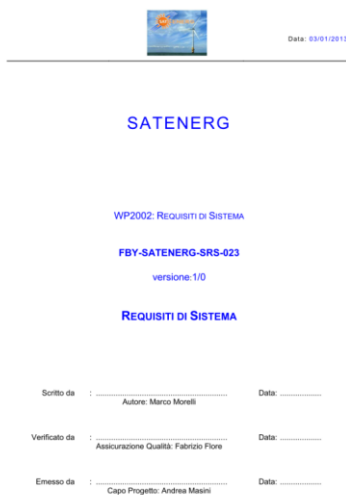
- “Stato dell’arte sull’elaborazione dati di EO per l’assistenza nella progettazione e nel monitoraggio di impianti solari a concentrazione ed eolici off-shore” (State of art on the elaboration of EO data for supporting the planning and the monitoring of concentrating solar plants and off-shore wind plants) - M3 deliverable of the ASI SATENERG project - 06/11/2012



- “Service EO subsystem definition” – M4 deliverable of the ASI SATENERG project - 27/01/2013



- “Requisiti di sistema” (System requirements) – M4 deliverable of the ASI SATENERG project - 03/01/2013



- “Definizione delle specifiche per la validazione del sistema e dei suoi component” (Definition of the specifics for the validation of the system and of its components) – M5 deliverable of the ASI SATENERG project - 29/03/2013



- “Procedure di validazione del sottosistema servizi di EO” (Validation procedures for the EO subsystem) – M5 deliverable of the ASI SATENERG project - 27/07/2013



- “Procedure di validazione del sistema integrato” (Validation procedures for the integrated system) – M5 deliverable of the ASI SATENERG project - 27/07/2013



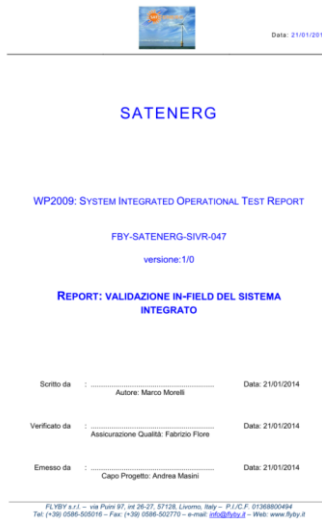
- “Report: validazione in-house del sottosistema servizi di EO” (Report: in-house validation of the EO services subsystem) – M5 deliverable of the ASI SATENERG project - 27/07/2013



- “Report: validazione in-house del sistema integrato” (Report: in-house validation of the integrated system) – M5 deliverable of the ASI SATENERG project - 27/07/2013



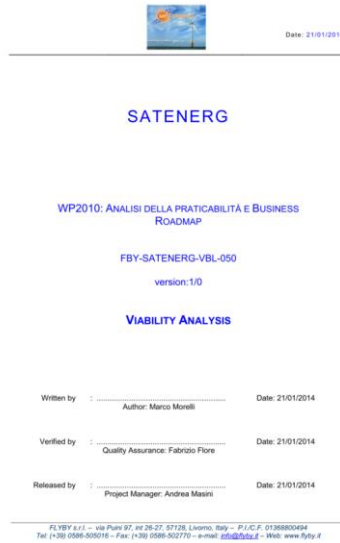
- “Report: validazione in-field del sistema integrato” (Report: in-field validation of the integrated system) – M6 deliverable of the ASI SATENERG project - 21/01/2014



- “User feedback analysis” – M6 deliverable of the ASI SATENERG project - 21/01/2014



- “Viability analysis” – M6 deliverable of the ASI SATENERG project - 21/01/2014



- “Implementation roadmap and recommendations” – M6 deliverable of the ASI SATENERG project - 21/01/2014



8.6.2 Public

In the following pages we enclose the 4 public research project deliverables where the Author is an author or a co-author:

- Deliverable D_R-RAD_3.1-1 of the FP7 MACC project
- Deliverable D402.1 of the FP7 ENDORSE project
- Deliverable D602.1 of the FP7 ENDORSE project
- Deliverable D602.2 of the FP7 ENDORSE project



Project MACC "monitoring atmosphere composition & climate"
Sub-project RAD "radiation"
Grant Agreement no. 218793

Service chain validation report for downstream test cases

Deliverable D_R-RAD_3.1_1, version 1.0

Author: Marco Morelli, Flyby S.r.l.
2011-12-22

Executive summary

This report shows a user's view on RAD services for downstream applications and a validation of the service chain in several test cases from the energy and materials sectors.

Some examples of possible integrations between the information retrieved from satellite images and the models of buildings, solar plants and materials are provided.

In particular the following services are presented:

- a tool that provide services concerning the design, production and financing management of new solar energy power plants;
- a system for the remote control of solar energy power plants, with a near-real-time (NRT) monitoring of power plant performances (daily energy production);
- a tool for NRT monitoring of the ultra-violet radiation (UV) intensity at ground level, allowing the user to prevent eventual materials damage (derived from UV radiation exposure) or for health care.

In addition some common requirements for these services, like user interface and integration with IT technology needs, are presented.

Table of contents

1. RAD downstream services and users	9
2. Common requirements	12
3. Test cases.....	14
3.1. Design, production and financing management of new PV and Thermal plants: PV/TH-Planner.....	14
<i>On-line sharing of projects and cost estimations</i>	14
<i>Web GIS technology</i>	14
<i>Advanced functionalities for design and marketing</i>	14
<i>Advantages offered by satellite analysis</i>	15
<i>Future work.....</i>	15
3.2. Web-satellite integrated system for the remote control of photovoltaic plants: PV-Controller.....	16
<i>Remote controlling based on satellite technology</i>	16
<i>PV plant efficiency is on-line</i>	16
A "plus" for every photovoltaic plant.....	17
Following the customer from design to maintenance.....	17
<i>Highest flexibility of customization.....</i>	17
<i>Users success cases</i>	17
<i>Future work.....</i>	20
3.3. UV.....	20
4. Conclusions	21

1. RAD downstream services and users

RAD services are useful for answering to different solar radiation knowledge related issues, like:

- solar energy power plants (Photovoltaic (PV) plants or Solar Thermal plants) design and monitoring;
- damage prediction of materials exposed to sun ultra-violet (UV) radiation;
- health care related to the ultra-violet radiation intensity at ground.

The main classes of users potentially interested in these services are:

- solar energy designers, interested in design and monitoring their plants;
- building designers, interested to energy efficiency design;
- energy utilities and plants installers for PV and Solar Thermal plants marketing and monitoring;
- automotive italian manufacturers, interested in an estimation of the ultra-violet radiation intensity at ground (for automotive parts ageing simulation).

The main GMES based downstream service currently provided by Flyby is the SolarSAT service, composed by:

- the PV/TH-Planner service, that provides assistance in the photovoltaic or Solar Thermal power plant design and planning stage;
- the PV-Controller service, that allows to monitor (near-real-time) the performances and the energy output of an existing photovoltaic plant;

Until now these services has been widely used, indeed we had:

- 17 main users of the SolarSAT PV-Controller service (medium or big italian enterprises, included Enel Green Power, the main electricity provider in Italy), that provide the service to other 235 end-users (typically small enterprises, with the exception of three public users that are three city administrations) ;
- One main user (Enel Green Power) for the SolarSAT PV/TH-Planner service, that is available online;

- about 52000 yearly accesses to the SolarSAT PV-Planner (for the photovoltaic systems) web-service;
- about 3000 yearly accesses to the SolarSAT TH-Planner (for the Solar Thermal systems) web-service.

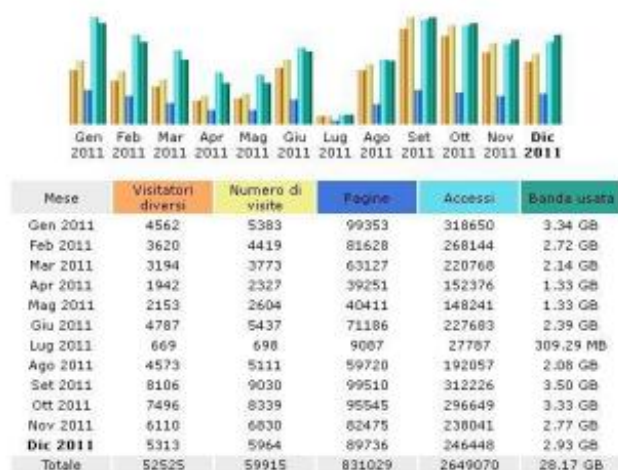


Figure 1.1. SolarSAT PV-Planner web-service monthly accesses statistics in the year 2011



Figure 1.2. SolarSAT TH-Planner web-service monthly accesses statistics in the year 2011

2. Common requirements

All the services ask for smart user friendly web GIS interfaces to allow both technical personnel and public to have access to solar radiation information in an easy way for consultation.



Figure 2.1. An example of the Web-GIS layout for the RAD downstream service PV-Planner (currently available online and realized for Enel Green Power)

Moreover, the downstream service should have the ability to be interfaced and integrated with existing user IT architecture and end-user front-end procedures (e.g. customers database contacts).

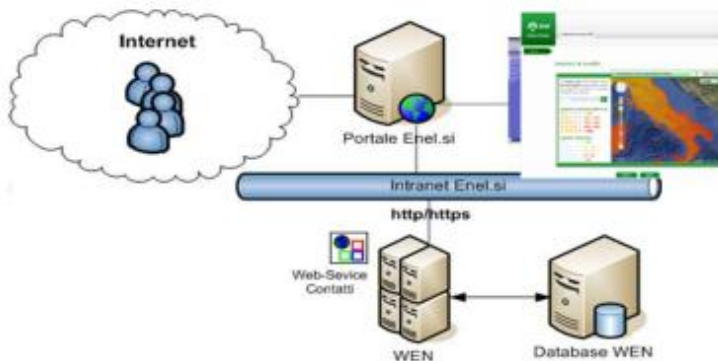


Figure 2.2. Scheme of a possible integration between GMES based downstream services and the end-user architecture

The service should also have the ability to present data in the new smart phones interfaces and to be distributed commercially according to the related business models (e.g. apps store).



Figure 2.3. Real time power plant management on a smart phone (this is an example image realized using a graphics software)

3. Test cases

In the following we present some cases of the use of EO information for provide services useful for the users classes specified in Section 1.

3.1. Design, production and financing management of new PV and Thermal plants: PV/TH-Planner

On-line sharing of projects and cost estimations

SolarSAT PV-Planner supports the job of all photovoltaic or Solar Thermal power plants installers (or designers, distributors, marketers) by providing a common standard within a single web tool. It allows the sharing of technical and commercial information regarding several plants by accessing a single database.

Web GIS technology

PV-Planner exploits the potential offered by web-GIS (Geographic Information System) technology, which allows to store geo-referenced information via web in a common database (e.g. regarding plant location, solar irradiance, temperature, wind speed and direction, but also technical information concerning the plant, like orientation and inclination of PV modules, modules features, inverters features, plant architecture, ...). The system also allows to interact with geographical maps, like solar irradiance ones.

Advanced functionalities for design and marketing

The PV-Planner service offers the following integrated functionalities:

- analysis of solar irradiance on both the selected site location and on the PV module plane through navigation in an interactive geographical map. The analysis is based on both solar irradiance data (derived from satellite archive) and on the features of the surrounding environment (e.g. albedo, shadowing, ...)
- PV plant dimensioning and preliminary characterization according to final user energy needs
- PV plant detailed design by choice of components (modules and inverters), optimization of their electric coupling in terms of strings and sub-fields, definition of solutions for the supporting structures (retrofit, flat roof, ...)
- analysis of plant producibility on the basis of its technical characteristics and of solar irradiance statistics deduced from satellite observations
- economical analysis: in order to evaluate the investment convenience, the most important economical parameters are calculated (e.g. Net Present Value, Internal Rate of Return, breakeven point, etc.). The estimation takes into account costs, incentive tariffs, taxes, inflation rate, weighted average cost of capital, etc.) all related to the final user specific case

Advantages offered by satellite analysis

Several factors make satellite archive data advantageous with respect to conventional databases:

- spatial resolution: the one used by SolarSAT is about 12 km and is based on last 10 years observations (20 years available on request). This identifies the typical climatic status of the deputy locality and hence the actual limit for producible energy of that plant. Such characteristics of SolarSAT appear unique if compared to data regarding the Italian UNI 10349 regulation, which are limited to about 100 Italian provinces, or with respect to Solar European Atlas data which have 50–100 km resolution. Moreover these latter ones do not take into account microclimatic effects and local orography as they are derived by interpolating local on-ground measurements.
- precision: solar irradiance estimation complies with the European standards (Joint Research Centre) over visible and infrared spectra, while data related to Italian UNI 10349 regulation are conceived to calculate energy fluxes for the building industry and tend to overestimate irradiance.
- area coverage: satellite observations cover the whole earth surface. SolarSAT exploits a coverage up to whole Europe and the Mediterranean basin, including facing African countries.

PV-Planner integrates together the satellite data and the opto-electronic models of the PV plant into a single user-friendly web interface. It's configurable as an application devised for the promotion of PV products (e.g. PV modules, inverters) or as an application for the spreading and promotion of solar PV energy. For such purposes, simplified user interfaces and intuitive functions can be realized for the use of the system by non-expert people.

The SolarSAT system is fully customizable for the company or institution which intends to offer such web services to its clients. SolarSAT can be integrated into existing web portals in outsourcing.

Future work

The service could be optimized further, for example, improving the irradiance calculation at ground and through a better knowledge of the plant location characteristics.

In particular the current spatial resolution of the available irradiance historical data - a fundamental input for the PV-Planner - is 3 Km x 3 Km. It could be useful in the next future to have more precise irradiance data retrieved from satellite, making further research to lower their difference from the effective irradiance data measured in-situ and improve their spatial resolution.

Another important input parameter for the service is the albedo: new studies on this property and an eventual albedo map at high spatial resolution (lower than 1Km x 1Km) could be important to improve the service accuracy and usefulness.

3.2. Web-satellite integrated system for the remote control of photovoltaic plants: PV-Controller

Controlling a photovoltaic plant is essential in keeping the efficiency of energy production as high as possible in the course of years and hence in achieving a fast payback. Moreover, putting in evidence the amount of produced energy gives the customer the perception of investment worthiness. SolarSAT PV-Controller springs up from a project carried out by Flyby, in collaboration with the European Space Agency (ESA), with the purpose of providing companies and Bodies devoted to PV plants installation and maintenance with an innovative solution for their clients.

Remote controlling based on satellite technology

In its basic version, PV-Controller allows for remote control of a photovoltaic plant by means of both real time monitoring of solar radiation through satellite and the acquisition of plant production data through a simple data logger (EasyLog), to be installed at the plant. The EasyLog is equipped with memory and with a GPRS modem and sends data regarding hourly energy production to the control station website. Produced energy is sensed locally by a pulse energy counter (S0 standard).

In its basic version, PV-Controller is then capable to retrieve the plant working status, without any need of interfacing to inverters or meteo sensors, and to present it on the web. Besides this, PV-Controller is also capable to acquire data from inverters and then provide PV plant diagnostics. For medium-size and large-size PV plants, PV-Controller includes the additional use of irradiance and meteo sensors to be interfaced with the more sophisticated SolarSAT data loggers models, LightLog and SuperLog. The latter one is also equipped with a graphic display to allow for a check of PV plant data directly at the place.

PV plant efficiency is on-line

PV-Controller evaluates the hourly producible energy and compares it to the produced one measured by the counter. It does so by exploiting an accurate opto-electronic model of the PV plant, where plant parameters are those furnished by the installer.

Producible energy is derived from solar irradiance and other parameters like PV module temperature, ambient temperature, wind speed and direction. On the website is then presented the plant efficiency level in terms of energy production and in terms of profitability, together with plant diagnostics (inverters efficiency, malfunction conditions, ...).

The installer or maintainer at anytime can obtain the plant diagnostics and receive eventual malfunction alarms. These services can always be accessed on the web portal which can even be customized for the company. PV-Controller allows the detection of possible inefficiencies in energy production and hence the estimation of consequent economical losses. Also the risk of false alarms is reduced thanks to satellite measurements.

A "plus" for every photovoltaic plant

The main advantages of PV-Controller are:

- *affordability and easiness*: the service is available also for small plants, so that even the single end user can verify at any time the value of the investment made. The basic model EasyLog is cheap and easy to install, requiring no interface with the plant, no connection to the Internet, no router configuration: just connect EasyLog to a counter and the data will be automatically transmitted to the website via GPRS link.
- *a single web standard for different PV plants*: the compatibility with the majority of inverter models ensured by SolarSAT data loggers allows to manage PV plants of different sizes and features through a unique web portal shared by the various operators (e.g. maintainers team).
- *reliability with no maintenance*: the monitoring of whole PV plant efficiency is done without the need to install sensors which would require periodical interventions for calibration and maintenance. The satellite data is accurate and its quality is continuously maintained.
- *management of PV plant maintenance*: the company or Body distributing the PV-Controller service can also include the management of eventual plant malfunction alarms, thus suggesting specific interventions of maintenance.
- *secure and diversified access to data*: plant diagnostics data are presented on an user-friendly interface, directly accessible by the operator or by the end user through a personal password on the website of the distributor company.

Following the customer from design to maintenance

By integrating the PV-Controller and PV-Planner modules, the SolarSAT system allows to follow the client during the entire PV plant life cycle: from feasibility check to design, cost estimation, test, monitoring of working status, maintenance. Such approach aims at the highest satisfaction of the end user by means of global quality and high added value services.

Highest flexibility of customization

The SolarSAT system is fully customizable for the company or Body which intends to offer such web service to its clients. SolarSAT can be integrated into existing web portals in outsourcing.

Users success cases

We report in Fig. 6 a diagram of the PV-Controller service.

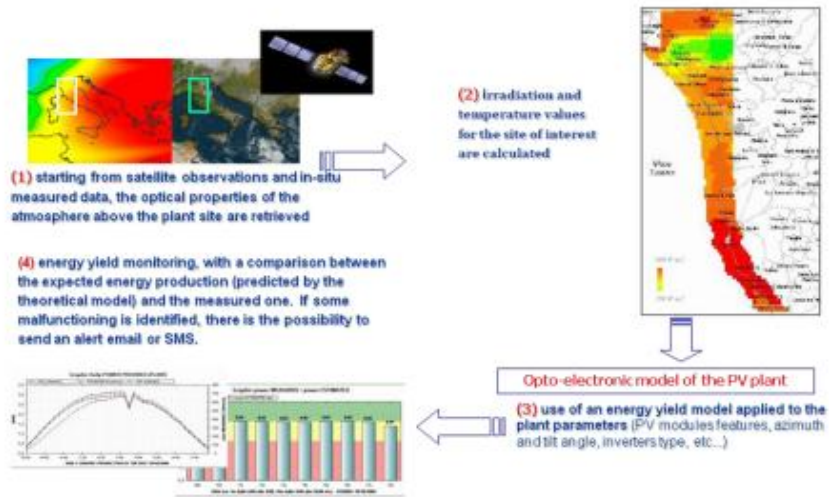


Figure 3.1. PV-Controller service model example

We activated the service in June 2010 and at this moment more than 200 plants are being monitored and there are still a lot of requests from the end-users.

The typical error in the power AC output prediction (respect to the real measured value) is less than 10-15 % and it is enough satisfactory for our end-users.



Figure 3.2. PV-Controller's energy yield monitoring service. Performance confidence interval has been evaluated of about 10% on statistical basis.

Based on plant modeling, the service offers also an extrapolation of the expected yearly energy yield, starting from the actual performance exploiting the satellite irradiation archive data.



Figure 3.3. As example, given the actual production in June, a web chart estimates which will be the production plant until the end of the year.

Finally, with the assistance of the PV-Controller service can be identified also possible malfunctioning or lack of calibration of the in-situ irradiance sensors.

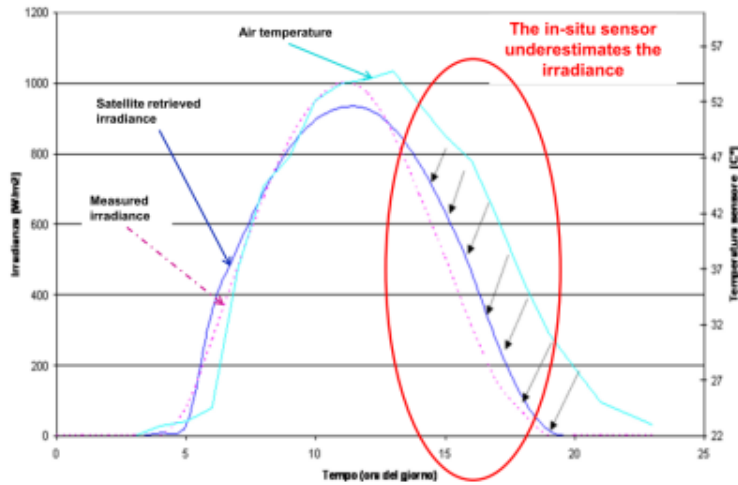


Figure 3.4. Identification of the malfunctioning of an irradiance in-situ sensor, caused by an uncorrected temperature compensation.

Future work

As for the PV-Planner service (see Section 3.1), also the PV-Controller service could be further improved with a better calculation of the irradiance data at ground (both improving spatial resolution and lowering the error respect to the actual in-situ measured values) and a better knowledge of the ground albedo.

In addition to this, also the knowledge of the spectral components of the incoming solar radiation could be important for the service improvement. The determination of the actual irradiation absorbed by the PV-plant could be determined more accurately knowing also the intensity of each spectral component of the incoming radiation itself.

Finally, another important input for the PV-Controller service could be determined better: the environment temperature, which is currently retrieved from Italian AirForce on a three-hourly base. A better estimation of this parameter could surely improve the cell temperature near-real-time calculation, which is a fundamental parameter for the Pac output determination.

3.3. UV

Synthetic polymers such as plastics, as well as naturally occurring polymer materials such as wood, are extensively used in building construction and other outdoor applications where they are routinely exposed to sunlight.

The UV-B content in sunlight is well known to affect adversely the mechanical properties of these materials, limiting their useful life.

A Web GIS service for estimating UV dose on open-door exposed materials has been proposed to automotive Italian manufacturers allowing for automotive parts ageing process simulation related to the geographic typical use of the cars.

At the moment the interest for this kind of service is under evaluation.

In fact the main problem for this issue is that the different parts of the car are manufactured by many different suppliers of the car manufacture company and the service should be mainly addressed to them.

4. Conclusions

The downstream services derived from the GMES services could be really useful for a great number of end-users like solar energy designers, building designers and PV or Thermal plants installers and designers.

In particular, a tool developed for the new PV or Thermal plants design– the PV-Planner service – and a tool developed for managing and monitoring the performances of existing PV or Thermal plants have been widely used and satisfied the end-users, while the interest for the tool developed for monitoring ground UV level (and the related materials ageing) is currently under evaluation.

In providing our services, we used the Soda irradiance data (a GMES core service). We had no relevant problems using both the web interface and the wget download procedure of the daily irradiance data (we made about 100 requests every day), with no delays in data delivery by Soda and really infrequent malfunctions of the Soda website.

Almost half hundred power plants have been constructed with the assistance of the PV-Planner (that in year 2011 has been used by more than 50000 users) and currently more than 200 power plants are monitored by the PV-Controller system.

We found a great interest for these services, especially from the PV installers and designers, and we received generally good feedbacks. We received also a few suggestions for developing them further and to improve their usefulness.

We report that the performances of these services could be further increased:

- improving the accuracy of the satellite irradiance data (for example lowering the distance from measured in-situ data and increasing the spatial resolution);
- with an high accuracy and high spatial resolution ground albedo map;
- with an high accurate and high spatial resolution near-real-time environment temperature map;
- knowing (near-real-time) the intensity of each spectral component of the incoming solar radiation.



Project ENDORSE

Energy Downstream Service
Providing energy components for GMES
Grant Agreement no 262892

Deliverable D402.1: Report on the Product S2 “Design CSPS”

Type of document: Product Report
Version Number and Revisions: 1.0
WP Number: WP402
Authors and Affiliation: Marco Morelli, Fabrizio Flore (Flyby S.r.l.)
Dissemination Level: PU
Estimated Indicative Person-Months: 10.75
Activity Type: RTD
Planned Delivery Date: September 2012
Actual Delivery Date: October 2012

CONTENTS

1. Document presentation	3
1.1. Purpose of the document.....	3
1.2. References.....	3
1.2.1. Applicable documents.....	3
1.2.2. Reference Documents.....	3
2. Product description	4
2.1. Definition of the product.....	4
2.2. Aim of the product	4
2.3. Embedded functionalities	4
2.4. Man-machine interfaces	4
2.5. Operational modes.....	5
2.6. Input data requirements	5
2.7. Output data produced.....	5
2.8. Performances	6
2.9. Limitations and constraints	6
3. Product development.....	8
3.1. User requirements.....	8
3.2. System requirements	8
3.3. Quality standards used.....	8
4. Product validation	9
4.1. Product results validation plan.....	9
4.2. Methods used for validation	9
5. User assessment.....	11
5.1. Compliance with initial User Requirements.....	11
5.2. Feedback from prime-users	11
5.3. Refinements after user feedback	11

1. Document presentation

1.1. Purpose of the document

This document is a report about the S2 product "Design CSPS" developed during the WP 402. Main functionalities, user assessment and results obtained (with their verification) are described giving an overall view about the product that has been developed and is now available.

1.2. References

1.2.1. Applicable documents

AD	Doc. Number	Iss / Rev	Date	Title
AD1	Annex I	3/1	2010-09-10	ENDORSE project Description of Work
AD2	D2.1	3/0	2011-05-24	Prime Users' Requirements for Product and Assessment Protocol
AD3	D5.1	1/0	May 2012	Summary of the assessment of products by users

1.2.2. Reference Documents

RD	Title	Authors	Date	Published by
RD1	Modeling daylight availability and irradiance components from direct and global irradiance	R. Perez, P. Ineichen, R. Seals, J. Michalsky and R. Stuart	1990	Solar Energy 44 , 271-289
RD2	Modeling and control of a solar thermal power plant with thermal energy storage	K. M. Powell and T. F. Edgar	2012	Chemical Engineering Science 71 , 138-145
RD3	Experimental and Model Based Performance Analysis of a Linear Parabolic Trough Solar Collector in a High Temperature Solar Cooling and Heating System	M. Qu, H. Yin and D. H. Archer	2010	Solar Energy Engineering 132 , 021004.1-021004.12
RD4	Energy Conversion	K. C. Weston	1992	PWS Publishing Company
RD5	Automatic control of a 30 MWe SEGS VI parabolic trough plant	T. Stuetzle, N. Blair, J. Mitchell and W. Beckman	2004	Solar Energy 76 , 187-193

2. Product description

2.1. Definition of the product

Software (algorithms and models) for calculating the production parameters of Concentrating Solar Power Systems starting from optical satellite imagery

2.2. Aim of the product

The software has a twofold application: it can be used for monitoring purposes, i.e. to assess the production efficiency of existing CSP plants by comparing the calculated energy with the measured one, or it can be used for planning purposes, i.e. to estimate what would be the production of a potential plant if it was installed in a specific location in Europe. EO optical satellite data are used. In the former case they are near-real time data, in the latter case data are from archive.

2.3. Embedded functionalities

The main new functionalities that have been developed and integrated into a unique software (written in IDL language), cover:

- remotely sensed irradiance and temperature values, respectively provided by Transvalor's Helioclim3 (developed into GMES-MACC project) and University of Genova (ENDORSE WP3);
- calculation of the direct irradiance on sun-tracking plane (DNI), mainly using the tilted irradiance model detailed in [RD1];
- calculation of the heat transferred from solar irradiance to the Heat Transfer Fluid (HTF) using solar field, absorber pipe and HTF models (mainly using the models presented in [RD3]);
- impact of the thermal energy storage (TES) system and heat losses during HTF flow (mainly using the models presented in [RD2]);
- DC electric power yield calculation using steam boiler and turbo-generator models (using the conversion efficiency presented in [RD4]) ;
- AC electric power yield calculation using an inverter model (embedded into the pre-existing Flyby's SolarSAT service).

The same functionalities are embedded in both monitoring and planning applications. The production parameters are calculated on a daily basis for monitoring, while on a monthly timescale for planning.

2.4. Man-machine interfaces

No interactive man-machine interfaces are available. The software retrieves the technical features of the CSP plant and the irradiance/temperature data from a local database, while the desired temporal range of the simulation is defined in a local configuration xml file. Once started, the software shows only the status of the simulation process in the form of a log-text prompted on the screen. When the process ends the 15-min AC power calculated values (for the selected temporal range) are stored in a dedicated table into the local database.

2.5. Operational modes

Only one operational mode is possible, as there are no different levels of performance and/or accuracy.

2.6. Input data requirements

Data sources (non GMES)		Comments and notes
Provider: ECMWF through Italian Air Force	Air ambient temperature (by interpolating ground measurements of network stations with 5 km ² spatial and 3 hours temporal resolution)	These data are used when the remotely sensed temperatures provided by University of Genova are missing

GMES service(s) used		Comments and notes
MACC-RAD core data Name: HelioClim database Provider: MINES ParisTech Service: SoDa	Near real-time or historical values (with 15-min temporal resolution) of solar horizontal irradiance at ground	The method to retrieve these data has been developed during GMES-MACC project (HC3 is a MACC Core Service)
Satellite: MSG Sensor: SEVIRI Provider: University of Genova	Near real-time or historical values (with 15-min temporal resolution) of temperature at ground	The method to retrieve these data has been developed in ENDORSE WP3

2.7. Output data produced

Model result (15-min values)	Output format	Description
HTF's temperature at the outlet of the solar field	Data inserted in a text file (.csv) or in a table of a local database	Daily Heat Transfer Fluid's temperature at the outlet of the solar field calculated starting from satellite imagery and sampled every 15 minutes
Energy absorbed by the Heat Transfer Fluid through the absorber tube	Data inserted in a text file (.csv) or in a table of a local database	Daily energy absorbed by the Heat Transfer Fluid through the absorber tube calculated starting from satellite imagery and sampled every 15 minutes
Energy loss from the absorber tube	Data inserted in a text file (.csv) or in a table of a local database	Daily energy loss from the absorber tube calculated starting from satellite imagery and sampled every 15 minutes

Instantaneous efficiency of the collector field	Data inserted in a text file (.csv) or in a table of a local database	Daily instantaneous efficiency of the collector field data calculated starting from satellite imagery and sampled every 15 minutes
HTF's temperature returning to the solar field	Data inserted in a text file (.csv) or in a table of a local database	Daily Heat Transfer Fluid's temperature returning to the solar field calculated starting from satellite imagery and sampled every 15 minutes
AC power yield	Data inserted in a text file (.csv) or in a table of a local database	Daily AC power data calculated starting from satellite imagery and sampled every 15 minutes (daily behaviour of the AC power yield by the CSP plant)

2.8. Performances

<p>Product's spatial resolution</p> <ul style="list-style-type: none"> Monitoring & Planning: 5 km² <p>Product's temporal resolution</p> <ul style="list-style-type: none"> Monitoring: 15 min Planning: 1 month <p>Production time:</p> <ul style="list-style-type: none"> Monitoring: 2 min (time to process 96 samples x 1 day) Planning: 24 min (time to process 96 samples x 12 days) <p>Delivery rate:</p> <ul style="list-style-type: none"> Monitoring: 1/day Planning: upon request <p>Accuracy:</p> <ul style="list-style-type: none"> Monitoring: to be validated as soon as the target plant will be active and production data will be released by the prime user. Nevertheless some interesting results were found by comparing calculated data with measured data retrieved from literature [RD2] and related to a similar plant: the difference for what concerns the AC power yield was within $\pm 20\%$. Planning: to be validated as soon as the target plant will be active and production data will be released by the prime user (after a sufficient working time).

2.9. Limitations and constraints

Data source	Limitations/Constraints
Remotely sensed temperature values (provided by the University of Genova)	The elaboration process developed by the University of Genova is not able, at the moment, to deliver these data daily

Air ambient temperature calculated by interpolating ground stations network measurements (provided by Italian Air Force)	These data have a poor temporal resolution (3 hours instead of 15 minutes)
--	--

3. Product development

3.1. User requirements

See deliverable D2.1 pp.17-21.

3.2. System requirements

Data / Process	Requirements
<i>Input data</i>	
Remotely sensed temperature data provided by University of Genova	~30 MB per plant per year
Remotely sensed solar irradiance data (both GHI and DNI) provided by Transvalor – HC3	70080 records in the database per plant per year (double type)
Temperature data calculated using ground stations measurements (provided by Italian Air Force)	~0.5 GB per year
Plant technical features	~30 records in the database per plant (double type)
<i>Output data</i>	
6 calculated parameters (see Section 2.7)	420480 records in the database per plant per year (double type)
<i>Processor power</i>	
Intel Xeon Quad-Core X5560 processor	2.80 GHz, 6 GB RAM

3.3. Quality standards used

The ISO9001 quality standards regarding processes and documentation are applied. In particular the involved processes are: requirements definition, design specifications, coding, verification and validation, configuration management and control.

The assigned project manager, with the support of the company Quality Manager, verifies all the activities in the project through dedicated milestones and verification procedures.

4. Product validation

This method was firstly applied to simulate the production of a 5 MW CSP parabolic plant with direct thermal storage located in Sicily (Italy). HTF outlet temperature, hot tank temperature and power yield were simulated for several days and meteorological conditions. The results showed good agreement with the same quantities measured for similar plants [RD2].

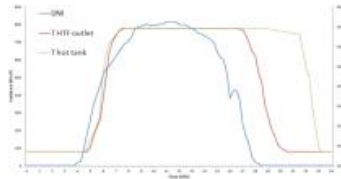


Figure 2: HTF outlet temperature and hot tank temperature simulated by S2 product for a 5 MW CSP energy plant at Priolo Gargallo (Sicily, Italy). Source data (DNI & temperature) are of 9th June 2012

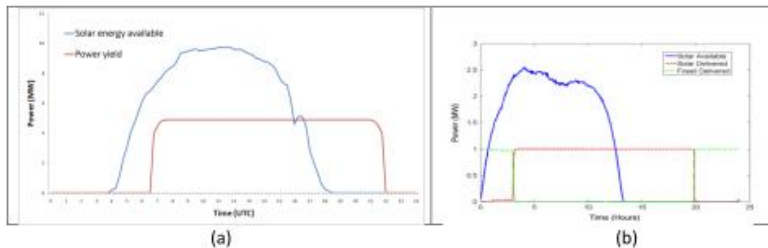


Figure 3: (a) AC power yield simulated by S2 product for a 5 MW CSP energy plant at Priolo Gargallo (Sicily, Italy). Source data (solar energy available & AC power yield) are of 9th June 2012 ; (b) AC power yield by a similar CSP plant in similar meteorological conditions (as reported in [RD2]).

4.1. Product results validation plan

At the moment the first results were successfully compared against measured power yield reported in literature for similar CSP plants. Results will be further validated using actual production data of Priolo Gargallo's CSP plant, as soon as it will be activated and the prime user Enel Green Power will make data available (hopefully within the end of the ENDORSE project).

4.2. Methods used for validation

The method used for validation is the direct comparison against measured values (reported in literature or in-situ measured in an active CSP plant) of the following parameters simulated by the S2 product:

- HTF's outlet temperature;
- energy absorbed by HTF through the absorber tube;
- instantaneous efficiency of the collector field;
- AC power yield by the plant;
- HTF's temperature returning to the solar field.

5. User assessment

The assessment was carried out in two steps:

- meeting in Rome (Viale Regina Margherita, 125 - Enel's Headquarters) on 27th February 2012;
- conference call on 13th June 2012.

In the first meeting Flyby presented the development status of the S2 product and the first results were discussed. Then in the conference call were discussed further results achieved in the meanwhile.

5.1. Compliance with initial User Requirements

As detailed in [AD3], the final version of the S2 product fulfilled all the user requirements defined in [AD2].

5.2. Feedback from Prime User (Enel Green Power)

- The user appreciated that all the important parameters for CSP plant characterization have been calculated; only some of them should be improved by further refining the modeling (turbo-generator and steam generator models);
- The user was interested in knowing that S2 results did match fairly well the production data given in [RD2] for a similar plant.

5.3. Refinements after Prime User feedback

The turbo-generator and steam boiler simulation parts were improved using the models reported in [RD4]. The new models replaced the previous energy conversion efficiency simple equations that were used before receiving user's feedback.



Project ENDORSE

Energy Downstream Service
Providing energy components for Gmes
Grant Agreement no 262892

Deliverable D402.1/D602.1: Report on the Product and the Service S2 “Design CSPS”

Type of document: Report
Version Number and Revisions: 1.0
WP Number: WP402 / WP602
Authors and Affiliation: Marco Morelli, Fabrizio Flore (Flyby S.r.l.)
Dissemination Level: PU
Estimated Indicative Person-Months: 10.75 (WP402) + 1.00 (WP602)
Activity Type: RTD / DEM
Planned Delivery Date: June 2013
Actual Delivery Date: October 2013

Coordination by Armines, 60, boulevard Saint-Michel, 75272 Paris cedex 06.
Contact : lucien.wald (at) mines-paristech.fr

TABLE OF CONTENTS

1	Document presentation	5
1.1	Purpose of the document.....	5
1.2	References.....	5
1.2.1	Applicable documents	5
1.2.2	Reference Documents	5
2	Product description	6
2.1	Definition of the product.....	6
2.2	Aim of the product	6
2.3	Embedded functionalities	6
2.4	Man-machine interfaces	6
2.5	Operational modes.....	7
2.6	Input data requirements	7
2.7	Output data produced.....	7
2.8	Performances	8
2.9	Limitations and constraints	8
3	Product development.....	10
3.1	User requirements	10
3.2	System requirements	10
3.3	Quality standards used.....	10
4	Product validation	11
4.1	Product results validation plan.....	11
4.2	Methods used for validation	11
5	User assessment.....	13
5.1	Compliance with initial User Requirements.....	13
5.2	Feedback from Prime User (Enel Green Power)	13
5.3	Refinements after Prime User feedback	13
6	Pre-market service description	14
6.1	Service requirements (reliability, availability, time of delivery)	14
6.2	Products used.....	14
6.3	Functional service elements.....	14
6.4	Technical implementation.....	15
6.5	User Interface.....	15

ENDORSE Deliverable D402.1: Report on the Product and the Service S2 "Design CSPS"

6.6	Main innovative features	15
7	Quality management concept	15
8	Service validation	15
8.1	Service test readiness status	15
8.2	Service test cases performed	15
8.3	Service test results	15
9	Marketing	16
9.1	Competitor's analysis	16
9.2	Own marketing approach/plans.....	16
10	Legal issues.....	16
10.1	Licenses required.....	16
10.2	IPR issues	16

— Page Intentionally Left Blank —

1 Document presentation

1.1 Purpose of the document

This document is an upgrade of the report about the S2 product "Design CSPS" developed during the WP402. An additional chapter has been dedicated to the description of the service based on the product developed in the WP402, following the guidelines decided during the July 2012 Progress Meeting #4.

1.2 References

1.2.1 Applicable documents

AD	Doc. Number	Iss / Rev	Date	Title
AD1	Annex I	3/1	2010-09-10	ENDORSE project Description of Work
AD2	D2.1	3/0	2011-05-24	Prime Users' Requirements for Product and Assessment Protocol
AD3	D5.1	1/0	May 2012	Summary of the assessment of products by users
AD4	D402.1	1/0	October 2012	Deliverable D402.1: Report on the Product S2 "Design CSPS"

1.2.2 Reference Documents

RD	Title	Authors	Date	Published by
RD1	Modeling daylight availability and irradiance components from direct and global irradiance	R. Perez, P. Ineichen, R. Seals, J. Michalsky and R. Stuart	1990	Solar Energy 44 , 271-289
RD2	Modeling and control of a solar thermal power plant with thermal energy storage	K. M. Powell and T. F. Edgar	2012	Chemical Engineering Science 71 , 138-145
RD3	Experimental and Model Based Performance Analysis of a Linear Parabolic Trough Solar Collector in a High Temperature Solar Cooling and Heating System	M. Qu, H. Yin and D. H. Archer	2010	Solar Energy Engineering 132 , 021004.1-021004.12
RD4	Energy Conversion	K. C. Weston	1992	PWS Publishing Company
RD5	Automatic control of a 30 MWe SEGS VI parabolic trough plant	T. Stuetzle, N. Blair, J. Mitchell and W. Beckman	2004	Solar Energy 76 , 187-193

2 Product description

2.1 Definition of the product

Software (algorithms and models) for calculating the production parameters of Concentrating Solar Power Systems starting from optical satellite imagery

2.2 Aim of the product

The software has a twofold application: it can be used for monitoring purposes, i.e. to assess the production efficiency of existing CSP plants by comparing the calculated energy with the measured one, or it can be used for planning purposes, i.e. to estimate what would be the production of a potential plant if it was installed in a specific location in Europe. EO optical satellite data are used. In the former case they are near-real time data, in the latter case data are from archive.

2.3 Embedded functionalities

The main new functionalities that have been developed and integrated into a unique software (written in IDL language), cover:

- remotely sensed irradiance and temperature values, respectively provided by Transvalor's Helioclim3 (developed into GMES-MACC project) and University of Genova (ENDORSE WP3);
- calculation of the direct irradiance on sun-tracking plane (DNI), mainly using the tilted irradiance model detailed in [RD1];
- calculation of the heat transferred from solar irradiance to the Heat Transfer Fluid (HTF) using solar field, absorber pipe and HTF models (mainly using the models presented in [RD3]);
- impact of the thermal energy storage (TES) system and heat losses during HTF flow (mainly using the models presented in [RD2]);
- DC electric power yield calculation using steam boiler and turbo-generator models (using the conversion efficiency presented in [RD4]) ;
- AC electric power yield calculation using an inverter model (embedded into the pre-existing Flyby's SolarSAT service).

The same functionalities are embedded in both monitoring and planning applications. The production parameters are calculated on a daily basis for monitoring, while on a monthly timescale for planning.

2.4 Man-machine interfaces

No interactive man-machine interfaces are available. The software retrieves the technical features of the CSP plant and the irradiance/temperature data from a local database, while the desired temporal range of the simulation is defined in a local configuration xml file. Once started, the software shows only the status of the simulation process in the form of a log-text prompted on the screen. When the process ends the 15-min AC power calculated values (for the selected temporal range) are stored in a dedicated table into the local database.

2.5 Operational modes

Only one operational mode is possible, as there are no different levels of performance and/or accuracy.

2.6 Input data requirements

Data sources (non GMES)		Comments and notes
Provider: ECMWF through Italian Air Force	Air ambient temperature (by interpolating ground measurements of network stations with 5 km ² spatial and 3 hours temporal resolution)	These data are used when the remotely sensed temperatures provided by University of Genova are missing

GMES service(s) used		Comments and notes
MACC-RAD core data Name: HelioClim database Provider: MINES ParisTech Service: SoDa	Near real-time or historical values (with 15-min temporal resolution) of solar horizontal irradiance at ground	The method to retrieve these data has been developed during GMES-MACC project (HC3 is a MACC Core Service)
Satellite: MSG Sensor: SEVIRI Provider: University of Genova	Near real-time or historical values (with 15-min temporal resolution) of temperature at ground	The method to retrieve these data has been developed in ENDORSE WP3

2.7 Output data produced

Model result (15-min values)	Output format	Description
HTF's temperature at the outlet of the solar field	Data inserted in a text file (.csv) or in a table of a local database	Daily Heat Transfer Fluid's temperature at the outlet of the solar field calculated starting from satellite imagery and sampled every 15 minutes
Energy absorbed by the Heat Transfer Fluid through the absorber tube	Data inserted in a text file (.csv) or in a table of a local database	Daily energy absorbed by the Heat Transfer Fluid through the absorber tube calculated starting from satellite imagery and sampled every 15 minutes
Energy loss from the absorber tube	Data inserted in a text file (.csv) or in a table of a local database	Daily energy loss from the absorber tube calculated starting from satellite imagery and sampled every 15 minutes

Instantaneous efficiency of the collector field	Data inserted in a text file (.csv) or in a table of a local database	Daily instantaneous efficiency of the collector field data calculated starting from satellite imagery and sampled every 15 minutes
HTF's temperature returning to the solar field	Data inserted in a text file (.csv) or in a table of a local database	Daily Heat Transfer Fluid's temperature returning to the solar field calculated starting from satellite imagery and sampled every 15 minutes
AC power yield	Data inserted in a text file (.csv) or in a table of a local database	Daily AC power data calculated starting from satellite imagery and sampled every 15 minutes (daily behaviour of the AC power yield by the CSP plant)

2.8 Performances

<p>Product's spatial resolution</p> <ul style="list-style-type: none"> Monitoring & Planning: 5 km² <p>Product's temporal resolution</p> <ul style="list-style-type: none"> Monitoring: 15 min Planning: 1 month <p>Production time:</p> <ul style="list-style-type: none"> Monitoring: 2 min (time to process 96 samples x 1 day) Planning: 24 min (time to process 96 samples x 12 days) <p>Delivery rate:</p> <ul style="list-style-type: none"> Monitoring: 1/day Planning: upon request <p>Accuracy:</p> <ul style="list-style-type: none"> Monitoring: to be validated as soon as the target plant will be active and production data will be released by the prime user. Nevertheless some interesting results were found by comparing calculated data with measured data retrieved from literature [RD2] and related to a similar plant: the difference for what concerns the AC power yield was within $\pm 20\%$. Planning: to be validated as soon as the target plant will be active and production data will be released by the prime user (after a sufficient working time).

2.9 Limitations and constraints

Data source	Limitations/Constraints
Remotely sensed temperature values (provided by the University of Genova)	The elaboration process developed by the University of Genova is not able, at the moment, to deliver these data daily

Air ambient temperature calculated by interpolating ground stations network measurements (provided by Italian Air Force)	These data have a poor temporal resolution (3 hours instead of 15 minutes)
--	--

3 Product development

3.1 User requirements

See deliverable D2.1 pp.17-21.

3.2 System requirements

Data / Process	Requirements
<i>Input data</i>	
Remotely sensed temperature data provided by University of Genova	~30 MB per plant per year
Remotely sensed solar irradiance data (both GHI and DNI) provided by Transvalor – HC3	70080 records in the database per plant per year (double type)
Temperature data calculated using ground stations measurements (provided by Italian Air Force)	~0.5 GB per year
Plant technical features	~30 records in the database per plant (double type)
<i>Output data</i>	
6 calculated parameters (see Section 2.7)	420480 records in the database per plant per year (double type)
<i>Processor power</i>	
Intel Xeon Quad-Core X5560 processor	2.80 GHz, 6 GB RAM

3.3 Quality standards used

The ISO9001 quality standards regarding processes and documentation are applied. In particular the involved processes are: requirements definition, design specifications, coding, verification and validation, configuration management and control.

The assigned project manager, with the support of the company Quality Manager, verifies all the activities in the project through dedicated milestones and verification procedures.

4 Product validation

This method was firstly applied to simulate the production of a 5 MW CSP parabolic plant with direct thermal storage located in Sicily (Italy). HTF outlet temperature, hot tank temperature and power yield were simulated for several days and meteorological conditions. The results showed good agreement with the same quantities measured for similar plants [RD2].

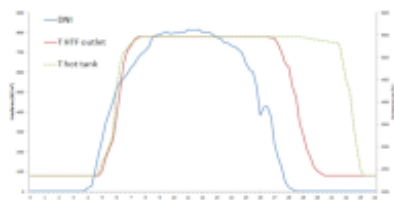


Figure 2: HTF outlet temperature and hot tank temperature simulated by S2 product for a 5 MW CSP energy plant at Priolo Gargallo (Sicily, Italy). Source data (DNI & temperature) are of 9th June 2012

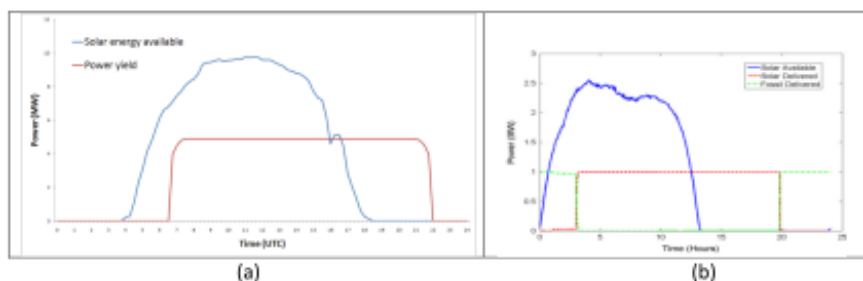


Figure 3: (a) AC power yield simulated by S2 product for a 5 MW CSP energy plant at Priolo Gargallo (Sicily, Italy). Source data (solar energy available & AC power yield) are of 9th June 2012 ; (b) AC power yield by a similar CSP plant in similar meteorological conditions (as reported in [RD2]).

4.1 Product results validation plan

At the moment the first results were successfully compared against measured power yield reported in literature for similar CSP plants. Results will be further validated using actual production data of Priolo Gargallo's CSP plant, as soon as it will be activated and the prime user Enel Green Power will make data available (hopefully within the end of the ENDORSE project).

4.2 Methods used for validation

The method used for validation is the direct comparison against measured values (reported in literature or in-situ measured in an active CSP plant) of the following parameters simulated by the S2 product:

- HTF's outlet temperature;
- energy absorbed by HTF through the absorber tube;
- instantaneous efficiency of the collector field;
- AC power yield by the plant;
- HTF's temperature returning to the solar field.

5 User assessment

The assessment was carried out in two steps:

- meeting in Rome (Viale Regina Margherita, 125 - Enel's Headquarters) on 27th February 2012;
- conference call on 13th June 2012.

In the first meeting Flyby presented the development status of the S2 product and the first results were discussed. Then in the conference call were discussed further results achieved in the meanwhile.

5.1 Compliance with initial User Requirements

As detailed in [AD3], the final version of the S2 product fulfilled all the user requirements defined in [AD2].

5.2 Feedback from Prime User (Enel Green Power)

- The user appreciated that all the important parameters for CSP plant characterization have been calculated; only some of them should be improved by further refining the modeling (turbo-generator and steam generator models);
- The user was interested in knowing that S2 results did match fairly well the production data given in [RD2] for a similar plant.

5.3 Refinements after Prime User feedback

The turbo-generator and steam boiler simulation parts were improved using the models reported in [RD4]. The new models replaced the previous energy conversion efficiency simple equations that were used before receiving user's feedback.

6 Pre-market service description

6.1 Service requirements (reliability, availability, time of delivery)

Service requirements	Description
Reliability	When tested, the service has demonstrated its capability to provide an accurate and timely information.
Availability	When tested, the service was available 24h/24h on the internet, by accessing the dedicated web portals. Generally speaking, the major constraint is the availability of the S2 product's inputs (satellite-based irradiance and air temperature in all cases and in-situ measured data in the CSP-Controller case)
Time of delivery	In case of CSP-Controller the service for a specific day is delivered with a maximum delay of 24h. In case of CSP-Planner the service is delivered within seconds from request.
Adaptivity	The service can be easily adapted also to other types of solar energy plants (e.g. Fresnel CSP plants, PV plants, CPV plants, etc..) by the upgrade of the modelling part inside the S2 product.

6.2 Products used

In the CSP-Controller case the products used for the service are those described in Section 2.6 plus the in-situ measured data. In the CSP-Planner case the product used are the same described in Section 2.6.

6.3 Functional service elements

The CSP-Controller part of the service compares the producible AC power (calculated from satellite data) with the actual one (measured in-situ) of the day before and gives an alert in case of misalignment. In this case it's also necessary to install a datalogger by the plant to read the produced AC power and other possible sensors.

The CSP-Planner part of the service provides the producible energy for a selected site together with a Return on Investment analysis based on the plant's technical features selected by the user.

In both cases the user receives the service in dedicated web portals.

6.4 Technical implementation

In the CSP-Planner case, after being granted the access to the web portal, the user has to select the plant's properties for use by the modelling. Then the user is provided with the results.

In the CSP-Controller case, after the installation of a datalogger by the plant and the provision of a plant's technical description, the user can access the dedicated web portal to monitor the produced AC power and receives an alert (by email or SMS) in case of misalignment with respect to the producible one.

6.5 User Interface

The user access the service through the dedicated web portals

6.6 Main innovative features

As far as we know this is the first service that combines satellite-based data, planning capabilities and near real-time monitoring capabilities.

7 Quality management concept

In addition to what specified in Section 3.3, the service status will be daily monitored by the assigned personnel. Moreover there will be also external web-tools checking the web accessibility continuously and alerting in case of malfunctions. Finally every complain by the user will be immediately taken into account by the assigned personnel.

8 Service validation

8.1 Service test readiness status

After successful tests, the service is ready to go operational for a specific geographical area (i.e Italy).

8.2 Service test cases performed

The service test has been based on the Prime User's CSP test plant (i.e. Priolo Gargallo's CSP). Since the test plant has not yet reached a steady production, the production data used in the test are those of a similar active plant found in literature.

8.3 Service test results

The plant modelling in the CSP-Controller part of the service has been tested against similar active CSP plant and the results are those reported in Section 4.

The CSP-Planner part of the service has been tested against a well known CSP plant simulator

(NREL's System Advisor Model – SAM), though not based on satellite data. The error between the two producible energies was lower than 4%.

9 Marketing

9.1 Competitor's analysis

As far as we know there are no competing services offering the CSP-Controller functionalities.

For what regards the CSP-Planner, the few existing products (not services) have different features like e.g. they don't use satellite data (SAM, Sandia Lab's DELSOL and SOLERGY).

9.2 Own marketing approach/plans

The service is intended to become a commercial service in 2015. Target customers will be designers and managers of CSP plants.

The service will be promoted jointly with other Flyby's products (PV and Wind Planner and Controller) during fairs dedicated to renewable energy, in specialized magazines, in scientific journals, by means of dedicated brochures, in international scientific conferences, etc..

The target for the first three years after market launch is to sell one CSP-Planner study and one CSP-Controller monitoring per year.

10 Legal issues

10.1 Licenses required

N/A

10.2 IPR issues

In view of the commercial service, some agreements will be established with the suppliers of the input data where the ownership of the data will be defined. Most probably the data ownership will remain with the supplier (e.g. in the CSP-Controller case the production data will belong to the customer).



Project ENDORSE

Energy Downstream Service
Providing energy components for GMES
Grant Agreement no 262892

Deliverable D602.2: Service S2 "Design CSPS" and final version of product

<i>Type of document:</i>	Demonstrator
<i>Version Number and Revisions</i>	1
<i>WP Number:</i>	WP602
<i>Authors and Affiliation:</i>	Marco Morelli (Flyby S.r.l.)
<i>Dissemination Level:</i>	PP
<i>Estimated Indicative Person-Months:</i>	2.5
<i>Activity Type:</i>	DEM
<i>Planned Delivery Date:</i>	March 2013 (Month 27)
<i>Actual Delivery Date:</i>	June 2013 (Month 30)

Coordination by Armines, 60, boulevard Saint-Michel, 75272 Paris cedex 06.
Contact : lucien.wald (at) mines-paristech.fr

- Page Intentionally Left Blank -

1. Objective of the present document

The pre-market services developed in ENDORSE have been made available to a selection of users for test in March 2013. The availability of services was the milestone MS#13. The European Commission requested this availability to be mentioned as a deliverable D60X.2 for each service. This deliverable is called a demonstrator.

A pre-market service may be a service on the Web or may deliver a report. In all cases, the demonstrator should be documented by a brief report that helps in keeping track of the availability of the demonstrator. This report may comprise different elements of the delivered products.

2. Objectives of the service S2

The service S2 is divided into two sub-services both dedicated to CSP plants: the first sub-service is called "CSP-Planner", while the other one is called "CSP-Controller".

The CSP-Planner sub-service offers support to identify the best site where to install a Concentrated Solar Power (CSP) plant, to configure the plant optimally and to estimate the profitability of the investment.

The CSP-Controller instead provides the capability to monitor in near real time the performances of an existing CSP plant.

Both the services exploit EO satellite based data and in-situ data. Products are delivered on the web using also GIS technology. Access to the service is allowed in a secure way. At the moment only parabolic-trough CSP plants are considered and the service covers only Italy (as planned in the ENDORSE DoW).

3. Two demonstrators for the service S2

In June 2013, two demonstrators were available online: one website for the CSP-Planner sub-service and another website for the CSP-Controller sub-service.

1) CSP-Planner

The screenshot displays the 'CSP-Planner' software interface. At the top, the 'Flyby' logo is visible next to the text 'Design your plant'. Below this, a blue arrow labeled 'Location' points to the 'Select location' section. The main area features a map titled 'Beam irradiation on normal plane' showing a color-coded irradiation map of the Mediterranean region. A search box on the left contains the text 'Search location or LAT,LOM' and an 'OK' button. A vertical color scale on the left indicates irradiation levels from 1330 kWh/m² (blue) to 2140 kWh/m² (red). A tooltip window is open over a location in southern France, displaying the following data: 'Selected location: SPS, Parco Nazionale dei Genargentini, 06030 Seui Og, Italia', 'Yearly Beam Normal Irradiation [kWh/m²]: 2175', 'Average wind intensity [m/s]: 5.5', and 'Air temperature [°C]: 15'. A 'Next' button is located below the map. At the bottom, a 'Notes' section lists: 'Yearly Beam Normal Irradiation has been averaged over the last 7 years.', 'Air temperature has been averaged over the last 5 years.', and 'Wind intensity has been averaged over the last 5 years.'. The footer contains the text: 'CSP-Planner is a Flyby 5.r.1. product, developed in the frame of the FP7 ENDORSE project - for more information: assistenza@solarat.eu' and 'Contact us'.

Location Technical features

Technical features

Fill the form with the technical characteristics of the CSP Parabolic Trough plant.

Solar collector modules

Number of modules

Aperture area (m²)

Mirrors reflectivity

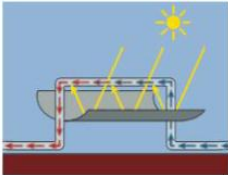


Heat Transfer Fluid (HTF)

Volume specific heat capacity (kWh/m³)

Inlet temperature (°C)

Flow rate (Kg/sec)



Glass envelope

Glass transmittivity

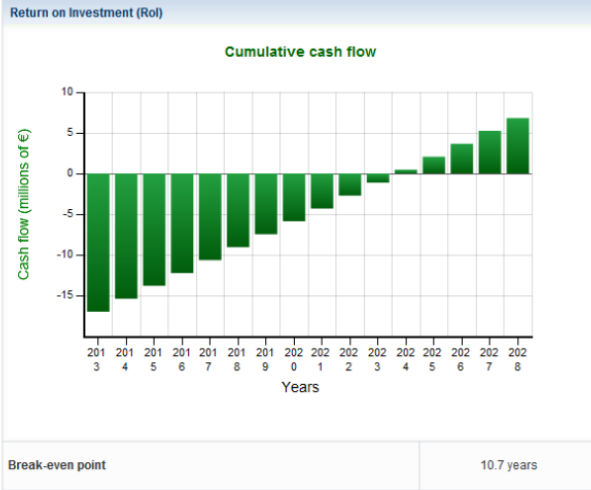
Outside diameter of the glass envelope (m)

Inside diameter of the glass envelope (m)



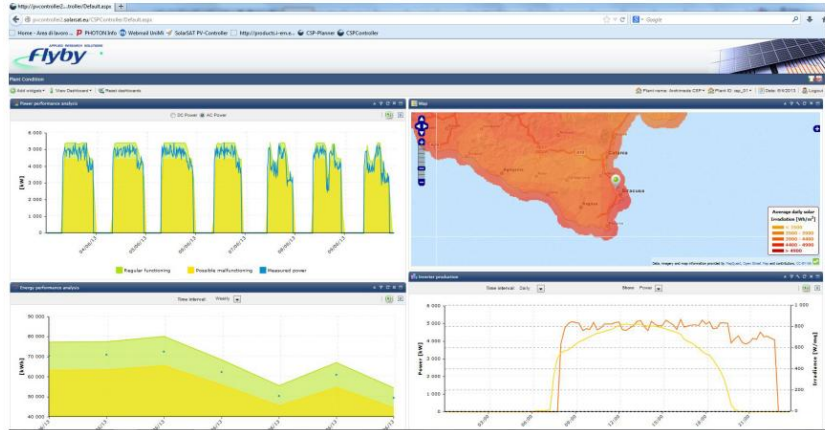


Global economic indicators	
Capital cost	17.01 millions of €
O&M annual cost	205391.00 €
Yearly incomes	1.79 millions of €



[Back](#) [Next](#)

2) CSP-Controller



<http://pvcontroller2.solarsat.eu/CSPController/Login.aspx>

